

1 How unstable was the environment during the Penultimate Glacial in
2 the South-Western Mediterranean? Vegetation, climate and human
3 dynamics during MIS 6.
4

5 **Charton Liz^{1,2}, Combourieu-Nebout Nathalie¹, Bertini Adele², Peyron Odile³, Robles Mary³,**
6 **Lebreton Vincent¹, Moncel, Marie-Hélène¹.**

a mis en forme : Anglais (Royaume-Uni)

7 1 : UMR 7194 HNHP- « Histoire Naturelle des Humanités Préhistoriques », MNHN / CNRS / UPVD, Paris, France.
8 liz.charton@mnhn.fr

9 2 : Dipartimento di Scienze della Terra, Università degli Studi di Firenze, Florence, Italy.

10 3: UMR 5554, ISEM-Institut des Sciences de l'Evolution de Montpellier, CNRS, Université de Montpellier, Montpellier, France.

11
12 **Correspondance** : [Liz charton \(liz.charton@mnhn.fr\)](mailto:liz.charton@mnhn.fr)

a mis en forme : Police :Gras

a mis en forme : Gauche

13 **Abstract**

a mis en forme : Anglais (États-Unis)

14 The impact of rapid climate variability on Neanderthal population in Europe during the Last
15 Glacial (Marine Isotope Stages 4-2), including Dansgaard-Oeschger cycles and Heinrich **eventsstadials**,
16 has been the subject of a long-standing debate. However, few studies have focused on the nature and
17 impact of such rapid variations on human population during earlier periods. A growing number of high-
18 resolution paleoclimatic archives supports the persistence of rapid oscillations during the penultimate
19 glaciation (**Marine Isotope Stage - MIS 6**), and the close response of Mediterranean ecosystems to
20 these. Still, few palynological sequences in the Mediterranean region offer sufficient resolution to
21 document vegetation dynamics during this time. Pollen records are especially lacking in the western
22 Mediterranean, a key region to understand the connection between North Atlantic and Mediterranean
23 climatic influences. This region is also traditionally considered a climatic refugium for human
24 population during unfavourable periods. We provide new palynological data covering MIS 6 from the
25 long and continuous marine record of **the ODP site 976** in the Alboran Sea. A total of 200 samples,
26 spanning the interval from 196 to 127 ka Before Present (BP), reveal both long-term trends and rapid
27 fluctuations in regional vegetation composition. A multi-method approach, including modern
28 analogues, regression, and machine learning approaches, was applied to **the ODP 976** pollen
29 assemblages to reconstruct the annual/seasonal temperatures and precipitation. Results show that
30 three phases can be identified. The first phase (187-166 ka BP) is characterized by significant
31 oscillations of temperate trees and rather cool and humid conditions during early MIS 6, coincident
32 with a sapropel layer deposition in both the western and eastern Mediterranean. In the second phase
33 (165-144 ka BP), arid herbaceous vegetation is dominant, marking the main imprint of glacial maxima

34 conditions and reduced climate variability. The third phase (144-129 ka BP) is marked by the
35 development of Ericaceae and increased annual precipitations. At the end of MIS 6 glaciation, an
36 episode of strong cooling and intense episode of steppe and semi-desert expansion is identified as
37 Heinrich Stadial 11 (135-129 ka BP), marking a distinct pattern for Termination II in the Western
38 Mediterranean. Rapid oscillations appear like a pervasive feature of the Penultimate glacial in the SW
39 Mediterranean, though they present reduced amplitude and frequency compared to the Last Glacial.
40 A synthesis of human occupation during MIS 6 shows that a mosaic of traditional (Mode 2) and
41 innovative (Mode 3) lithic technological features is observed in the archaeological record. Although
42 the data are scarce, Neanderthals seems to have continuously inhabited Western Mediterranean
43 regions across the penultimate glacial. The severe climate conditions during Heinrich Stadial 11 (~133-
44 129 ka BP) might have played a role in the apparent population contraction at the end of MIS 6, and
45 perhaps also in the definitive abandonment of Lower Palaeolithic industries.

46 1. Introduction

47 Rapid climate oscillations occurred during the last Glacial period (MIS 4-2). Dansgaard-
48 Oeschger (DO) cycles have been well identified in ice-core records (Bond et al., 1999; Dansgaard et al.,
49 1993; Johnsen et al., 1992; Rasmussen et al., 2014) and recognized in Atlantic sedimentary cores (e.g.
50 Bond et al., 1993, 1997; Roucoux et al., 2005; Sánchez Goñi et al., 2002; Shackleton et al., 2000,
51 Zumaque et al., 2025). Short periods of intense cold named Heinrich Stadials (HS) and linked with
52 intense iceberg discharges were also evidenced in Atlantic sediments (Bond et al., 1992; Heinrich,
53 1988; Hemming, 2004; Rasmussen et al., 2003; Ruddiman, 1977; Shackleton et al., 2004). Major cooling
54 events also occurred during MIS 5 and the penultimate deglaciation (e.g. Chapman & Shackleton, 1999;
55 Oppo et al., 2001). These high-frequency oscillations reflect major changes at global scale in the
56 oceanic circulation and the Atlantic Meridional Overturning Circulation (AMOC), that are important
57 features particularly during glacial terminations (Barker and Knorr, 2021). The Mediterranean region
58 has been very sensitive to the rapid climate oscillations of MIS 5 to MIS 1, with changes recorded in
59 both marine and continental environments (Cacho et al., 1999, 2006; Combourieu-Nebout et al., 2002,
60 2009; Fletcher et al., 2010; Martrat et al., 2007; Penaud et al., 2016; Sánchez Goñi et al., 2002, 2022).

61 The penultimate glacial (MIS 6) took place between ~185 and 130 ka BP and presented a
62 different ice-sheet and global climate configuration compared to the last glacial (MIS 4-2). It is
63 considered among the coldest glacial periods of the past 800 ka BP (Masson-Delmotte et al., 2010),
64 characterized by larger European Ice-Sheet and smaller Laurentide ice-sheet extension (Colleoni et
65 al., 2016; Ehlers et al., 2018; Ehlers & Gibbard, 2007; Rohling et al., 2017). In Europe, it corresponds to
66 the Riss glaciation in the Alpine area, and to the late Saalian glaciation complex in northern and central

a mis en forme : Anglais (Royaume-Uni)

67 Europe, with two major ice-sheet advances identified in Germany: the Drenthe advance (~170-155 ka
68 BP) characterized by the maximum ice extent in Europe, and the less extensive Warthe advance during
69 the younger stage of MIS 6 (Ehlers et al., 2011). The exact chronology of the Penultimate Glacial
70 Maximum (i.e. the maximum extension of the northern hemisphere ice-sheet) is still not well
71 constrained (Svendsen et al., 2004), but is usually considered around 140 ka BP (Colleoni et al., 2016).
72 Five marine isotopic substages were identified from MIS 6e to 6a, reflecting variations of global sea
73 temperatures : three cold substages (6e : ~180 ka BP, 6c : ~160 ka BP, 6a : ~136 ka BP) with increasing
74 cold intensity, and two warm substages (6d : ~170 ka BP and 6b : ~149 ka BP) (Railsback et al., 2015).
75 Different speleothem records revealed that MIS 6 glaciation in Europe, including the Mediterranean
76 region, was characterized by wetter conditions in comparison with the last glacial (Ayalon et al., 2002;
77 Koltai et al., 2017; Nehme et al., 2018; Regattieri et al., 2014). Furthermore, various studies highlighted
78 the apparent higher stability of the Laurentide ice-sheets during the penultimate glacial, leading to the
79 absence of typical “Heinrich layers” in the North Atlantic sediments, with the exception of the large
80 event recorded at the MIS 6 to MIS 5 transition, HS11 (~135-129 ka BP) (de Abreu et al., 2003;
81 McCarron et al., 2021; McManus et al., 1999; Obrochta et al., 2014; Ovsepyan and Murdmaa, 2017;
82 Shackleton et al., 2003).

83 Human Palaeolithic groups in Europe were likely affected by rapid climate changes
84 (Bradtmöller et al., 2012; Dennell et al., 2011; Raia et al., 2020; Willis et al., 2004). The South-Western
85 Mediterranean probably played a major role as one of the climate refugia areas around the
86 Mediterranean Basin during the most unfavourable climatic periods, permitting the persistence of
87 “source” population able to recolonize the northernmost areas during more favourable periods (Bailey
88 et al., 2008; Bicho & Carvalho, 2022). Neanderthal presence in very distinct ecotones in Eurasia proves
89 they could adapt to a very wide range of environments. However, recent niche modelling approaches
90 together with palaeoecological data from archaeological sites strengthened the view that warm
91 forested landscapes like the MIS 5e environments represented the most suitable habitats for
92 Neanderthals, where they could persist during colder periods (Carrión et al., 2026; Ochando et al.,
93 2019; Stewart et al., 2019; Trájer, 2023). This conception leads to the overlap of the notions of
94 refugium for vegetation and human populations, despite the greatest adaptability and niche extension
95 of humans. Many studies focused on the potential impact of abrupt environmental changes on
96 Neanderthal populations, especially those associated with Heinrich Stadials during MIS 3 (e.g. Charton
97 et al., 2025; D’Errico & Sánchez Goñi, 2003; Finlayson & Carrión, 2007; Melchionna et al., 2018). During
98 the previous climatic cycles of the Middle Pleistocene, when Early to Middle Palaeolithic cultures
99 developed, repeated climate instability has been brought forward as an explanation for the large
100 variability in the lithic production (Dennell et al., 2011; Foerster et al., 2022; Sánchez-Yustos and Diez-

Code de champ modifié

101 Martín, 2015), and the non-linearity of ~~the biological processes linked with~~ Neanderthal biological
102 evolution (Bermúdez de Castro & Martínón-Torres, 2013; Hublin, 2009). Still, the short and long-term
103 resilience of human populations in a globally unstable environment is poorly understood, and partially
104 hindered by our limited knowledge of fast millennial-scale climate oscillations in older glaciations prior
105 to MIS 4-2.

106 While the Greenland ice does not provide an adequate record for periods older than 123 ka BP
107 (Chappellaz et al., 1997), the description of a precise stratigraphy of climatic events at sub millennial
108 scale for the previous glacial/interglacial cycles remains complex, and relies on the Antarctic isotope
109 record (Bazin et al., 2013; Jouzel et al., 2007), the study of marine sediments (de Abreu et al., 2003;
110 Lisiecki & Raymo, 2005; Margari et al., 2010, 2014; McManus et al., 1999; Obrochta et al., 2014) and
111 high-resolution continental archives such as speleothems (Burns et al., 2019; Held et al., 2024; Hodge
112 et al., 2008; Wainer et al., 2013; Wang et al., 2018; Wang et al., 2001). Benthic and planktonic isotopic
113 ratios together with Sea Surface Temperatures (SSTs) reconstructions in the North Atlantic and the
114 Western Mediterranean showcased the persistence of D-O-like events and interhemispheric bipolar
115 see-saw heat transport during MIS 6, in addition to important reorganization of the water circulation
116 during sapropel S6 deposition ~175 ka BP (Margari et al., 2010, 2014; Martrat et al., 2004, 2007, 2014;
117 Rousseau et al., 2020; Siero & Andersen, 2022). Nevertheless, MIS 6 is much less well documented
118 than the last glacial in Mediterranean Europe. Few palynological sequences are available to document
119 the vegetation changes across this interval (Camuera et al., 2019, 2022; Follieri et al., 1988; Margari et
120 al., 2010; Okuda et al., 2001; Roucoux et al., 2011; Sadori et al., 2016; Sinopoli et al., 2019; Tzedakis et
121 al., 2006; Wilson et al., 2021). Among them, only one in SW Europe provides sufficient resolution to
122 document high-frequency changes: ~~the deep-sea core MD01-2444~~ (Margari et al., 2010, 2014). This
123 record from the deep-sea core MD01-2444 showed that several ~~While D-O like~~ millennial-scale climatic
124 events impacting impacted the vegetation the vegetation have been identified in this record especially
125 during the lower part of MIS 6 (Margari et al., 2010). ~~The core is located out of the Mediterranean~~
126 Sea, along the Portuguese margin in the Atlantic Ocean. Therefore, questions remain open concerning
127 the impact of such rapid events on the Western Mediterranean region, considered a Pleistocene
128 refugium for human populations.

129 To fill this gap, our study provides high-resolution pollen data and quantitative climate
130 reconstructions from ODP site 976 in south-western Mediterranean focusing on MIS 6. We aim to (i)
131 reconstruct the vegetation and climate changes in the SW Mediterranean during the penultimate
132 glacial, (ii) identify abrupt millennial-scale climatic changes ~~including potential Heinrich like and D-O~~
133 ~~like events~~ and connect-correlate them with other Atlantic and Mediterranean paleoenvironmental
134 records, (iii) compare the nature of millennial-scale climate and vegetation dynamics during the last

135 glacial period and the penultimate glacial using a single, continuous pollen record and (iv) explore the
136 potential impact of these climatic changes for Early Middle Palaeolithic human groups, with particular
137 attention to the presence of climate refugia during the most extreme glacial phases.

138 2. Study site

139 Ocean Drilling Program (ODP) Site 976 (36°12 N, 4°18W, 1108 m depth) core was retrieved in
140 1995 in the Alboran Sea (Zahn et al., 1999). The site is located about 110 km east of the Gibraltar Strait,
141 70 km south of the Spanish coast, and 100 km north of Morocco (Fig. 1).

142 The Alboran Sea is the westernmost extensional basin of the Mediterranean Sea, bordered to
143 the north by the Betic Cordillera and to the south by the Moroccan Rif mountains. Oceanic currents
144 result from the water masses exchanges between the Atlantic Ocean and the Mediterranean Sea
145 through the Gibraltar Strait. The surface currents are governed by the inflow of low-salinity Atlantic
146 waters (Atlantic Jet) forming two anticyclonic gyres named Western and Eastern Alboran Gyres (WAG
147 and EAG) (Renault et al., 2012) (Fig. 1). The Mediterranean high-salinity water masses flow out in the
148 Atlantic basin through the intermediate depth currents.

149 The modern climate in the Alboran Sea region is typically Mediterranean, defined by long, hot,
150 dry summers and mild and cool winters (Lionello et al., 2006; Sánchez-Laulhé et al., 2021). Atlantic
151 westerlies dominate during winter, while subtropical high pressure masses generate intense drought
152 during summer (Sumner et al., 2001). The current vegetation distribution on the Alboran borderlands
153 follows a strong altitudinal climatic gradient : dry steppe elements such as *Artemisia* and *Lygeum* grow
154 in the most arid lowlands along the coast, sclerophyllous evergreen taxa, including *Quercus ilex*, *Olea*
155 and *Pistacia* are the main representatives of the thermo-to meso-Mediterranean belts, while
156 temperate vegetation with deciduous trees constitutes the overlying supra-Mediterranean belt
157 (Quézel, 2000). Finally, coniferous forests of *Abies* and *Pinus* and *Picea* grow in the oro-Mediterranean
158 belt (above approximately 1200 m), with the presence of *Cedrus* in altitudinal vegetation of the
159 Moroccan Rif mountains.

160 The main sedimentation processes in the area originate from the strong erosion in the Betic
161 Cordillera (Alonso et al., 1999; Lique et al., 2005; Lobo et al., 2006) and the material transported by
162 the surface Atlantic waters (Auffret et al., 1974), although a significant but unknown proportion of
163 particles including pollen was transported by African winds as evidenced by the presence of Saharan
164 clay particles and *Cedrus* pollen across the Pleistocene (Bout-Roumzeilles et al., 2007; Jiménez-
165 Moreno et al., 2020; Magri & Parra, 2002). Therefore, the pollen assemblage is interpreted as reflecting
166 the regional vegetation of the southern Iberian Peninsula, with smaller but variable contribution from
167 Northern Africa. Previous studies have shown that the Alboran Sea palynological record displays close

a mis en forme : Anglais (Royaume-Uni)

Code de champ modifié

168 similarities with the Padul record in SE Spain (Camuera et al., 2019), indicating that ODP 976 is a valid
169 archive to reconstruct the southern Iberian Peninsula vegetation changes (Fletcher & Sánchez Goñi,
170 2008; Charton et al., 2025).

171 Two Organic-Rich Layers (ORLs) were identified in ODP 976 core during the MIS 6 interval, bed
172 607 (50.43-49.93 m), and bed 606 (41.6-40.4 m) (Murat, 1999). The ages were recalculated based on
173 the updated age model for MIS 6 presented here, giving 178.07-174.53 ka BP for bed 607, and 132.64-
174 129.16 ka BP for bed 606. With a Total Organic Carbon (TOC) of 1.18% and 1.85% respectively, these
175 layers have been described as “ghost sapropels”, as they present a lower organic matter content than
176 the Eastern Mediterranean sapropels (Rogerson et al., 2008). Their relevance for hydrological and
177 climatic inferences in the Alboran Sea will be discussed in the light of the vegetation dynamics.

a mis en forme : Anglais (États-Unis)

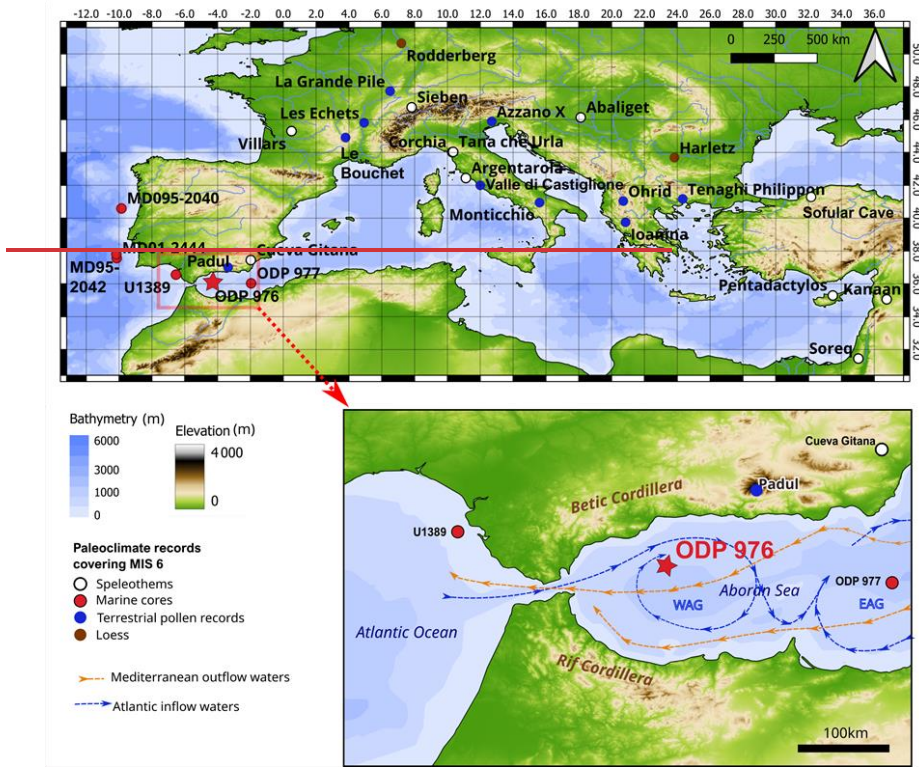




Fig. 1. Map showing the location of ODP 976 core together with other paleoenvironmental and paleoclimate records covering part or all of MIS 6, as discussed in the text.

178

3. Methods

179

3.1. Age Model

180

181

The age model for the study interval uses three previously published tie-points between ODP 976 Mg/Ca-derived SST (Jiménez-Amat and Zahn, 2015) and the speleothem temperature records from Dongge cave in China (Kelly et al., 2006, [see Supplement Fig. S1](#)). [Several other marine records covering MIS 6 in the region are chronologically tuned to speleothems \(e.g. Sierra & Anderson, 2022; Tzedakis et al., 2018\).](#) -For the lower interval, the low resolution of planktonic isotopic data available for ODP 976 did not allow direct [correlation to global temperature stacks or orbital configuration](#) ~~orbital or temperature calibration~~ (von Grafenstein et al., 1999). Instead, we chose to align the higher-resolution pollen record produced in this study with the one from MD01-2444 core on the Portuguese margin (Margari et al., 2010, 2014; Tzedakis et al., 2018). Previous studies highlighted the strong similarities

183

184

185

186

187

188

189

a mis en forme : Anglais (Royaume-Uni)

190 between pollen records on the Atlantic margin and the Alboran Sea during the last glacial period
 191 (Fletcher et al., 2010; Fletcher & Sánchez Goñi, 2008; Sánchez Goñi et al., 2002), supporting this
 192 approach. MD01-2444 chronology is based on the alignment of benthic isotopic events with the
 193 Antarctic temperature record, on AICC2012 timescale (Jouzel et al., 2007; Margari et al., 2010; Shin et
 194 al., 2020). [The eleven tie-points between MD01-2444 core and EPICA Dome C can be found in
 195 Supplement \(Table S1\).](#) Five peaks of temperate forest in MD01-2444 were used as control-points for
 196 ODP 976 (Table 1). [The main assumptions of these tuning approaches to the Dongge cave speleothem
 197 and the Antarctic record are discussed in detail in Jiménez-Amat and Zahn \(2015\) and Margari et al.
 198 \(2010\) respectively. The obtained chronology for ODP 976 core for MIS 6 prevents any assessment of
 199 the southwestern Mediterranean vegetation response to global climatic events.](#)

a mis en forme : Anglais (États-Unis)

a mis en forme : Anglais (États-Unis)

a mis en forme : Anglais (États-Unis)

Event type	ODP 976 meters composite Depth (mcd)	Age (ka BP)	References
Dongge cave speleothem D3	40.25	128.73	Jiménez-Amat and Zahn, 2015; Kelly et al., 2006
Dongge cave speleothem D2	42.61	135.57	Jiménez-Amat and Zahn, 2015; Kelly et al., 2006
Dongge cave speleothem D1	44.14	142.09	Jiménez-Amat and Zahn, 2015; Kelly et al., 2006
Temperate pollen peak in MD01-2444	46.4	149.43	(Margari et al., 2010; Shin et al., 2020)
Temperate pollen peak in MD01-2444	48.5	160.00	(Margari et al., 2010; Shin et al., 2020)
Temperate pollen peak in MD01-2444	49.3	170.07	(Margari et al., 2010; Shin et al., 2020)
Temperate pollen peak in MD01-2444	50.48	178.42	(Margari et al., 2010; Shin et al., 2020)
Temperate pollen peak in MD01-2444	53.2	193.758	(Margari et al., 2010; Shin et al., 2020)

a mis en forme le tableau

a mis en forme : Anglais (Royaume-Uni)

200 **Table 1. List of control points used to calibrate the ODP 976 record for the MIS 6 interval.** The tie-
 201 points on MD01-2444 temperate pollen curve are on AICC2012 timescale.

202 A linear regression was applied to obtain a continuous age for the study interval, spanning from
 203 126.4 to 196.6 ka BP, with a mean resolution of about 350 years for the record (Fig. 2).

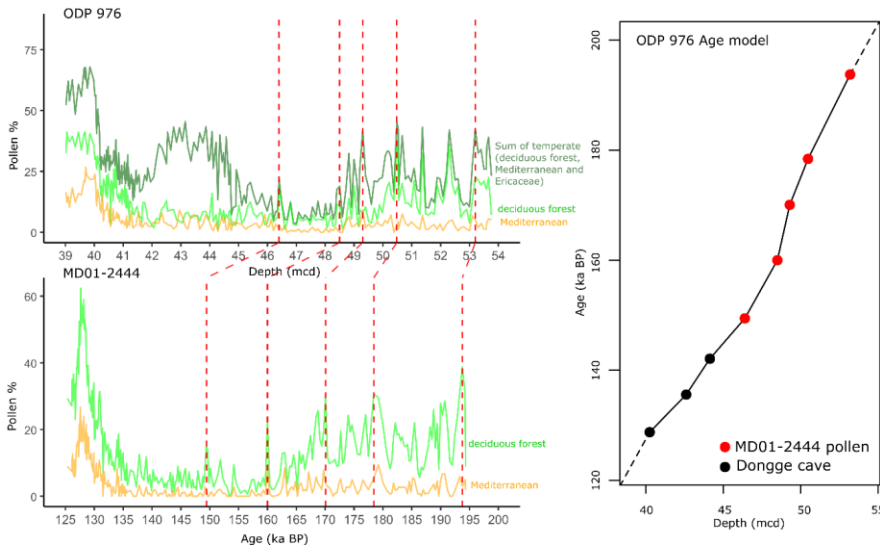


Fig. 2. Age versus depth model for the MIS 6 part of ODP 976 record, based on correlation between the Mg/Ca-based SST curve (Jiménez-Amat and Zahn, 2015) and the Dongge cave speleothem temperature record (Kelly et al., 2006) (black dots), and graphical correlation of the temperate pollen curve with the MD01-2444 palynological record (red dots and dotted lines) on AICC2012 timescale (Margari et al., 2010; Shin et al., 2020).

204

205 3.2. Pollen analyses

206 Two hundred samples have been analysed [herein this study](#), between 40 and 54 m (mcd)
 207 depth. The sample processing followed the traditional steps used for pollen extraction (Faegri and
 208 Iversen, 1964) and previously applied to the ODP 976 core (Combourieu-Nebout et al., 2002; 2009;
 209 Sassoon et al., 2023, Charton et al., 2025). It included sample weighing between 5 and 10 g of
 210 sediments, a 150 μm sieving for ~~the~~ retrieving of macrofossils and macroparticles, followed by 10%
 211 HCl, 40% HF, 20% HCl and a final 10 μm sieving.

212 A minimum of 150 pollen grains were counted for each sample, excluding *Pinus* as it is usually
 213 overrepresented in marine sequences (e.g. Combourieu-Nebout et al., 2002; Fletcher et al., 2010b;
 214 Mudie, 2011 and references therein), and represents often more than 50% of the total pollen sum
 215 [along in](#) the study interval (see Fig. 3).

216 Ecological groups of pollen taxa were defined following previous studies of the ODP 976 record
 217 (Charton et al., 2025; Combourieu-Nebout et al., 2009; Sassoon et al., 2023). The percentage pollen
 218 diagram was constructed using the *rioja* R package (Juggins, 2023). Constrained Incremental Sum-of-

219 Squares (CONISS) cluster analysis was applied for pollen zonation, using the *vegan* package on R
220 (Oksanen et al., 2024).

221 3.3. Pollen-inferred climate reconstructions: a multi-method approach

222 Four methods were applied to the ODP 976 record to reconstruct past climate changes during
223 MIS 6. This is the first time this approach is used for the entire MIS 6 interval (Sinopoli et al., 2019). ~~As~~
224 ~~already pointed out, t~~ The multi-method approach allows for a more accurate climate reconstruction
225 (trends and rapid events) compared to the traditional single-method approach (Chevalier et al., 2020;
226 Peyron et al., 2011, 2013; Salonen et al., 2019; Sassoon et al., 2025). It also allows us to compare the
227 reliability and biases of the different methods, which are based on different ecological principles and
228 mathematical algorithms. Four methods were used in this study.

229 The Modern Analogue Technique (MAT) is the first “assemblage” method ever developed to
230 estimate climate parameters based on pollen assemblages, and is still the most widely used (Guiot,
231 1990). It is based on the calculation of a dissimilarity index between the fossil samples and samples
232 from a modern pollen dataset. The values of the closest modern analogues selected (here, 4) are
233 averaged to reconstruct the climate parameters for each fossil sample. Weighted-Averaging Partial
234 Least Squares (WA-PLS) (ter Braak and Juggins, 1993) is the second most widely used method, and is
235 based on a different mathematical approach using non-linear regression. Assuming that taxa are most
236 abundant where they find their optimum climatic conditions, WA-PLS models the plant/climate
237 relationships from the modern calibration dataset, weighing the climatic values based on the pollen
238 taxa percentage. These plant pollen abundance / climate transfer functions are then used to calculate
239 the climate parameters of the fossil samples. The last two methods, Random Forest (RF) and Boosted
240 Regression Trees (BRT), rely on a completely different approach using machine learning: they generate
241 a large set of regression trees based on a randomised pollen dataset by bootstrapping (with pollen
242 taxa selected randomly). Contrary to RF (Prasad et al., 2006), BRT (Salonen et al., 2012) assigns a higher
243 probability to select samples that have not been selected before (boosting), increasing the
244 performance of the model for elements that are less well predicted (Chevalier et al., 2020). The
245 application of these machine learning methodologies in paleoclimatology is very promising, especially
246 for BRT, and they have already been validated through different European and Mediterranean pollen
247 records, for different time periods (Charton et al, 2025; D’Oliveira et al., 2023; Robles et al., 2022,
248 2023; Salonen et al., 2019; Sassoon et al., 2025).

249 The four methods were run on R using the *Rioja* packages *Rioja* for MAT and WA-PLS (Juggins,
250 2024), *dismo* for BRT (Hijmans et al., 2023) and *randomForest* for RF (Liaw and Wiener, 2022).

251 We used the modern pollen dataset compiled by Peyron et al. (2013, 2017) and updated by
252 Dugerdil et al. (2021a) and Robles et al. (2023). Samples belonging to non-relevant biomes for this
253 study were excluded (Taiga, Tundra, Pioneer Forest, warm steppe and hot desert), resulting in 2373
254 samples for calibration dataset spanning ~~across~~ Eurasia and NW Africa (see Supplement, Fig. S2). A
255 total of 103 harmonized pollen taxa are included in the dataset, excluding *Pinus* and aquatic taxa.

a mis en forme : Police :Italique

256 Six climate variables were reconstructed: PANN (annual ~~precipitations~~precipitation), MAAT
257 (annual temperatures), SUMMERPR (summer ~~precipitations~~precipitation), WINTERPR (winter
258 ~~precipitations~~precipitation), MTWA (mean temperature of the warmest month) and MTCO (mean
259 temperature of the coldest month). The climatic tolerance spectra of the ten most abundant pollen
260 taxa in the ODP 976 record have been reconstructed based on the modern dataset (Supplement, Fig.
261 S3). They show that steppe and semi-desert taxa display the highest tolerance to low winter
262 temperature and precipitation, while Mediterranean taxa (*Olea* and *Quercus ilex*-type) are the most
263 tolerant taxa to high annual and summer temperature, and *Cedrus* and *Ericaceae* to higher annual and
264 seasonal precipitation. SUMMERPR ~~and MTWA values were~~was poorly reconstructed according to the
265 accuracy indicators (Table 2). This is in agreement with previous studies showing the poor reliability of
266 summer parameters (e.g. Camuera et al., 2022). Therefore, we chose to represent seasonal
267 parameters as contrast values for a better visualization: TCON (temperature contrast) = MTCO -
268 MTWA, and PCON (precipitation contrast) = WINTERPR – SUMMERPR. The MTWA and SUMMERPR
269 results can be found in Supplementary Supplement (Fig. S4).

a mis en forme : Police :Italique

a mis en forme : Police :Italique

a mis en forme : Police :Italique

a mis en forme : Police :Italique

270 For comparison with the present-day climate, and the calculation of anomalies, the modern
271 values were extracted from ERA 5 reanalysis of the ECMWF (European Centre for Medium-Range
272 Weather Forecasts), based on data assimilation into meteorological modelling from 1960 to 2022
273 (Hersbach et al., 2020). Pollen dispersal is reduced beyond a radius of 175 km (Rojo et al., 2016).
274 However, other studies suggest that pollen can be transported up to distances of 200-300 km
275 (Fernández-Rodríguez et al., 2014) and even over distances greater than 500 km (Bayr et al., 2023;
276 Damialis et al., 2017). Sediments from marine cores such as ODP 976 can therefore include close and
277 long-distance pollen. To account for these observations, ~~An~~ averaged value of the climate parameters
278 on a 400 km radius around the ODP 976 site was extracted (Supplement, Fig. S5), giving MAP = 478
279 mm, MAAT = 16.78°C, MTCO = 13.78 °C, WINTERPR = 172 mm, TCON = -9.59, PCON = 141.5 mm. These
280 values for modern climate, averaged temporally and spatially, provide a better basis for understanding
281 the nature of the climate signal extracted from a marine palynological sequence at a regional pluri-
282 annual scale.

a mis en forme : Anglais (Royaume-Uni)

a mis en forme : Anglais (Royaume-Uni)

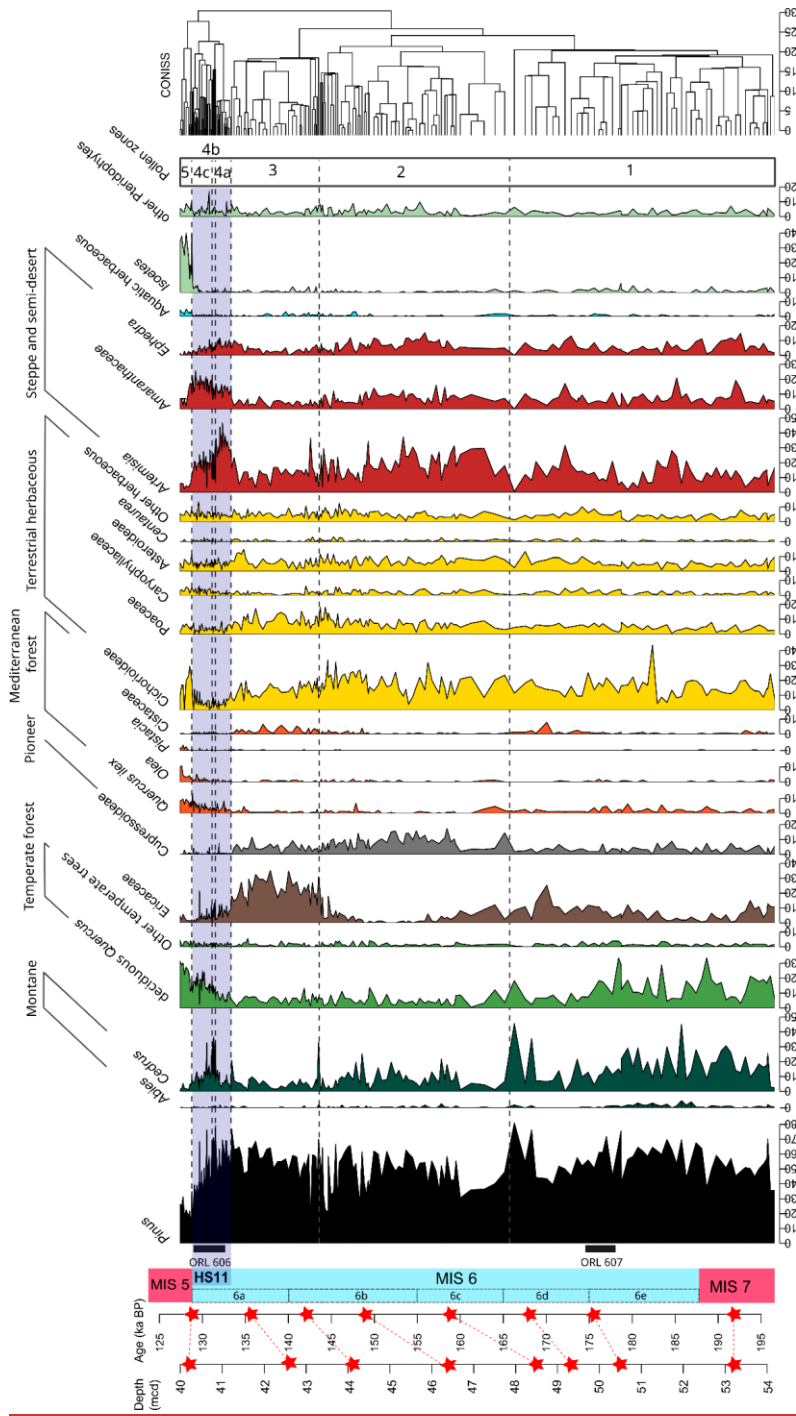
a mis en forme : Anglais (Royaume-Uni)

283 The reliability of the different methods and climate parameters reconstructed is evaluated with
284 bootstrapping cross-validation through two indicators: the correlation coefficient between the
285 variables (R^2) and the root mean square error (RMSE).

286 4. Results

287 4.1. Pollen record

288 The pollen diagram shows the vegetation dynamics between 196.6 and 127.5 ka BP, spanning
289 late MIS 7 to early MIS 5 (Fig. 3). Five pollen zones were separated by CONISS cluster analysis, with
290 zone 4 being divided in three subzones (Table 2).



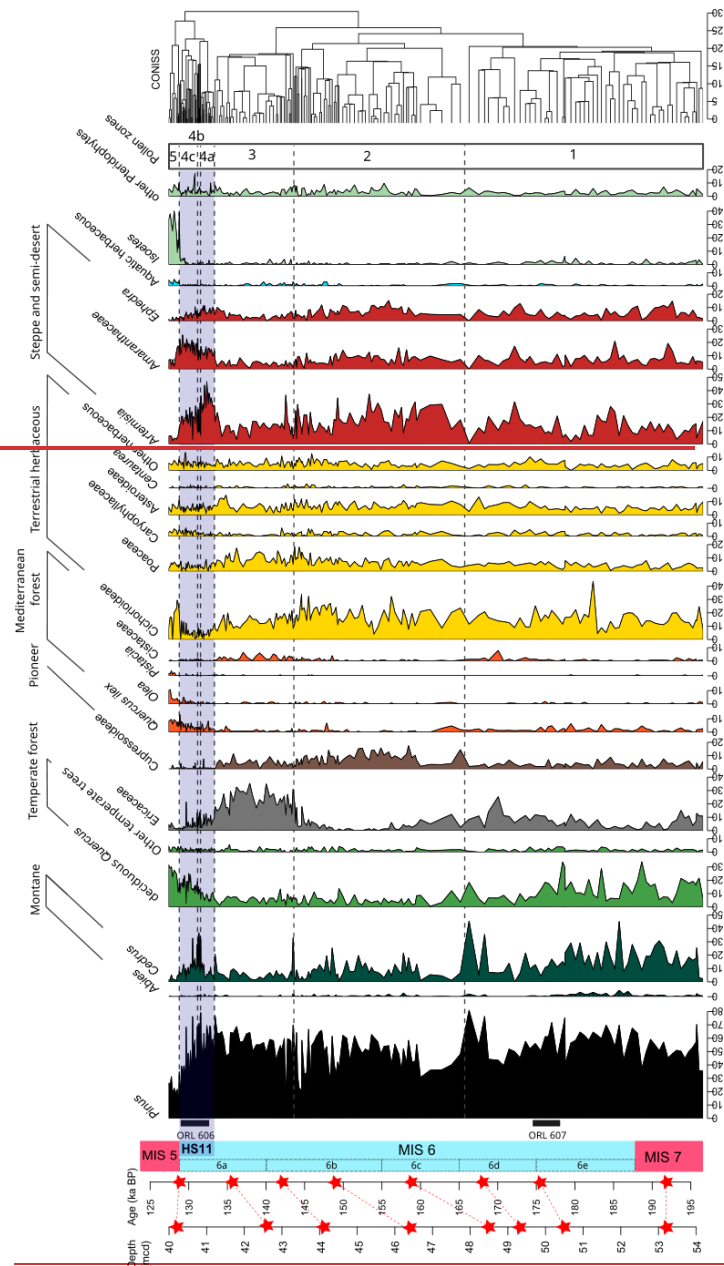


Fig. 3. Pollen diagram of selected taxa for MIS 6 interval in the ODP 976 record, plotted against age. Taxa are grouped by ecological groups (see Table 2). Red stars indicate control points used for the age calibration, and their correspondence with mcd (meters composite depth) (see Table 1). The blue bar indicates Heinrich Stadial 11. ORL : Organic Rich Layers from ODP 976 (Murat, 1999).

292 Zone 1 most represented taxa are deciduous *Quercus* and *Cedrus*, with important abundance
293 variability showing an unstable ~~and rather cool and humid~~ phase at the transition from MIS 7 to MIS
294 6e and 6d. Zone 2 displays the maximum expansion of steppe and semi-desert vegetation together
295 with other open vegetation taxa and Cupressoideae, ~~characteristic of the vegetation maximum glacial~~
296 ~~stage~~ during the MIS 6b and 6c. An additional noteworthy observation within this interval is the
297 presence of gastropod shells identified as *Limacina retroversa* (Jeanne Rampal, personal
298 communication, [2023](#)), recovered during sieving of a sample at 46.4 m, corresponding to around
299 155.5 ka BP (Fig. 4). This species is usually most abundant in temperate to subpolar waters in the
300 North-Atlantic (Thabet et al., 2015). Zone 3 is mainly characterized by the abundance of Ericaceae ~~and~~
301 ~~indicates cold and humid conditions~~ at the final stage of MIS 6 (6b and 6a). Zone 4, at the end of MIS
302 6a, is divided into 3 subzones which display fast vegetation changes during the transition from MIS 6
303 to MIS 5 (Termination II), and Heinrich Stadial 11. The fast expansion of steppe and semi-desert taxa
304 (*Artemisia*, *Amaranthaceae*, *Ephedra*) occurs simultaneously with the first increase of deciduous
305 temperate and Mediterranean forest indicative of the initialization of interglacial conditions (zone 4a).
306 This episode of arid vegetation dominance is interrupted in zone 4b by the fast expansion of montane
307 vegetation mainly represented by *Cedrus*. A new steppe and semi-desert vegetation increase is
308 observed in zone 4c, while the deciduous temperate forest and the Mediterranean vegetation
309 continue to expand. Finally, zone 5 is characterized by the maximum abundance of mesophilous and
310 thermophilous elements, mainly represented by deciduous *Quercus* and *Quercus ilex*, typical of the
311 MIS 5 interglacial ~~optimum~~.

312

313

314

315

316

317

318

319

320

321

322

323

324

325

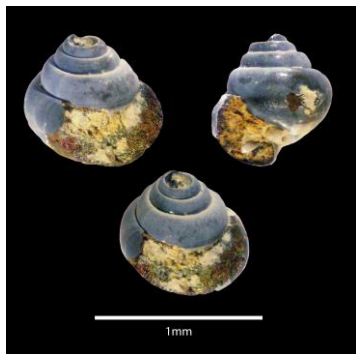
Pollen zone	Depth (mcd) and Age (ka BP)	Description of the pollen assemblage (Fig. 3)	Climate reconstructions (Fig. 5)
5	40.25-39.98 m 128.73-127.47 ka BP	Peak abundance of deciduous <i>Quercus</i> (up to 32%), <i>Quercus ilex</i> (4-10%), <i>Olea</i> (2-11%), <i>Pistacia</i> (up to 4%), aquatic herbaceous (up to 5%) and <i>Isoetes</i> (up to 38%). High values of Cichorioideae (up to 30%). Low percentages of <i>Pinus</i> (<35%), <i>Artemisia</i> (<11%), Amaranthaceae (<18%) and <i>Ephedra</i> (<3%).	Rapid increase of temperature, precipitation and seasonal contrast close to the modern value
4c	41.08-40.28 m 131.13-128.81 ka BP	New increase of <i>Artemisia</i> (up to 29%) and Amaranthaceae (up to 26%). High values of <i>Cedrus</i> (5-28%), and increasing percentages of deciduous <i>Quercus</i> (10-23%), Cichorioideae (0-14%) and <i>Quercus ilex</i> (1-13%). Decrease of Ericaceae (13-0%). Increasing percentages of <i>Isoetes</i> (0-5%) and Pteridophytes spores (0-17%).	First decrease, and then increase in temperatures and precipitations precipitation, with low PCON.
4b	41.21-41.09 m 131.51-131.16 ka BP	Peak abundance of <i>Cedrus</i> (up to 37%). Decrease of <i>Artemisia</i> (30-7%), Amaranthaceae (6-13%) and <i>Ephedra</i> (6-4%). Notable abundance of deciduous <i>Quercus</i> (6-15%) and <i>Quercus ilex</i> (1-3%).	Abrupt rise in precipitation contrast, but still cold conditions.
4a	41.82-41.22 m 133.28-131.54 ka BP	Peak abundance of <i>Artemisia</i> , (24-47%), Amaranthaceae (14-6%) and <i>Ephedra</i> (5-11%). Decreasing trend of Ericaceae percentages (12-2%), and progressive increasing of deciduous <i>Quercus</i> (4-11%) and <i>Quercus ilex</i> (1-8%). Decrease of Cichorioideae (<11%) and Cupressoideae (<8%).	Rapid decrease in temperature, precipitation and seasonal contrast.
3	44.57-41.85 m 143.49-133.37 ka BP	Peak abundance of Ericaceae (12-35 %), and high values of Cichorioideae (8-22%). Notable presence of Cupressoideae (2-11%). Peak abundance of <i>Artemisia</i> (37%) at 44.28 m / 142.54 ka BP and <i>Cedrus</i> (33%) at 44.57 m/143.49 ka BP.	Increase of temperatures (but still lower than present), and important precipitations precipitation rise until values higher-than-present. Seasonal contrast close to present-day.
2	48.91-44.63 m 165.16-143.68 ka BP	High percentages of Cichorioideae (11-34 %), Poaceae (4-18%), <i>Artemisia</i> (4-	Decline of temperatures and precipitations precipitation, both lower than the modern

		37%), Amaranthaceae (3-16%) and <i>Ephedra</i> (3-12%). Cupressoideae maximum between 150-160 ka BP (up to 17%), and abundant <i>Cedrus</i> (up to 25%). Very low values of deciduous <i>Quercus</i> (<10%), Mediterranean taxa (<4%) and Ericaceae (<12%), with minimum values between 150 and 158 ka BP.	values, reaching a minimum between ~164-155 ka BP. Afterwards, progressive rise in temperature, precipitation and seasonal contrast.
1	53.76-49 m 196.15-166.29 ka BP	High percentages of <i>Cedrus</i> (8 to 45%) and deciduous <i>Quercus</i> (4 to 34%), with important variations. Abundant Cichorioideae (up to 43%) and Ericaceae (up to 25%), with notable presence of <i>Abies</i> (up to 5%), <i>Quercus ilex</i> (up to 6%) and <i>Isoetes</i> (up to 6%). Relatively low values of semi-desert elements (<i>Artemisia</i> , Amaranthaceae, <i>Ephedra</i>) but with two increases at 49.6 m /172 ka BP and at 51.6 m / 185 ka BP.	Rather stable conditions expressed by the smoothed lines, but important and numerous rapid oscillations. In general, values of precipitation and seasonal contrast are close or higher than the modern value, while temperature is cooler than present.

326

327 **Table 2. Description of the pollen zones identified through CONISS cluster analysis, including the**
 328 **main characteristics of their pollen assemblage and associated climate reconstructions.**

329



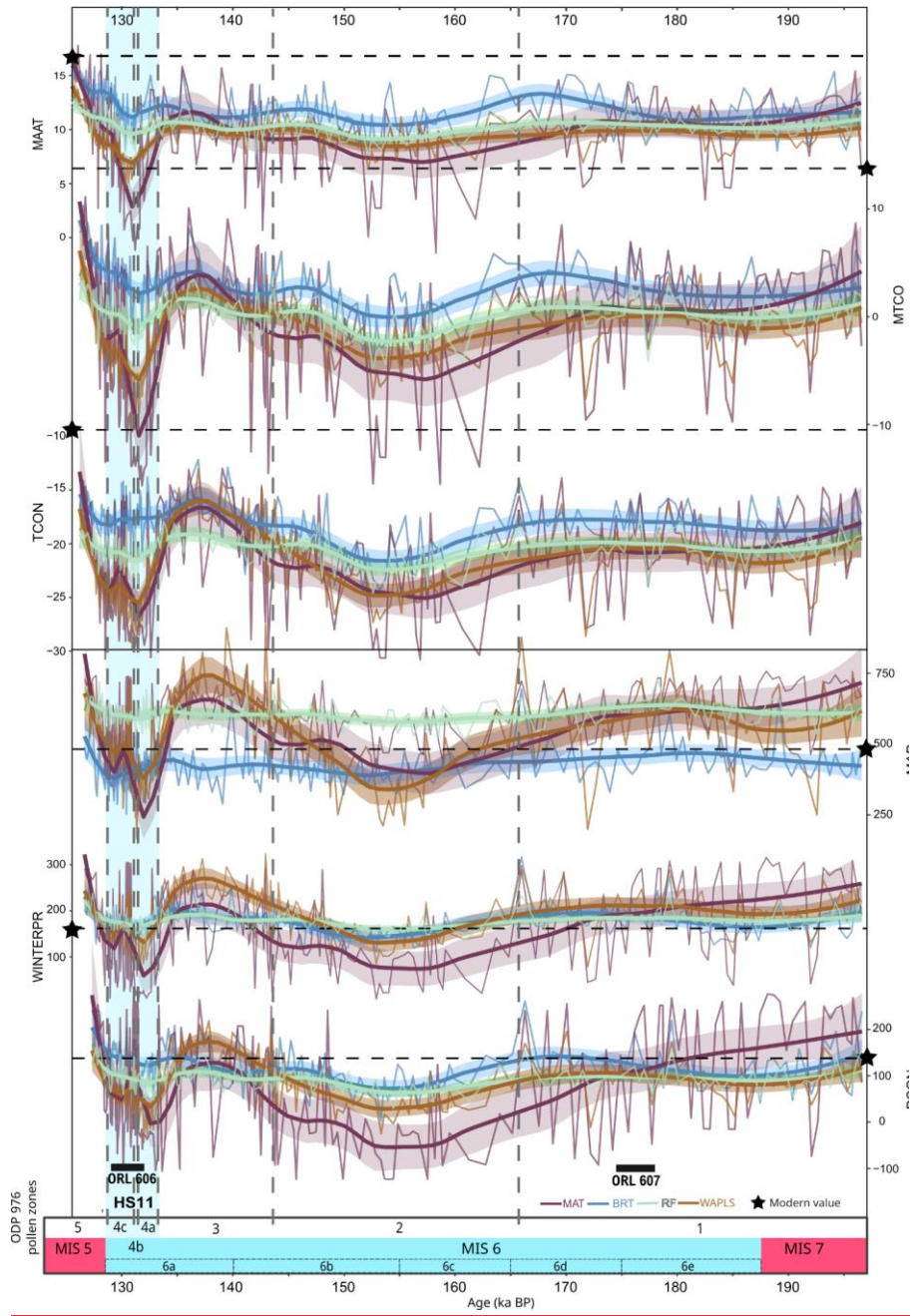
330 **Fig. 4. *Limacina retroversa* specimen found in sample B6H4 130-132** (identification: Jeanne Rampal personal communication, 2023). Photo: Dael Sassoon.

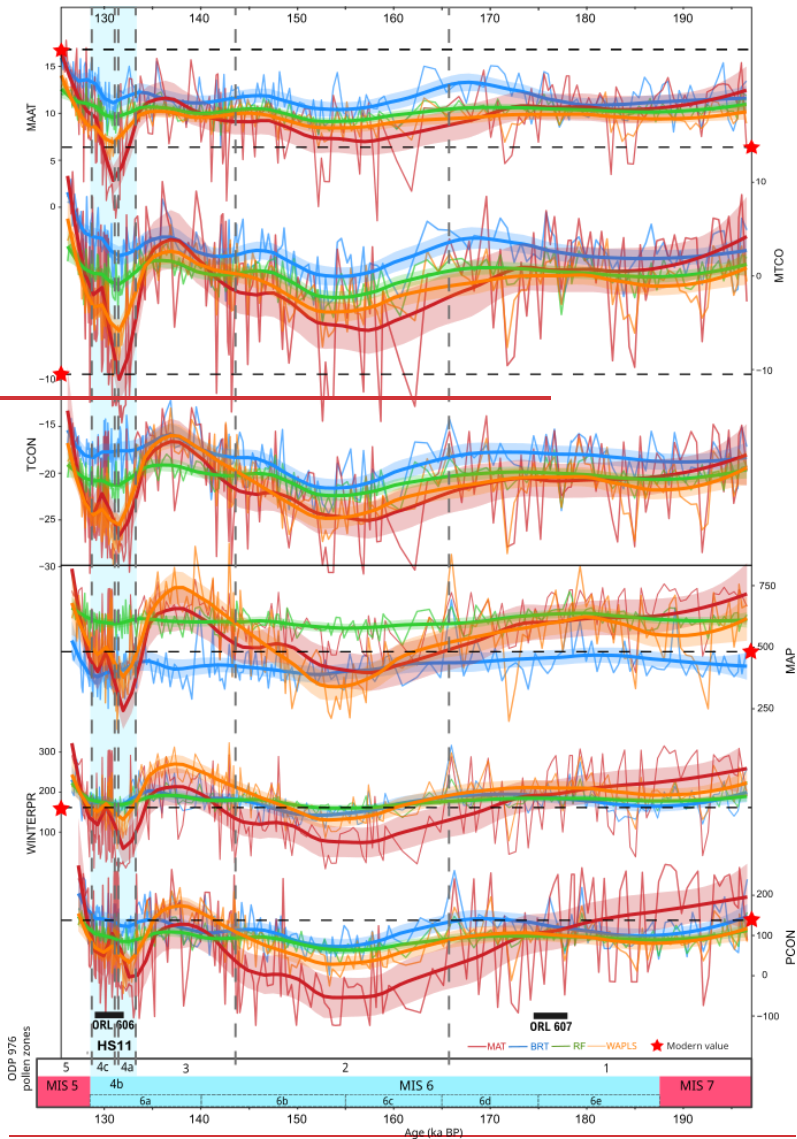
331 4.2. Pollen-inferred climate reconstructions

332 Results show significant temperatures and precipitation variations in connection with the
333 glacial / interglacial cyclicality and shorter-term variability (Fig. 5, Table 2). The most reliable methods
334 according to the two R^2 and RMSE indicators are MAT and BRT, and the most accurately reconstructed
335 parameters are MAAT and MTCO (Table 3). The four methods are in agreement for the general trends,
336 although MAT shows the widest amplitude of variations, and RF has the smoothest curve.

337 Temperatures are lower than the present ~~all along during the complete~~ MIS 6 interval, except
338 at the onset of MIS 5. A cooling trend is reconstructed during the final stage of MIS 7 (pollen zone 1,
339 MIS 6e and 6d), while MTCO and the seasonal temperature contrast (TCON) are stable. The methods
340 do not agree on the precipitation patterns during this phase, with MAT showing a trend toward aridity,
341 decreasing WINTERPR and seasonal precipitation contrast (PCON), while the three other methods
342 display a slight precipitation increase and stable PCON. From 166 ka BP onward (pollen zone 2, MIS 6c
343 and 6b), both temperatures and precipitation decrease, and the seasonal contrast between winter and
344 summer climate conditions reduced progressively. The MIS 6 minimum temperatures and precipitation
345 are reconstructed in pollen zone 2 between around 150 and 160 ka BP, corresponding to the transition
346 between MIS 6c and 6b. Subsequently, both temperatures and precipitation increase progressively in
347 the late pollen zone 2 and early pollen zone 3 (MIS 6b to 6a). Between 140-135 ka BP (early MIS 6a),
348 the four methods reconstruct temperatures similar to late MIS 7, a seasonal contrast close to the
349 present, and precipitation higher than the present (except for BRT). This climate optimum is abruptly
350 interrupted by the HS11 extreme arid event between ~134 and ~129 ka BP (pollen zone 4, late MIS 6a),
351 during which temperatures, precipitation and seasonal contrasts are significantly reduced, reaching
352 climate conditions similar to the MIS 6 glacial maxima ~155 ka BP. A short climate amelioration is
353 evidenced at ~132 ka BP (pollen zone 4b), where precipitation and seasonal contrasts increase
354 abruptly. Finally, after 130 ka BP the climate amelioration toward the MIS 5 interglacial conditions
355 happens very fast (pollen zone 5).

356





357 **Fig. 5. Pollen-based climate reconstructions for MIS 6 interval from the ODP 976 record.** MAAT (Mean
 358 Annual Temperature), MTCO (Mean Temperature of the Coldest Month), TCON (Temperature
 359 Contrast, see methods), MAP (Mean Annual ~~Precipitations~~Precipitation), WINTERPR (Winter
 360 ~~Precipitations~~Precipitation) and PCON (Precipitation contrast, see methods) for the four different
 361 methods applied: MAT (Modern Analogue Technique), WA-PLS (Weighted Averaging Partial Least
 362 Square), BRT (Boosted Regression Trees) and RF (Random Forest). The light-coloured interval
 363 represents the 95% confidence window, and the bold curves the loess smoothed values ($\alpha = 0.25$).
 364 Modern values (see methods)- are indicated by the horizontal dashed line and the ~~red-black~~ star. Grey
 365 vertical dashed lines separate the pollen zones defined by CONISS cluster analysis.

366

	BRT		MAT		WA-PLS		RF	
	R ²	RMSE	R ²	RMSE	R ²	RMSE	R ²	RMSE
MTCO	0.87	2.96	0.88	3.19	0.71	4.44	0.77	3.88
MAAT	0.83	2.31	0.83	2.48	0.66	3.22	0.69	3.00
SUMMERPR	0.77	44.86	0.82	46.61	0.52	66.87	0.65	56.48
MAP	0.77	148.52	0.79	163.70	0.50	225.68	0.66	182.32
MTWA	0.76	2.25	0.79	2.33	0.53	3.16	0.61	2.81
WINTERPR	0.69	60.69	0.72	65.81	0.43	82.58	0.59	69.34

a mis en forme : Police :Gras

a mis en forme : Police :Gras

a mis en forme : Police :Gras

a mis en forme : Police :Gras

367

368 **Table 3. R² (coefficient of determination) and RMSE (Root Mean Square Error) values for the different**
 369 **climate parameters reconstructed with the four methods applied.** The lower the RMSE and the higher
 370 the R² (in bold), the more reliable the reconstruction.

371

372 5. Discussion

373 5.1. Paleoenvironment of MIS 6 and Termination II in the western Mediterranean

374 Important changes are recorded during MIS 6, that are consistent with orbital-scale variability
 375 during the different glacial substages ~~and with D-O like dynamics.~~

376 Three phases can be discerned. The early phase (pollen zone 1) spans late MIS 7, MIS 6e and
 377 6d (~196-166 ka) and is characterized by high percentages of deciduous *Quercus*, *Cedrus* and
 378 Cichorioideae, with marked variability and several abrupt semi-desert and steppe increases under cool
 379 and humid climate conditions, with seasonal contrast similar to present-day. The middle phase (pollen
 380 zone 2) extends from MIS 6c to late 6b (~165-143 ka), and displays the maximum expansion of steppe
 381 and semi-desert taxa together with very low temperatures and precipitation between ~160 and ~150
 382 ka BP, a chronology compatible with the maximum Drenthe ice advance (Ehlers et al., 2011). Finally,
 383 the late phase (pollen zone 3), spanning late MIS 6b and 6a (~143-133 ka), is marked by a major
 384 expansion of Ericaceae vegetation associated with higher reconstructed precipitation and winter
 385 temperatures, as well as enhanced seasonal contrast during this phase.

386 Previous studies are consistent with a subdivision of MIS 6 is traditionally divided into three
 387 phases characterized by different general trends and amplitude of millennial-scale oscillations
 388 (Margari et al., 2014; Nehme et al., 2020). Margari et al. (2014) described an early phase between 185
 389 and 160 ka BP, with warmer and wetter conditions and important rapid climate variability, a middle
 390 transitional phase between 160 and 150 ka BP, and a late phase with stable glacial conditions between
 391 150 and 135 ka BP. This three-phasing for MIS 6 glaciation matches our interpretation of ODP 976
 392 pollen zones 1, 2 and 3.

393

394

395

396

397

398

399

400

401

402

403

404

405

406

407

408

409

410

411

412

413

414

415

416

417

418

419

420

421

422

423

424

425

a mis en forme : Espace Avant : 12 pt

a mis en forme : Non Surlignage

The final phase of MIS 6 is characterized by important changes in vegetation and climate, indicating a rapid ~~reorganization—modification~~ of vegetation communities and atmospheric configuration at the transition between MIS 6 and MIS 5. Termination II (TII), defined as the period of fast reorganization of the climate system from full glacial (MIS 6) to full interglacial (MIS 5) conditions, is indeed characterized by extreme and fast internal dynamics including a major Heinrich Stadial, HS11 (Broecker & Henderson, 1998; Gouzy et al., 2004; Martrat et al., 2014; Moseley et al., 2015; Ovsepyan & Murdmaa, 2017). The ~~t~~ timing for TII has been estimated based on the initialisation and termination of Weak Asian Monsoon evidenced in the Dongge cave speleothems, lasting from ~136 to 129 ka BP (Bajo et al., 2020; Kelly et al., 2006; Menviel et al., 2019). These boundaries for TII give a total duration of about 7 ka. The timing of TII in the ODP 976 marine record is directly dependent on the Dongge Cave chronology (see methods, section 3.1). Approximately the same duration is observed in the ~~Alboran Sea~~ vegetation response to TII, but with ~1 ka delay; ~~the~~ the imprint of HS11 on the vegetation in the Western Mediterranean region is indeed recorded here between 133.3 – 128.8 ka BP (pollen zone 4). This delay in marine and terrestrial proxies may reflect the vegetation response to the first cold pulse of HS11. ODP 976 provides for the first time a very detailed record of vegetation successions during this arid event (pollen zones 4a, 4b and 4c), in agreement with other SSTs and speleothem records that depict a three-phases or “double-UW” pattern for the event (see section 56.4). After the first rapid increase of steppe and semi-desert taxa (pollen zone 4a), the middle phase shows an abrupt decrease of steppe and semi-desert vegetation, and a fast increase of montane trees (mainly *Cedrus*) percentages (pollen zone 4b). Climate reconstructions reflect this event through a fast increase of both precipitation and temperatures. This pattern is fully compatible with the ODP 976 SSTs trend (Jiménez-Amat and Zahn, 2015; Martrat et al., 2014), although a delay of about 1 kyr is observed between the abrupt drop in alkenone-based SSTs at the onset of HS11 and the expansion of steppe and semi-desert vegetation. ~~In~~ the same way, the abrupt sea surface warming in the middle of HS11 (~133 ka BP) is shifted in the pollen record, to around 131.5 ka BP (pollen zone 4b).

5.2. Atmospheric-Hydroclimate connection with ORLs deposition during MIS 6

Pollen analyses help us to characterize the processes behind Organic Rich Layers (ORLs) deposition in this western Mediterranean region. Like sapropels, ~~they~~ ORLs reveal important changes in the water stratification and circulation, with reduced bottom water ventilation and enhanced organic productivity in straight-direct connection with (i) increase in the freshwaters Atlantic inflow at times of deglaciation and (ii) enhanced rivers runoff regionally linked with increased precipitation (Murat, 1999; Pérez-Asensio et al., 2020; Rogerson et al., 2008). Although they are often considered as “ghost

426 sapropels”, their timing and the mechanism behind them may differ from those of Eastern
427 Mediterranean sapropels (Rogerson et al., 2008).

428 ORL bed 607 coincides with a period of enhanced precipitation around 176 ka reconstructed
429 through our pollen-based approach (Fig. 7). Its basis appears almost synchronous with the onset of
430 Sapropel S6 layer deposition in the Eastern Mediterranean (Emeis et al., 2003; Rohling et al., 2015;
431 Savannah et al., 2024). Its duration also appears shorter than Sapropel S6, possibly indicating an
432 interruption of favourable climate conditions in the Western Mediterranean region by a stadial event
433 occurring around 172 ka BP and marked by an abrupt decrease in precipitation (Fig. 7).

434 ORL bed 606 was deposited during the second half of Termination II, at a time of deglaciation and
435 directly following the first aridity pulse of HS11. Pollen-based reconstructions show enhanced
436 precipitation and seasonal contrast during this time, suggesting intense precipitation together with
437 deglacial freshwater input as combined causes for ORL deposition in the Western Mediterranean,
438 which finds no counterpart in the Eastern Mediterranean. The implications of such organic layer
439 deposition occurring at times of enhanced ~~precipitations~~precipitation or deglaciation will be further
440 discussed in section 6.2.6.4.

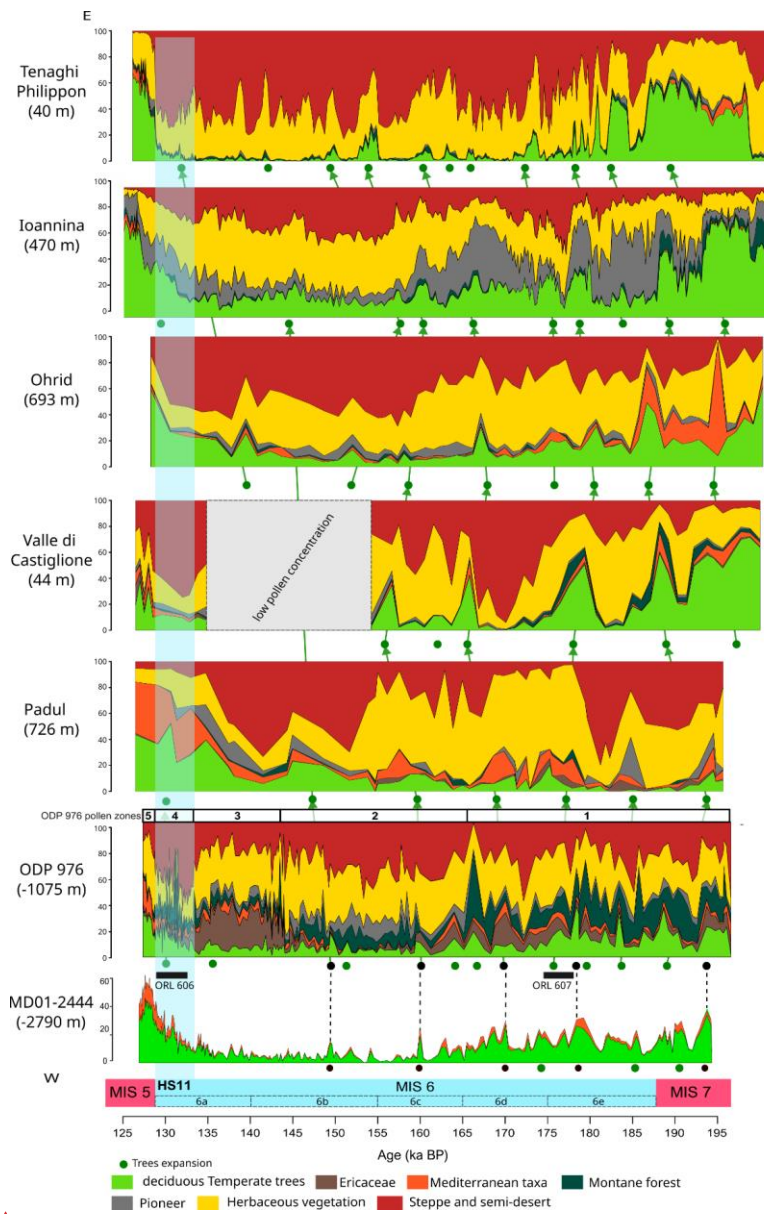
441 5.3. Mediterranean vegetation changes during the penultimate glaciation: a 442 synthesis

443 The ODP 976 pollen record documents MIS 6 vegetation changes in the Western
444 Mediterranean with a temporal resolution comparable to the most detailed terrestrial palynological
445 sequences from the Eastern Mediterranean (Tenaghi Philippon and Ioannina). ~~This~~A W-E transect of
446 Mediterranean palynological records offers valuable insights on the spatial pattern of vegetation
447 changes during the penultimate glaciation (Fig. 6).

448 At the MIS 7-6 transition, no abrupt decline of temperate forest is recorded in the ODP 976 and
449 Padul records, in contrast with central and Eastern pollen records such as Tenaghi Philippon, Ioannina,
450 Ohrid and Castiglione where the transition is very abrupt (Follieri et al., 1988; Koutsodendris et al.,
451 2023; Roucoux et al., 2011; Sadori et al., 2016). ~~At these sites, a higher contrast has been described
452 between interglacial periods with very high percentages of temperate deciduous forest taxa and glacial
453 periods with very reduced tree cover (Tzedakis, 1993; Tzedakis et al., 2006). The western
454 Mediterranean region, at the contrary, was generally characterized by a high proportion of herbaceous
455 taxa, even during interglacial periods, attenuating the vegetation contrasts during transitions to glacial
456 periods. This difference is probably linked with the lower percentages of deciduous forest in the
457 Western Mediterranean region.~~

a mis en forme : Anglais (Royaume-Uni)

458 The first half of MIS 6 (~185-165 ka BP) is marked by relatively high percentages of arboreal
459 pollen across all records, especially deciduous forest (Roucoux et al., 2011; Margari et al., 2010, 2014).
460 The abundance of montane taxa (mainly *Cedrus*) is characteristic of ODP 976 record, and reflects the
461 development of altitudinal trees on the Moroccan Rif-mountains. Montane elements also increase
462 during early MIS 6 at Valle di Castiglione, mainly represented by *Fagus* and *Abies* (Follieri et al., 1988),
463 and at Ioannina, mainly represented by *Pinus* (Roucoux et al., 2011). No equivalent pattern is recorded
464 in Padul where herbaceous vegetation is largely dominant. The scarcity of palynological data from the
465 western Mediterranean, especially from North Africa, limits our understanding of the spatio-temporal
466 significance of *Cedrus* expansions during MIS 6, and past glaciations in general.



a mis en forme : Anglais (Royaume-Uni)

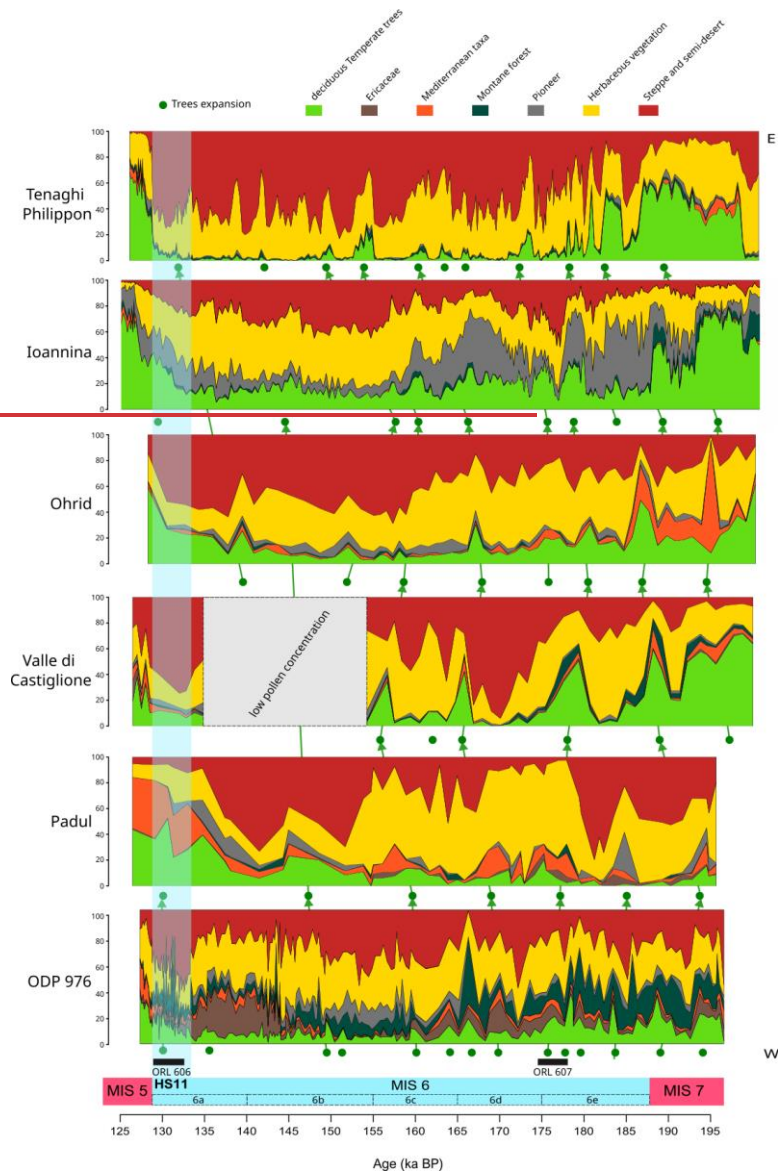


Fig. 6. Synthesis of vegetation changes in the Mediterranean during MIS 6 based on available palynological sequences, from west (bottom) to east (top): MD01-2444 (Margari et al., 2010; Tzedakis et al., 2018), from east (top) to west (bottom): ODP 976 (this study), Padul (Camuera et al., 2019), Valle di Castiglione (Follieri et al., 1988), Ohrid (Sadori et al., 2016), Ioannina (Roucoux et al., 2011), Tenaghi Philippon (Koutsodendrīs et al., 2023). Each synthetic pollen diagram is plotted according to its own age model. ODP 976 and Ioannina's chronologies are based on alignment with MD01-2444 temperate pollen curve on AICC2012 timescale. The ecological groups are the same as for ODP 976, except *Pinus* was included in pioneer vegetation at Ioannina, as it is the only record

Code de champ modifié

where *Pinus* is not over-represented. Green dots indicate temperate vegetation increases, with tentative correlations between records. The two Organic Rich Layers (ORLs) identified in the ODP 976 core (Murat, 1999), were placed at the bottom.

a mis en forme : Police :Italique

The main phase of steppe and semi-arid vegetation is recorded between ~165-145 ka BP in the Alboran Sea record, consistent with Ohrid and Ioannina pollen sequences (Fig. 6.6 Fig. 6). In Padul, however, the maximum expansion of steppe and semi-desert taxa occurs later, between ~155 and ~137 ka BP. This time window corresponds to the glacial maximum recorded at Azzano X (northern Italy) between 148 and 135 ka BP (Pini et al., 2009), and to a period of low pollen concentration at Valle di Castiglione, likely reflecting full glacial conditions. The ~10 ka lag in the vegetation glacial maxima between ODP 976 and Padul is probably the result of the low temporal resolution of the latter, in addition to differences in the age models used. However, the presence of pioneer vegetation and to a lesser extent of montane elements in Padul during the maximum glacial phase matches the ODP 976 pattern in pollen zone 2, where Cupressaceae and *Cedrus* display high abundance.

A distinctive feature of the Western Mediterranean vegetation recorded during the final stage of MIS 6 (pollen zone 3) is the marked increase in Ericaceae observed in the ODP 976 record, and whereas Ericaceae are almost absent in the rest of the Mediterranean region. A similar expansion is observed in the Atlantic margin, where core MD01-2444 recorded patterns of Ericaceae expansion matching the three insolation minima during MIS 6 (Margari et al., 2014). Ericaceae development during minimal summer insolation is particularly favoured by reduced summer evaporation at times of low seasonal contrast in precipitation, as already noted in the Alboran Sea during the last glacial (Fletcher and Sánchez Goñi, 2008). Following the same interpretation, the expansion of heathland vegetation in the Iberian Peninsula as recorded in ODP 976 during the final stage of MIS 6 therefore marks the renewed influence of westerlies and Atlantic moisture preceding the onset of the transition to MIS 5 interglacial (Margari et al., 2014). Supporting this interpretation, an increase in temperate deciduous forest at the end of MIS 6 is also seen in Padul, Ohrid and Ioannina records before the transition to MIS 5.

a mis en forme : Anglais (Royaume-Uni)

Despite some discrepancies due to the differences in age models and temporal resolutions, all records display comparable variations in temperate pollen percentages during the penultimate glacial. These variations support the persistent sensitivity of Mediterranean plant ecosystems to global-scale millennial climate variability during the penultimate glaciation, with modulation of the vegetation response depending on the local geography. Strong similarities can be observed between ODP 976 and Padul, despite the lower temporal resolution of Padul record. In both sequences, temperate pollen percentages reached ~25-30% of total pollen as a maximum during the rapid forest expansions events in the first half of MIS 6. This similarity supports the validity of the ODP 976 marine record to

498 reconstruct the SW Iberian Peninsula temperate forest history. However, ODP 976 sequence provides
499 a more regional image of the vegetation, including higher percentages of Ericaceae pollen coming from
500 the Atlantic coast, and *Cedrus* pollen from the Moroccan ~~Rif~~ mountains (Jiménez-Moreno et al., 2020),
501 compared to Padul where percentages of Mediterranean taxa and hygrophyte herbaceous are higher
502 due to the local nature of the signal (Camuera et al., 2019). Looking further east, Valle di Castiglione
503 recorded various temperate trees expansions and contractions during the lower MIS 6, before the full
504 glacial conditions. In the Italian Peninsula, various interstadials have also been identified further north
505 at Azzano X (Pini et al., 2009). In the Balkans, Tenaghi Philippon shows the highest percentages of semi-
506 desert and herbaceous vegetation ~~aeross-throughout~~ MIS 6, with more abrupt changes than all the
507 other Mediterranean records, and more amplitude of the trees' contractions. This pattern was already
508 described during the last climatic cycle and reflects the exacerbated vegetation dynamics locally, with
509 episodes of rapid and enhanced colonization by tree vegetation ~~and probably linked with the lower~~
510 altitude of the site (Koutsodendris et al., 2023; Tzedakis, 2005; Tzedakis et al., 2004). This has been
511 mainly explained by the location of the site in a low altitudinal plain characterized by a more
512 continental climate with lower winter precipitation; tree populations at lower altitudinal location are
513 closer to their ecological threshold in term of precipitation, and are likely to be very affected even by
514 minimal changes in the amount of rainfall. On the contrary, the Ioannina record shows the highest
515 deciduous forest percentages of all the records presented here, supporting its character as a local trees
516 refugium (Roucoux et al., 2011).

a mis en forme : Anglais (Royaume-Uni)

517 Termination II displays a particular pattern in vegetation records from the Mediterranean
518 region: while the expansion of trees and temperate vegetation is fast and continuous, HS11 represents
519 at the same time a remarkable episode of abrupt steppe and semi-desert expansion. Although this
520 event is visible in almost all the records, it is particularly prominent in the ODP 976 record (pollen zone
521 4), and appears less pronounced in the eastern Mediterranean sequences. This observation is
522 compatible with previous observations that Heinrich stadials during the last glacial had a minor impact
523 on the eastern Mediterranean vegetation compared to the western Mediterranean, likely due to the
524 already limited presence of tree vegetation in the eastern records during glacials (Tzedakis, 2005). A
525 similar interpretation can be proposed for the differential response of eastern and western
526 Mediterranean vegetation to HS11, supporting the major sensitivity of the southwestern
527 Mediterranean vegetation to North Atlantic cold events. In Padul, no major expansion of xerophyte
528 vegetation is detected, but a small decrease of temperate deciduous taxa was interpreted as the HS11
529 imprint (Camuera et al., 2019), and the signal might be hindered by the low resolution of the record.
530 A pattern of fast arid vegetation increase contemporaneous to the temperate forest expansion is also

a mis en forme : Anglais (Royaume-Uni)

531 found in central Italy at Lago Grande di Monticchio, which was not presented in ~~Fig. 6.6~~Fig. 6 as its
532 record does not extend beyond 132 ka BP (Allen and Huntley, 2009; Brauer et al., 2007).

a mis en forme : Anglais (Royaume-Uni)

533 ~~To sum up~~Finally, all palynological sequences reveal high-frequency oscillations of temperate
534 and semi-desert pollen, compatible at first look with DO-like variability based on their duration and
535 intensity with DO-like variability. They, and which are represent a particularly distinctive feature of the
536 lower part of MIS 6.

537 5.4. Rapid climate variability during MIS 6: a regional multiproxy comparison

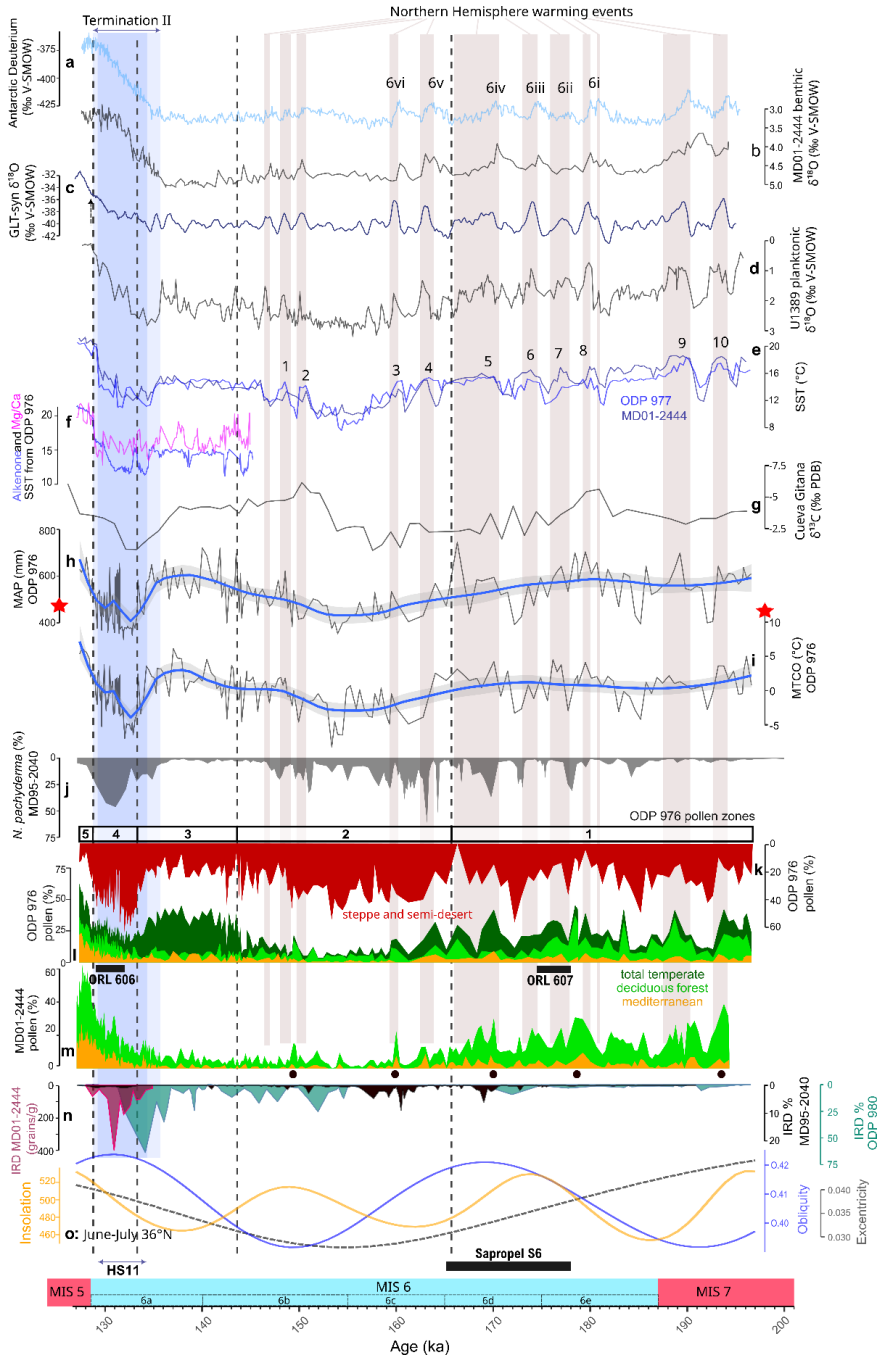
538 In order to ~~disentangle-investigate~~ the character of rapid climate variability during MIS 6, a
539 comparison with regional and global climatic archives is essential. The ~~events of increases in~~arboreal
540 pollen ~~increase~~ observed in the ODP 976 record ~~are show percentages and timing consistent with~~
541 comparable to those from the Portuguese margin core MD01-2444 (Margari et al., 2010, 2014;
542 Tzedakis et al., 2018) (Fig. 7, m). However, the ODP 976 record generally presents lower ~~percentages~~
543 values of temperate deciduous pollen percentages compared to the Atlantic record, due to its more
544 ~~semiarid the~~Mediterranean influence as previously evidenced for the last glacial period (Charton et
545 al., 2025; Fletcher et al., 2010b). To better capture temperate vegetation dynamics, we added
546 Ericaceae, a clear marker of Atlantic influence in the ODP 976 record, to the deciduous temperate
547 forest, to obtain a “total temperate pollen sum” which enhances the main warming peaks and
548 strengthens the correlation between the two marine cores on both sides of Gibraltar Strait (Fig. 7, m
549 and l). ~~Another striking correlation appears between the~~The ODP 976 pollen-inferred climate
550 reconstructions ~~show generally consistent patterns with~~ the SSTs trends based on alkenones (Martrat
551 et al., 2004, 2007), and the southern Iberian humidity recorded in the speleothem from data from
552 Cueva Gitana (Hodge et al., 2008) (Fig. 7, e and g). The ODP 976 pollen and climate record therefore
553 appears to reflect well regional variations in both temperature and humidity across MIS 6.

554 Warm events in the northern hemisphere are generally well-correlated to peaks in the ODP
555 976 temperate pollen curve (Fig. 7, c and l). An active bipolar seesaw dynamics was described during
556 the penultimate glacial Davtian & Bard, 2023; EPICA Community Members, 2006; Stocker, 1998), and
557 the Antarctic record was used to elaborate the Greenland GL_T-syn (Greenland temperature synthetic)
558 curve showing predicted $\delta^{18}\text{O}$ ~~D-O~~millennial-scale events for the past glacial eight climatic cycles,
559 which are not directly recorded in Greenland ice (Barker et al., 2011; Bazin et al., 2013; Jouzel et al.,
560 2007). Six Antarctic Isotopic maxima (AIM) events were recognized on the Deuterium curve during MIS
561 6 (6i to 6vi), correlated with increases in CO₂ concentrations and benthic isotope minima in the North
562 Atlantic (Barker et al., 2011; Hodell et al., 2023; Margari et al., 2010, 2014; Shin et al., 2020) (Fig. 7, a-
563 c). These AIM and benthic minima in the Atlantic are not easily correlated with steppe expansions in

564 the ODP 976 record, indicating a limited response of vegetation in the Western Mediterranean to the
565 Antarctic warm events.

566 Barker et al. (2011) predicted the occurrence of eleven ~~millennial-scale warming events~~ ~~events~~
567 ~~events~~ during MIS 6 (Fig. 7, c), while nine interstadials were recognized in the Alboran Sea from the
568 alkenone record (Fig. 7, e). (Martrat et al., 2004, 2007). In the loess record of Harletz in central Europe,
569 ten interstadials were described (Rousseau et al., 2020), strongly matching the Chinese speleothems
570 records of stadial and interstadial events related to the Asian Monsoon dynamics (Cheng et al., 2006;
571 Li et al., 2014; Wang et al., 2018; Wang et al., 2001; Xue et al., 2019). The global nature of fast climate
572 oscillations in the northern hemisphere thus appears controlled by the coupled influence of Atlantic
573 cold events, and tropical monsoon variations as evidenced by the eastern Mediterranean speleothems
574 records from Sofular, Soreq and Kanaan caves (Ayalon et al., 2002; Held et al., 2024; Matthews et al.,
575 2021; Nehme et al., 2018).

576



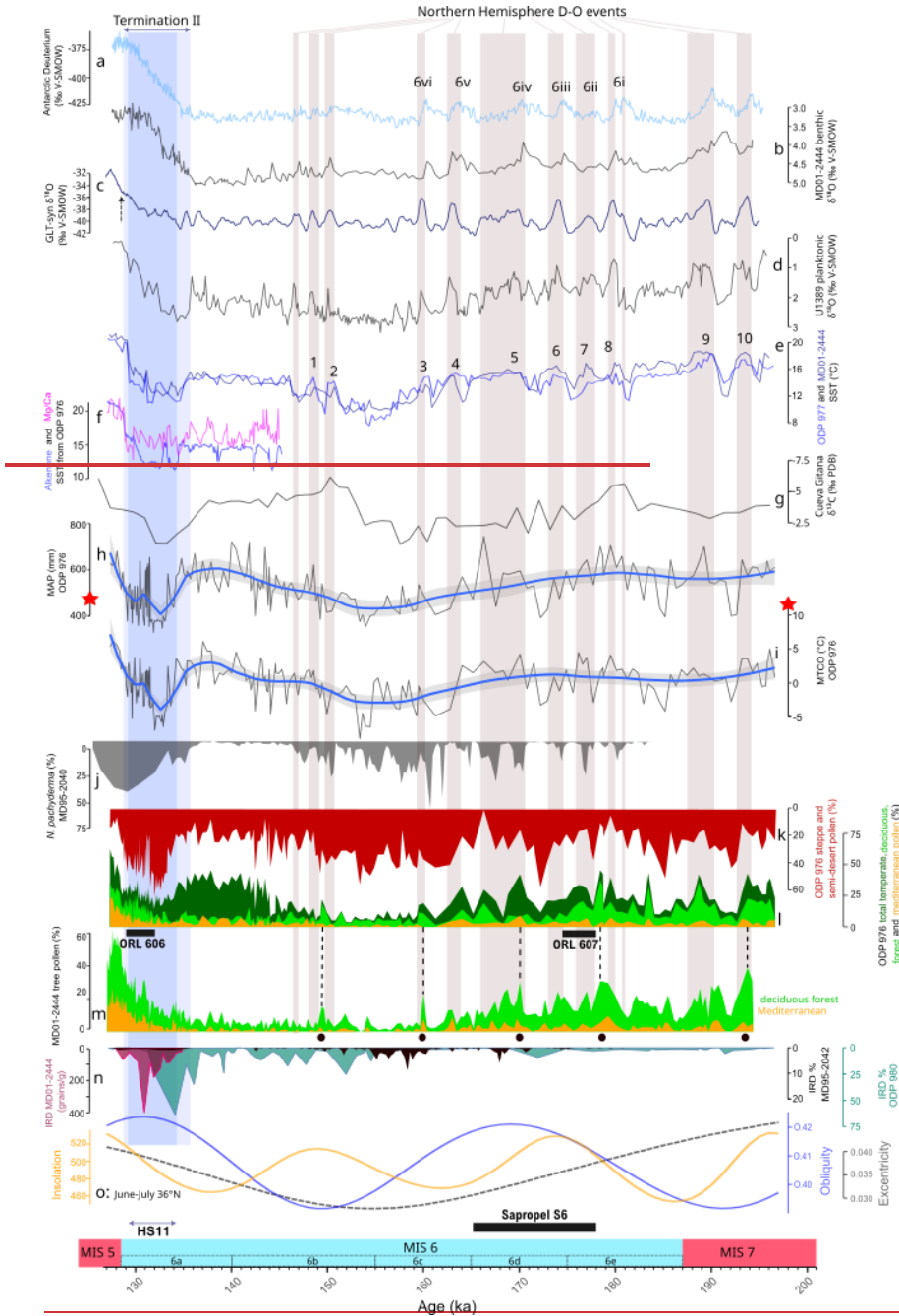


Fig. 7. Millennial-scale climate changes during MIS 6. a) Antarctic Dome C δD (Bazin et al., 2013; Jouzel et al., 2007); **b)** Benthic $\delta^{18}O$ from MD01-2444 (Margari et al., 2010); **c)** Greenland synthetic

Code de champ modifié

$\delta^{18}\text{O}$ (Barker et al., 2011); **d**) Planktonic $\delta^{18}\text{O}$ from U1389 (Sierra & Andersen, 2022); **e**) alkenone-based SST from ODP 977 (darker blue) and MD01-2444 (lighter blue) (Martrat et al., 2004, 2007); **f**) Alkenone-based SST (Martrat et al., 2014) and Mg/Ca-based SST (Jiménez-Amat and Zahn, 2015) from ODP 976; **g**) $\delta^{13}\text{C}$ from Cueva Gitana (Hodge et al., 2008); **h**) Mean Annual Precipitation (MAP) reconstructed from ODP 976 pollen assemblage, mean of the four methods used in this study (MAT, WA-PLS, RF, BRT), with the red star showing the modern value; **i**) Mean Temperature of the Coldest Month (MTCO) reconstructed from ODP 976 pollen assemblage, mean of the four methods used in this study (MAT, WA-PLS, RF, BRT), with the red star showing the modern value; **j**) *N. pachyderma* percentages from MD95-2040 (de Abreu et al., 2003; Voelker & de Abreu, 2011); **k**) ODP 976 pollen percentages of semi-desert and steppe taxa, with ODP 976 pollen zones (this study); **l**) ODP 976 pollen percentages of total temperate taxa including temperate deciduous forest + Ericaceae + Mediterranean (dark green), deciduous forest (light green), Mediterranean (orange) (this study); **m**) MD01-2444 pollen percentages of temperate tree (light green) and Mediterranean (orange) taxa (Margari et al., 2010; Tzedakis et al., 2018); **n**) Ice-Rafted Debris (IRD) percentages from MD01-2444, 37° N (pink) (Skinner & Shackleton, 2006) redrawn from Tzedakis et al. (2018), MD95-2040 (red/black), 40°N (de Abreu et al., 2003) and ODP 980 (blue), 55°N (McManus et al., 1999; Oppo et al., 2001, 2006); **o**) orbital parameters (Laskar et al., 2004) calculated for June-July at 36°N: Eccentricity (black), Obliquity (blue) and Insolation (yellow). The black rectangle indicates the interval of deposition of Sapropel layer S6 in the eastern Mediterranean (Ziegler et al., 2010). The marine substages MIS 6a-e follow (Railsback et al., 2015). All data are plotted on AICC2012 chronology (Bazin et al., 2013) following Sierra et al. (2020, 2022), except for the IRD records and Gitana Cave which is plotted on its own age model based on U-series absolute dating. The vertical grey bars indicate the Northern Atlantic interstadial events based on the planktonic isotope record and the predicted millennial-scale warming $\delta^{18}\text{O}$ -events from Greenland synthetic record, with the numbers of the Alboran interstadials (AI-1 to AI-10) from Martrat et al. (2004, 2007). Numbers 6i-6vi correspond to the Antarctic Isotope Maxima (AIM) from Margari et al. (2010). The vertical blue bar represents Heinrich Stadial 11 (HS11). Black dots and dotted lines show the five temperate pollen peaks in MD01-2444 used as control points for ODP 976 chronology.

MIS 6 is traditionally divided into three phases characterized by different general trends and amplitude of millennial scale oscillations (Margari et al., 2014; Nehme et al., 2020). Margari et al. (2014) described an early phase between 185 and 160 ka BP, with warmer and wetter conditions and important rapid climate variability, a middle transitional phase between 160 and 150 ka BP, and a late phase with stable glacial conditions between 150 and 135 ka BP. This three phasing for MIS 6 glaciation matches our interpretation of ODP 976 pollen zones 1, 2 and 3.

The three phases identified during MIS 6 based on the ODP 976 vegetation and climate record can be compared with regional and global records to be interpreted in a broader context, based on general climatic trends and the expression of climatic instability;

Early MIS 6 (187-166 ka BP): warm/wet conditions and instability. The first phase encompasses the two substages MIS 6e and 6d, and is characterized by humid and rather warm climate conditions in the Mediterranean at the transition from MIS 7 to MIS 6. This phase aligns well with the deposition of ORL bed 607 in the Alboran Sea, and the sapropel layer S6 in the Eastern Mediterranean, associated with the maximum summer insolation and increased intensification of the summer monsoonal system

a mis en forme : Non souligné

a mis en forme : Non souligné

a mis en forme : Non souligné

592 in the eastern Mediterranean between 178.5 to 165.5 ka (Emeis et al., 2003; Rohling et al., 2015;
593 Ziegler et al., 2010). At the same time of S6 deposition, Cheddadi and Rossignol-Strick (1995) described
594 an increase in temperate pollen in the Nile region, and Soreq cave speleothem records climatic
595 conditions typical of an interglacial (Ayalon et al., 2002). Sapropel depositions usually occur during
596 interglacial periods as MIS 1 (Holocene), which makes sapropel S6 an exceptional feature of early MIS
597 6. It reflects particularly warm and humid conditions, and intense freshwater input in the
598 Mediterranean which can result from various sources, including increased rainfall and monsoon
599 activity, Atlantic freshwater entrance, and enhanced river discharges (Sierra & Andersen, 2022). The
600 long speleothem records in China report a period of northern shift of the Intertropical Convergence
601 Zone associated with enhanced Asian Monsoon activity during this phase (Wang et al., 2018). Higher
602 pluviometry is also supported by foraminifera isotopic and SSTs signal throughout the Mediterranean
603 Sea, which were used to reconstruct past salinity and freshwater budget regionally (Kallel et al., 2000).
604 Enhanced rainfall in the Balkans is evidenced by the Ioannina lake deepening (Wilson et al., 2021), and
605 a more humid period is documented in speleothem records from Argentarola cave in Italy (Bard et al.,
606 2002) and Gitana cave in southern Spain (Hodge et al., 2008) (Fig. 7, g). Therefore, humid conditions
607 during this phase were not restricted to the eastern Mediterranean where the sapropel deposition
608 occurred. ODP 976 organic layer 607 together with the pollen-based climate reconstructions support
609 this view, with enhanced seasonal precipitation contrast during this interval driven by enhanced winter
610 precipitationsprecipitation (Fig. 5). Comparison with Padul pollen-based hydroclimate reconstructions
611 (Camuera et al., 2022) further strengthens this scenario: despite the chronological delay between the
612 two sequences, this early MIS 6 humid phase and ORL deposition likely matches the Western
613 Mediterranean Humid Period (WMHP 6) dated between 180-155 ka BP (Fig. 8). The same study made
614 the case for a co-occurrence of humid periods in the Western Mediterranean and in West Africa
615 (African Humid Periods) during periods of high precipitationsprecipitation seasonality and enhanced
616 West African Monsoon. Pollen-inferred climate reconstructions from lake Ohrid have also shown the
617 phase relationship between African Monsoons and periods of high winter precipitationsprecipitation
618 in the Mediterranean region (Wagner et al., 2019; Sinopoli et al., 2019).

619 Another characteristic of this early MIS 6 phase is the strong variations in pollen and isotopic
620 curves in the Atlantic and Western Mediterranean (Fig. 7, a-d and l-m). Variations in temperate
621 deciduous and Ericaceae percentages are observed in the ODP 976 record, in close correspondence
622 with the Atlantic record from MD01-2444. The largest interstadial peak in ODP 976 around 179 ka BP
623 is also identified in all the different records and marked by warmer conditions in the sea, and more
624 effective precipitationsprecipitation in SE Iberia (Hodge et al., 2008). It is well correlated with the
625 stadial following Antarctic event 6i (Margari et al., 2010), the associated predicted millennial-scale

626 ~~warming D-O~~ event in Greenland synthetic curve, and the Alboran Sea SST interstadial event 8 (Martrat
627 et al., 2004). In Padul record, the temperate deciduous, Mediterranean and *Abies* percentages increase
628 correlates well with this event (Camuera et al., 2019). It could also match the WMHP 6.1 interstadial
629 (Camuera et al., 2022) (Fig. 8). This large interstadial was suggested to be at the origin of the
630 initialisation of the sapropel S6 deposition (Sierro & Andersen, 2022), and could also have participated
631 in the initialization of ORL 607 deposition in the Alboran Sea (Murat, 1999). On the other hand, the
632 most important tree population decline and semi-desert expansion in ODP 976 is recorded at ~172 ka
633 BP, which could match Antarctic event 6iv, and is associated to a moderate increase of IRD deposition
634 at the latitude of ODP 980 (Fig. 7, n). A similar stadial can be observed in the Ioannina and Tenaghi
635 Philippon records with a close chronology (Roucoux et al., 2011) (Fig. 6). Dry conditions at this time are
636 also recorded in the eastern Mediterranean as shown in the Pentadactylos and Soreq speleothems
637 (Ayalon et al., 2002; Nehme et al., 2018).

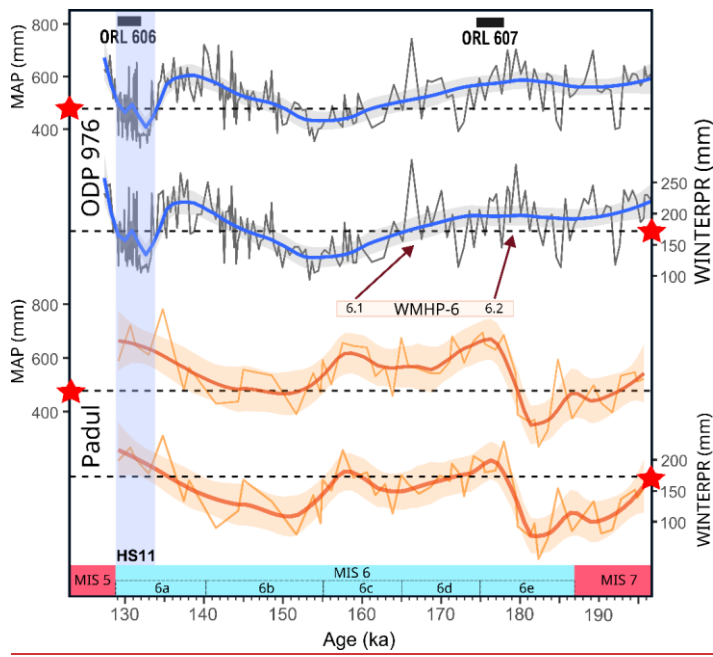
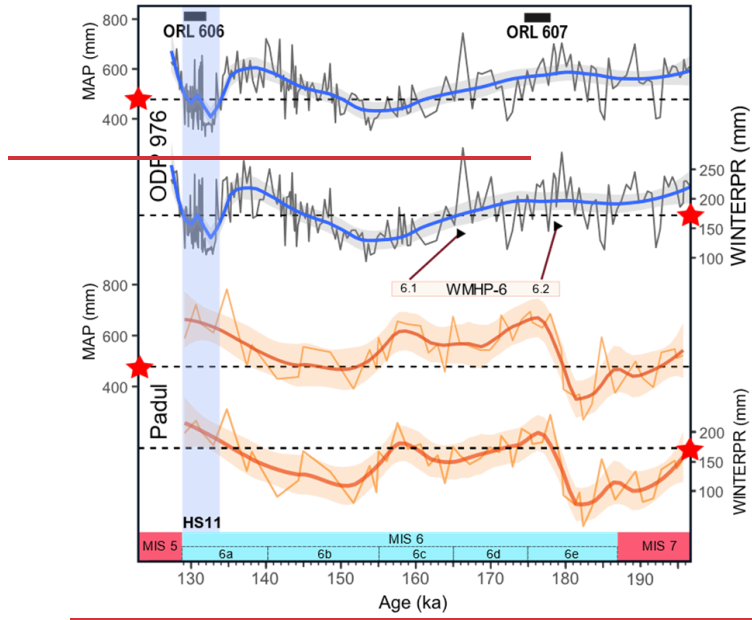


Fig. 8. Comparison between the precipitation pattern reconstructed from ODP 976 with our multi-method approach (mean) (this study) and from Padul with only the WA-PLS method (Camuera et al., 2022). Mean Annual Precipitation (MAP) and Winter Precipitation (WINTERPR) are represented, together with the two Organic Rich Layers (ORLs) identified in ODP 976 (Murat, 1999) and the Western Mediterranean Humid Period (WMHP) 6 defined by Camuera et al. (2022). Red arrows indicate tentative correlation between the two phases of WMHP 6, and the precipitation reconstructions from ODP 976. Red stars and dashed lines indicate the modern climate value (see methods).

638 Middle MIS 6 (165-144 ka BP): maximum glacial conditions and stability. This phase is marked
639 by the maximum expansion of semi-desert vegetation and the almost complete collapse of forest
640 vegetation between ~163 and 150 ka BP, according to the ODP 976 pollen and MD01-2444 records,
641 synchronous with the minimum in orbital eccentricity. This is in agreement with the lowest SSTs values
642 reconstructed in the Alboran Sea from the alkenone record occurring around 155 ka BP, and low SSTs
643 in the Gulf of Lions too (Cortina et al., 2015). At the same time, high percentages of the cold species *N.*
644 *pachyderma*, together with important ice-detritus pulses, are recorded on the Portuguese margin (de
645 Abreu et al., 2003; Voelker & de Abreu, 2011), (Fig. 7, j and n). The occurrence of the cold Atlantic
646 species *Limacina retroversa* shells in the ODP 976 sediments at ~155 ka BP is consistent with the
647 enhanced entrance of cold subpolar water masses in the Alboran sea at the time of full glacial
648 conditions. In parallel, there is an intensification of “Fleuve Manche” paleo river discharges evidenced
649 in various sedimentary cores from the Bay of Biscay (Boswell et al., 2019; Eynaud et al., 2007; Penaud
650 et al., 2009, 2016; Toucanne et al., 2009), and a fluvial aggradation linked with reduced vegetation
651 cover in Spanish river basins (Macklin et al., 2002). A long-term aridification is recorded in SE Spain in
652 Gitana cave close to the ODP 976 location (Hodge et al., 2008). The glacial maximum in Soreq cave
653 speleothem is also recorded around 154 ka BP (Bard et al., 2002), and might be responsible for the
654 hiatus in the Pentadactylos speleothem in Cyprus (Nehme et al., 2020). In Italy, the Tana che Urla cave
655 also recorded cooling and aridification between 159-132 ka BP, indicated by both the carbon and
656 oxygen isotopic ratio (Regattieri et al., 2014). The coolest phase in Abaliget Cave speleothem in central
657 Europe is also recorded at that time (Koltai et al., 2017). Climate conditions reconstructed at ODP 976
658 site during this phase show the maximum aridity and cold temperatures, which are consistent and fall
659 within the range of reconstructed temperatures and ~~precipitations~~precipitation at the same time at
660 Ohrid (Sinopoli et al., 2019). This main phase of glaciation in Europe took place after 163 ka BP,
661 corresponding to the Drenthe glacial advance (Ehlers et al., 2018; Margari et al., 2014). The maximum
662 ice expansion probably led to the almost complete collapse of temperate vegetation across the
663 Mediterranean region, except in specific climate refugia-~~s~~ like Ioannina or Padul (Fig. 6-6Fig. 6). The
664 Mediterranean vegetation taxa were particularly affected and almost disappeared at this time in the
665 ODP 976 record.

Code de champ modifié

a mis en forme : Français (France)

a mis en forme : Français (France)

666 Few interstadial events are observed during this cold and dry phase, probably due to the
667 extended ice volume reaching a critical threshold (McManus et al., 1999) and leading to higher climate
668 stability at time of glacial maximum expansion (Sierro and Andersen, 2022). One moderate interstadial
669 event around 150 ka BP is expressed in the ODP 976 and MD01-2444 records through an increase in
670 temperate deciduous tree taxa (Fig. 7, l and m). It may correspond to the interstadial recognized in
671 Gitana Cave speleothem approximately at the same time, and is compatible with the Alboran
672 Interstadial events 1 or 2 (Martrat et al., 2004), while a larger trees increase in Padul record is also
673 observed (Camuera et al., 2019) (Fig. 6). It is also compatible with interstadials recognized in other
674 speleothem records in eastern and central Mediterranean (Ayalon et al., 2002; Bard et al., 2002;
675 Regattieri et al., 2014). Sierro et al. (2022) described a major event of low Mediterranean overturning
676 and high freshwater entrance through the Gibraltar Strait at that time and contemporaneous to the
677 insolation maximum (Fig. 7, o). This configuration was similar to the one contemporaneous to sapropel
678 S6 and ORL 607 deposition during early MIS 6, but did not lead to any new sapropel deposition at 150
679 ka BP, probably because the climate conditions were more favourable but not enough for a sapropel
680 deposition.

a mis en forme : Anglais (Royaume-Uni)

Code de champ modifié

a mis en forme : Anglais (États-Unis)

681 Late MIS 6 (144-129 ka BP): increased precipitation during the last glacial, and arid conditions
682 during Heinrich Stadial 1+HS11. Between 150 and 140 ka BP, warmer and wetter conditions are
683 indicated by ODP 976 pollen percentages of Ericaceae (pollen zone 3). Ericaceae expansions in the
684 Iberian margin sediments were found to be associated to insolation minima in core MD01-2444
685 (Margari et al., 2014). This pattern is consistent with the ODP 976 Ericaceae curve (Fig. 6-7 Fig. 7, j). The
686 climate reconstructions evidenced high ~~precipitations~~precipitation and especially high WINTERPR
687 values. These higher humidity and temperature values are supported by the carbon isotope record
688 from Gitana Cave (Hodge et al., 2008) and the Alboran Sea SSTs (Martrat et al., 2007) (Fig. 7, e-g). In
689 central Europe, Abaliget Cave speleothem also shows more favourable climate conditions during this
690 phase (Koltai et al., 2017). Climatic oscillations appear subdued in the Western Mediterranean pollen
691 records during this last phase. The high resolution ODP 976 record shows some SST variations
692 (Jiménez-Amat and Zahn, 2015; Martrat et al., 2014) : Ericaceae pollen contractions and semi-desert
693 elements expansions could be correlated to three abrupt drops in alkenone-based SSTs at 144, 142,
694 and 139 ka BP (Fig. 6-7 Fig. 7, f, k and l). Fifteen Chinese Interstadials (CIS) were identified at Hulu Cave
695 during late MIS 6, linked with Asian Monsoon dynamics (Q-Wang et al., 2018), and the ultra-high-
696 resolution record of planktonic isotope ratio at U1389 by Sierro and Andersen (2022) also expresses
697 some variability. However, the vegetation response in the SW Mediterranean was apparently limited.

698 Following the Ericaceae expansion, the most prominent feature of the late MIS 6 phase is the
699 large and fast expansion of steppe and semi-desert vegetation during HS11, between 133 and 129 ka

700 BP (pollen zone 4). It is characterized by a first large IRD peak at high latitude (ODP 980) around 134 ka
701 BP, and later at the MD01-2444 latitude, around 131 ka BP (Skinner & Shackleton, 2006; Tzedakis et
702 al., 2018). This event also corresponds to an increase in the oxygen isotopic ratio at the Portuguese
703 margin (especially planktonic, starting around 136 ka BP), also broadly synchronous to an important
704 decrease in SSTs of the Atlantic and the Mediterranean Sea (Jiménez-Amat and Zahn, 2015; Martrat et
705 al., 2004, 2007, 2014). A pronounced increase in *N. pachyderma* (sinistral) abundance is also recorded
706 on the Portuguese margin (Voelker & de Abreu, 2011). Climate reconstructions show particularly harsh
707 conditions in the Western Mediterranean region during this event, compatible with the
708 reconstructions from Lake Ohrid (Sinopoli et al., 2019) and from three French sites (Les Echets, la
709 Grande Pile and Le Bouchet) for the latest phase of MIS 6 (Guiot et al., 1989, 1993). An arid phase is
710 also evidenced at Gitana Cave (Hodge et al., 2008), which closely matches the trend of the ODP 976
711 precipitation curve (Fig. 8). Aridity is evidenced in other speleothem records in Europe like Villars
712 (Wainer et al., 2011), Sieben in the Alps (Moseley et al., 2015), and Abaliget cave in central Europe
713 (Koltai et al., 2017). Dryness over western Europe is also supported by an episode of intense loess
714 deposition in Rodderberg crater in northern Germany between 136-129 ka BP (Zhang et al., 2024). If
715 HS11 is also recorded in China speleothems (Wang et al., 2018), it appears subdued in the eastern
716 palynological Mediterranean records (Fig. 6), indicating that the Western Mediterranean region was
717 more severely impacted by the dry and cold pulse of HS11. The “~~double-uW~~” shape of HS11 described
718 in section 5.1 for the ODP 976 record matches well the Hulu cave record, where the particular event
719 in the middle of HS11 was linked with a strong Asian Monsoon episode that could represent an
720 analogue to the Bølling-Allerød during Termination I (Wang et al., 2018). The fast and multiphase
721 vegetation and climate dynamics evidenced in the ODP 976 record is in agreement with the description
722 of a “HS11 complex” with multiple phases (Tzedakis et al., 2018), and will require more focused
723 attention in the future.

724 HS11 has been described as a “pause” in the glacial termination II (Gouzy et al., 2004; Hodge
725 et al., 2008). However, in the ODP 976 and MD01-2444 records, temperate vegetation keeps increasing
726 all along the event, despite the supposed cessation of the warming and moistening trend for almost
727 2000 years. Therefore, the trend toward increased temperate vegetation during Termination II did not
728 seem to be strongly affected by the abrupt arid event, following the continuous climate amelioration
729 described in various speleothem records from Italy covering Termination II, at Corchia cave, Tana che
730 Urla and Argentarola (Bard et al., 2002; Drysdale et al., 2005; Regattieri et al., 2014). On the contrary,
731 the Gitana Cave speleothem records a strong moisture deficit (Fig. 7, g), supporting a stronger impact
732 of HS11 in the SW Mediterranean compared to the Italian Peninsula.

a mis en forme : Anglais (Royaume-Uni)

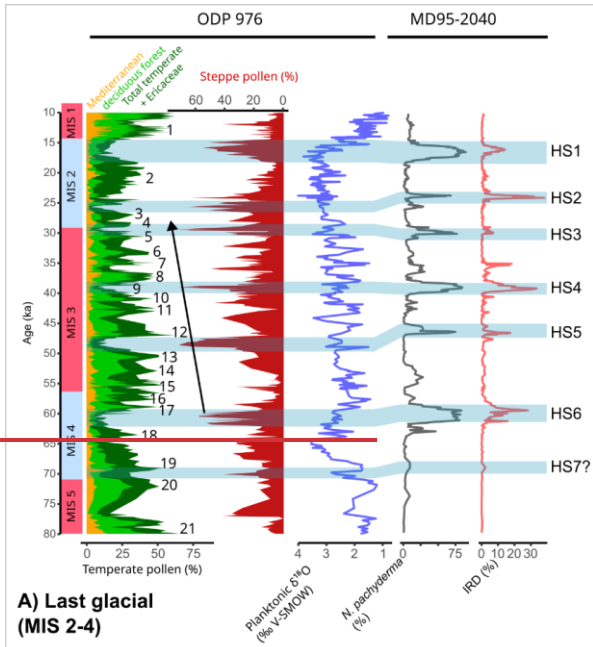
a mis en forme : Polonais

a mis en forme : Anglais (Royaume-Uni)

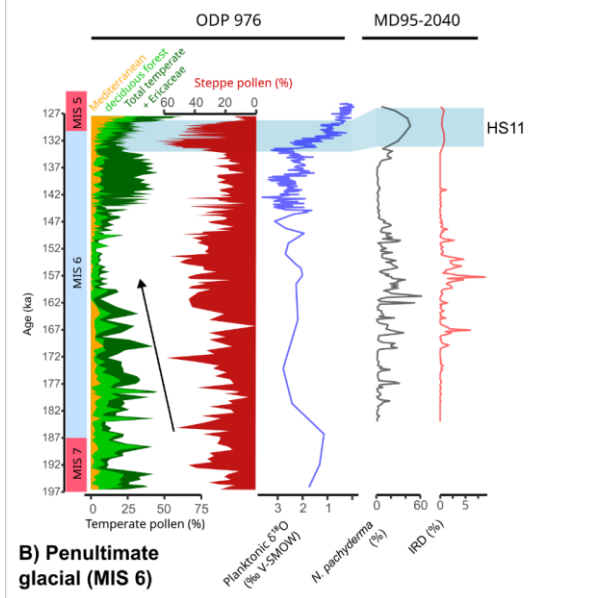
733 Finally, it is to be pointed out that HS12, occurring around 140 ka BP (Lisiecki & Stern, 2016),
734 apparently did not have any imprint on the vegetation record of ODP 976, implying a subdued impact
735 of this event on Mediterranean vegetation compared to HS11.

736 5.5. Comparison of MIS 6 with the last glacial period (MIS 4-2)

737 Various studies have pointed out strong similarities between the millennial-scale oscillations
738 of the last glacial period and the penultimate glacial period, with the division between MIS 3 and MIS
739 2 being analogous to the early and mid-late phase of MIS 6 respectively (Held et al., 2024; Margari et
740 al., 2010, 2014; Roucoux et al., 2011; Rousseau et al., 2020; Shin et al., 2020; Sierro et al., 2020). The
741 same studies argued in favour of pervasive impact of stadial events on the continental climate and
742 vegetation in the Mediterranean region, even in absence of typical Heinrich layers (Roucoux et al.,
743 2011). The ODP 976 record shows a cooling and aridification trend during the first half of MIS 6 (Fig.
744 9), with decreasing intensity of interstadials events, that recalls the pattern of MIS 3 D-O cycles (Bond
745 et al., 1993).



A) Last glacial (MIS 2-4)



B) Penultimate glacial (MIS 6)

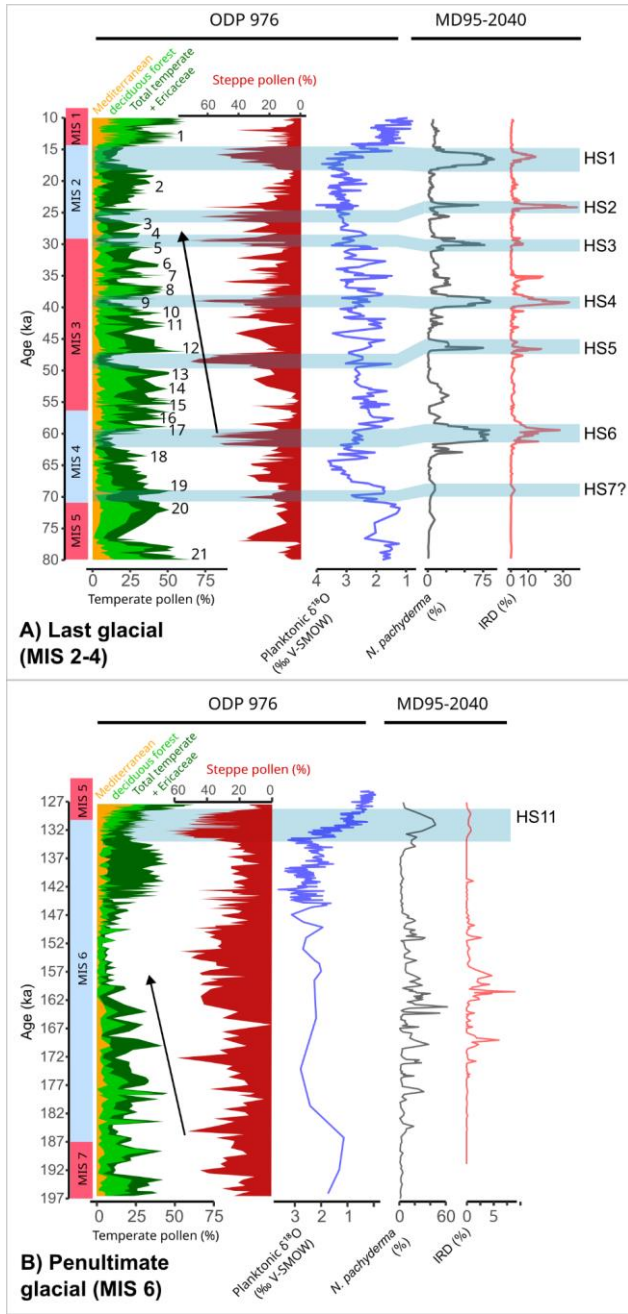


Fig. 9. Comparison of millennial-scale changes during A) the last glacial (MIS 2-4) and B) the penultimate glacial (MIS 6), including the main pollen data from ODP 976 (Charton et al., 2025; Combourieu-Nebout et al., 2002, 2009, and unpublished data for the last climatic cycle, and this

study for MIS 6), the ODP 976 planktonic isotopic ratio from *G. bulloides* (Combourieu-Nebout et al., 2002; Jiménez-Amat & Zahn, 2015; von Grafenstein et al., 1999, and unpublished data), and the *N. pachyderma* and IRD record from core MD95-2040 (de Abreu et al., 2003; Voelker and de Abreu, 2011). Marine Isotope Stages follow the boundaries from Lisiecki & Raymo (2005). Numbers on the Last Glacial correspond to the Greenland D-O events chronology (Fletcher et al., 2010a; Rasmussen et al., 2014). Black arrows mark the aridification trend and decreasing interstadials intensity during MIS 3 and early MIS 6.

a mis en forme : Anglais (Royaume-Uni)

746

747 However, the absence of clear successions of stadial events and especially Heinrich stadials,
748 together with the more subdued expression of interstadials in the vegetation record, limits the
749 resemblance between the two glacial periods. The pacing of interstadial peaks also seems to be
750 reduced compared to the last glacial period high-frequency oscillations, as previously highlighted from
751 the high-resolution speleothem record from Sofular cave in Turkey (Held et al., 2024).

752 A comparison of millennial-scale changes during the past two glacial periods based on the ODP
753 976 and MD95-2040 records, on either side of the Gibraltar Strait, supports our view (Fig. 9). The last
754 glacial period (encompassing MIS 4 to MIS 2) was characterized in the Alboran Sea by high-intensity
755 oscillations in both temperate and semi-desert vegetation correlated with D-O cycles and intense ice-
756 rafting events HE1 to HE7 in MD95-2040. During interstadial events, temperate and Mediterranean
757 vegetation (deciduous forest + Mediterranean + Ericaceae) could reach values above 60 % of total
758 pollen; during stadial events, the semi-desert pollen values reached values as high as 70% of total
759 pollen (during HS3, HS4 and HS5). In comparison, the penultimate glacial (MIS 6) displays much lower
760 intensity events, with interstadials characterized by 45% as a maximum value for temperate
761 vegetation, and stadials with 65% for the steppe and semi-desert vegetation (during HS11). High-
762 intensity cold episodes during MIS 6 are limited to the HS11, and the ~172 ka BP event. This is
763 consistent with the multiproxy record of core MD95-2040 on the Portuguese margin, which evidenced
764 reduced variability in the *N. pachyderma* abundance and IRD deposition during the penultimate glacial
765 compared to the last glacial (de Abreu et al., 2003; Voelker & de Abreu, 2011). The ice rafting episodes
766 appear to be of different nature during MIS 6 (Hodell et al., 2008; Liu et al., 2018; McCarron et al.,
767 2021), with the main iceberg discharges originating from the European ice sheet, contrary to the typical
768 Hudson Strait origin of the last glacial Heinrich events layers. SST reconstructions in the western
769 Mediterranean also show less intense cooling during MIS 6 than during MIS 3 (Martrat et al., 2004,
770 2007), supporting limited incursions of polar waters in the Mediterranean during MIS 6 compared to
771 MIS 3 coldest stadials, and especially Heinrich stadials (Cacho et al., 1999).

772 Like ODP 976, Ioannina records lower intensity arboreal pollen oscillations during early MIS 6
773 compared to the last glacial (Roucoux et al., 2011). In comparison, the Atlantic pollen record from
774 MD01-2444 core displays similar amplitude of tree percentages during the last and the penultimate

775 glacial (Margari et al., 2010). This difference can be explained by the different climate conditions, and
776 the higher sensitivity to cold and aridity of sclerophyllous and deciduous forest vegetation on the
777 Mediterranean side, as recorded in the ODP 976 and Ioannina palynological sequence. It appears that
778 temperate vegetation in SW Mediterranean responded to millennial-scale climatic oscillations with
779 higher intensity during the last glacial compared to the penultimate, probably because the climate in
780 Europe was colder during MIS 6 compared to MIS 2. This is supported by larger European ice-sheet
781 extension during the penultimate glacial (Ehlers et al., 2011; Ehlers & Gibbard, 2007; Shackleton, 1987),
782 favouring the long-term establishment of open landscapes mainly composed by steppe and semi-
783 desert plants. The differences in humidity might not be as easily interpretable, with an early MIS 6
784 more humid, and a MIS 6 glacial maximum more arid, compared to MIS 3 and MIS 2 as also suggested
785 by the Ioannina record (Roucoux et al., 2011). Future climate reconstructions applied to the complete
786 last glacial cycle in ODP 976 and other Mediterranean long pollen sequences will help understanding
787 the different climate configurations between the last two glacial periods.

788 5.6. Human occupation during MIS 6 in SW Europe

789 Only a limited number of sites in South-Western Europe have yielded archaeological layers
790 attributed to MIS 6, and even fewer of them have been radiometrically dated allowing for a robust
791 comparison with the environmental changes during MIS 6 (Fig. 10 and supplementary Supplements
792 table S24). The environmental proxies available in the archaeological layers (pollen, charcoal, macro
793 and microfauna) can help the chronological attribution, but are often insufficient to establish a precise
794 correlation with the high-resolution chrono-environmental framework of marine and glacial archives.
795 Even when absolute dates are available, their large uncertainty range and the poor resolution of the
796 archaeological record represent a major limitation and makes it difficult to correlate the human
797 occupation phases with a specific substage of MIS 6.

798 It is generally accepted that the northern part of Europe was almost completely depopulated
799 during MIS 6, with very few sites identified compared to the southern European fringes, indicating
800 discontinuous occupation during more favourable climatic episodes (Hérisson et al., 2016) or total
801 abandonment like in the British lands (Scott, 2011; Shaw et al., 2016; White and Pettitt, 2011).
802 Southern France, Italy and the Iberian Peninsula could have represented climate refugia during the
803 most extreme ice-cap advances (Bicho and Carvalho, 2022). Notably, Italy is particularly deprived of
804 sites well-dated to MIS 6 including the isolated Neanderthal of Altamura, the short episode of elephant
805 scavenging at Poggetti Vecchi, and the long sequence of San Bernardino cave which chronological
806 range extends up to ~154 ka BP, a period marked by the most extensive glacial conditions of MIS 6.
807 Some other few archaeological layers have been attributed to MIS 6, but they lack a robust

a mis en forme : Anglais (Royaume-Uni)

808 chronological attribution (Aureli & Ronchitelli, 2018; Fontana et al., 2010, Fig. 6.4 Fig. 10). One can
 809 hypothesise that regional climate conditions in the peninsula were particularly harsh after 150 ka, and
 810 that potential refugia sites remain to be identified in Italy. Palaeoecological reconstructions at the
 811 Poggetti Vecchi site indicated cold and dry open environment (Aranguren et al., 2019; Benvenuti et al.,
 812 2017). Interestingly, the chronological range for the site could coincide with a major stadial event at
 813 171 ka BP identified in the ODP 976 core, and particularly well expressed in the Valle di Castiglione
 814 record (Fig. 6).

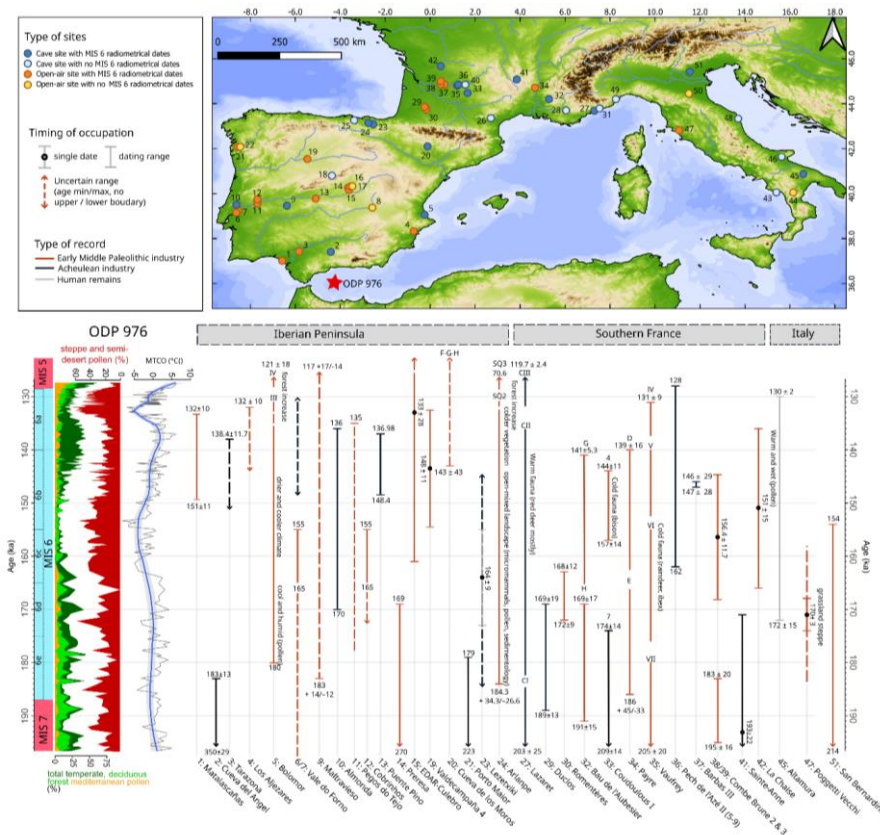


Fig. 10. Distribution of archaeological sites and radiometrically dated human occupation in western Mediterranean attributed to MIS 6, with some relevant palaeoecological information when available. The dates used and references can be found in Supplementary table S32. Sites on the map are numbered from south to north in each country: 1: Matalascañas ; 2: Cueva del Angel ; 3: Tarazona ; 4: Los Aljezares ; 5: Cueva del Bolomor ; 6: Vale do Forno ; 7: VF3 (Milharos) ; 8: El Provencio ; 9: Cueva de Maltravieso ; 10: Almonda ; 11: Pegos do Tejo ; 12: Cobrinhos ; 13: Puente Pino ; 14: Preresca ; 15: EDAR-Culebro 2 ; 16: Arriaga II/III ; 17: Arganda II (Valdocarros) ; 18: Villacastin ; 19: Valdecampana ; 20: Cueva de los Moros de Gabasa ; 21: Porto Maior ; 22 : Arbo ; 23: Lezetxiki ; 24 : Arlanpe ; 25: Ventalaperra ; 26: Aldènes ; 27 : Grotte du Lazaret ; 28 : Baume Bonne ; 29 : Duclos

; **30**: Romenteres ; **31**: Grotte du Prince ; **32**: Bau de l'Aubesier; **33**: Coudoulous I ; **34**: Payre ; **35**: Grotte Vaufrey ; **36** : Pech de l'Aze II ; **37**: Barbas III ; **38**: Combe Brune 3 ; **39**: Combe Brune 2 ; **40**: Grotte Sirogne; **41**: Sainte -Anne ; **42**: La Chaise ; **43**: Riparo del Poggio; **44**: Rosaneto; **45**: Altamura; **46**: Riparo Paglicci; **47**: Poggetti Vecchi ; **48**: Monte Conero; **49**: Grotta del Colombo; **50**: Due Pozzi/Scornetta; **51**: Grotta di San Bernardino.

a mis en forme : Interligne : simple

815 In Southern France and the Iberian Peninsula, according to available radiometric dates, human
816 occupation appears to have been continuous across MIS 6, even during the glacial maximum, with both
817 cave and open-air sites. France provides a comparable number of cave and open-air sites mainly
818 concentrated in the southwestern region. The Portuguese record is mainly constituted by open-air
819 sites in fluvial terrace systems of the lower Tagus, offering important insights into short-term
820 occupations during the full-glacial stage, but with complex chronological attribution (Cunha et al.,
821 2012, 2017; Pereira et al., 2019). The Spanish record includes various open-air settlements in the upper
822 Tagus valley (Panera et al., 2011, 2014; Yravedra et al., 2019), as well as the Duero (Diez-Martín, 2010)
823 and the Guadalquivir (Caro Gómez et al., 2011) valleys. Cave sites are fewer and are mainly located
824 closer to the coast (Cueva del Bolomor, Cueva del Angel, Lezetxiki, Arlanpe, Ventalaperra), with the
825 two exceptions of Cueva de Maltravieso and Villacastín. Key sites like Lazaret ~~C~~eave (Late Acheulean,
826 France) and Cueva del Bolomor (Middle Palaeolithic, Spain) evidence the persistence of human groups
827 in possible climate refugia ~~where large game hunting of red deer was prevailed (Michel et al., 2013;~~
828 ~~Valensi et al., 2013).~~ (Ochando et al., 2019; Valensi et al., 2005). ~~Cueva del Bolomor stands out in the~~
829 ~~Iberian Peninsula record as it provides an exceptionally long and continuous record of human~~
830 ~~presence, and the oldest evidence of fire use in Spain during the Middle Palaeolithic (Vidal-Matutano~~
831 ~~et al., 2019). Climate changes during MIS 6 are documented in the cave's sediments through multiple~~
832 ~~proxies, with a more humid and cool phase at the beginning, and the most arid phase taking place at~~
833 ~~the middle of Phase III (layers X VIII) (Arsuaga et al., 2012; Fernández-Peris et al., 2008). The site is~~
834 ~~described as a climate refugia where Mediterranean vegetation persisted during the colder phase of~~
835 ~~MIS 6 thanks to the coastal reservoir character of the site (Ochando et al., 2019). ~~where large game~~~~
836 ~~hunting of red deer was prevailed (Valensi et al., 2013).~~

a mis en forme : Français (France)

a mis en forme : Français (France)

Code de champ modifié

Code de champ modifié

Code de champ modifié

Code de champ modifié

Code de champ modifié

a mis en forme : Anglais (États-Unis)

837 MIS 6 in Europe saw the final stage of the cultural transition from the Lower to the Middle
838 Palaeolithic industries (MIS 8-5), mainly characterized by the emergence of more complex core
839 technologies such as Levallois debitage and changes in subsistence strategies. No rupture is observed
840 between the technocomplexes, as cultural diversity and the permanence of Acheulean bifacial tools
841 associated to technological innovation mark these Early Middle Palaeolithic industries in Southern
842 Europe (Santonja et al., 2016; Terradillos-Bernal et al., 2023). The distribution of archaeological sites
843 and timing of human occupation in South-Western Mediterranean at that time reflects this pattern. A
844 mosaic of traditional and innovative behavioural traits can be observed, with late Acheulean and Early

845 Middle Palaeolithic coexisting continuously (Cueto et al., 2016; de Lumley, 2018; Mathias et al., 2020;
846 Moncel et al., 2025; Santonja et al., 2022; Torres et al., 2024; Valensi et al., 2013). Acheulean
847 technocomplexes are progressively abandoned ~~aeross-during~~ MIS 6 in Europe (Álvarez-Alonso, 2014;
848 Key et al., 2021), with the latest chronologies found possibly in the Manzanares basin in central Iberia
849 at Arriaga sites (Panera et al., 2014; Rubio-Jara et al., 2016; Rubio-Jara and Panera, 2019; Silva et al.,
850 2013), or at Lazaret cave (Michel et al., 2022), and dated to the beginning of MIS 5. No clear explanation
851 is accepted for the emergence and generalization of the Levallois debitage, and while cognition might
852 not be the only factor, some authors suggested that MIS 6 glaciation could have played a role in the
853 final abandonment of Acheulean industries (Moncel et al., 2020; Valensi et al., 2005). It is hard to claim
854 that specific environmental pressures favoured Levallois technology over bifacial production, as these
855 lithic technologies seem to have co-existed in Western Europe since MIS 12-11 over several
856 glacial/interglacial cycles (Baena et al., 2017; Moncel et al., 2020), including extremely cold stages (like
857 MIS 12 and 10). This “mosaic” pattern for the lower to middle palaeolithic transition, although at least
858 partly imputable to the large dating uncertainties, points toward more complex processes leading to
859 the generalization of Middle Palaeolithic industries from MIS 5. Interestingly, the end of the Lower to
860 Middle Palaeolithic transition is also associated with a shift in the morphology of human remains, from
861 “Early Neanderthals” (MIS 7-5) to “Classical Neanderthals” (MIS 5-3) (Di Vincenzo and Manzi, 2023).
862 Sites like La Chaise (Abri Suard), Lazaret and Altamura provide fossil evidence for these “Early
863 Neanderthals” which share characteristics with earlier Middle Pleistocene populations, and with later
864 Neanderthals (Buzi et al., 2025; Couture-Veschambre et al., 2021; de Lumley, 2018). Genetic data also
865 support an important population shift in western Europe sometimes around the transition from MIS 6
866 to MIS 5 (Peyrègne et al., 2019). Therefore, an important population reorganization seems to have
867 occurred at the time of the final Acheulean industries, leading to the onset of the so-called “Classical
868 neanderthal world” in western Eurasia, with generalized Middle Palaeolithic industries and established
869 Neanderthal morphological features. The role of environmental changes occurring during MIS 6 in this
870 population reorganization remains poorly understood.

871 Changes in land use and mobility pattern have been evidenced in north-central Iberia, and can
872 be viewed as adaptations to the severe climatic conditions of MIS 6 evidenced in the ODP 976 sequence
873 during pollen zone/phase 2-: increasing mobility, more short-term occupations and reliance on more
874 local resources for subsistence strategies (Diez-Martín, 2010; Diez-Martín et al., 2008; Rios-Garaizar,
875 2016; Sánchez-Yustos, 2009). According to this view, the emergence of the “classical Neanderthal”
876 world in Europe after the MIS 6/5 transition corresponds to the initialization of dynamics of repeated
877 population contraction and expansion in response to the Upper Pleistocene instability (Sánchez-
878 Yustos, 2009). However,

a mis en forme : Anglais (États-Unis)

a mis en forme : Anglais (États-Unis)

a mis en forme : Anglais (États-Unis)

a mis en forme : Anglais (États-Unis)

Code de champ modifié

Code de champ modifié

879 -identifying cultural phases in the archaeological sequences linked with specific climatic
880 episodes is generally hindered by the poor resolution of the archaeological record and chronological
881 data. Among the sites identified in this synthesis, Lazaret and Bolomor caves probably present the
882 most informative and well-dated sequences with several archaeological layers dated to MIS 6.

a mis en forme : Espace Avant : 0 pt

883 Cueva del Bolomor stands out in the Iberian Peninsula record as it provided an exceptionally
884 long and continuous record of human presence, and the oldest evidence of fire use in Spain during the
885 Middle Palaeolithic (Vidal-Matutano et al., 2019). Climate changes during MIS 6 documented in
886 Bolomor's sediments through multiple proxies are consistent with the different phases identified in
887 the ODP 976 record, with a more humid and cool phase at the beginning of MIS 6, and the most arid
888 phase taking place at the middle of Phase III (layers X-VIII) (Arsuaga et al., 2012; Fernández Peris et al.,
889 2008). The site is described as a climatic refugium where Mediterranean vegetation persisted during
890 the colder phase of MIS 6 thanks to the coastal reservoir character of the site (Ochando et al., 2019).
891 No clear change in lithic production has been identified in the MIS 6 layers of Bolomor: according to
892 Fernández Peris et al. (2008), archaeological layers XII to VII (Phase III, MIS 6) are all dominated by
893 limestone flakes with few retouches, few recycling, and the presence non-Acheulean macro-lithic
894 elements. These layers are characterized by expeditive flaking (including Levallois *débitage*) relying on
895 local raw-material, pointing toward a high degree of mobility and search for immediate effectiveness.
896 It is thus hard to distinguish different techno-cultural tendencies during this phase. The most visible
897 change in the archaeological sequence occurs in layer VI (MIS 5) which shows an intensification of lithic
898 production dominated by flint, the production of more specialized tools including microlithic elements
899 and associated to more intense and stable occupation in the cave (Fernández Peris et al., 2008).
900 Therefore, a clear behavioural change in the technological and economical exploitation of raw
901 materials is identified at the beginning of MIS 5. Faunal remains show a large and constant diversity,
902 including abundant micro supporting both short-term and long-term not-specialized occupation, with
903 no clear change in the site's function across the sequence (Blasco et al., 2013).

a mis en forme : Anglais (Royaume-Uni)

a mis en forme : Anglais (Royaume-Uni)

904 Lazaret Cave, in south-eastern France, shows a very distinct scheme: the lower to middle
905 Palaeolithic transition is well documented in the archaeological sequence (Unit CII and CIII), with the
906 progressive replacement of large bifacial tools production by more standardized and smaller flakes
907 (Cauche, 2012). Levallois *débitage* is already present and well-mastered in the lower MIS 6 levels,
908 although rare, and becomes dominant in the upper levels (early MIS 5). Therefore, a subdivision of unit
909 CII can be made with a lower interval rich in handaxes, and an upper layer characterized as "final
910 Acheulean" with rare handaxes and more abundant flakes. Faunal assemblages are very constant
911 throughout MIS 6, with the large dominance of red deers and rare presence of cold species (*Rangifer*

a mis en forme : Police :Italique

912 tarandus, Coelodonta antiquitatis). Thus, the climatic oscillations of MIS 6 do not seem to have
913 influenced different hunting strategies or prey selection by human populations at Lazaret Cave, as large
914 game hunting of red deer prevailed (Valensi et al., 2013).

a mis en forme : Anglais (Royaume-Uni)

915 Therefore, Lazaret and Bolomor caves are examples of different strategies of site exploitation*
916 and technological evolution during MIS 6: Lazaret Cave represents a specialized red-deer hunting camp
917 evidencing a progressive change from Lower to Middle Palaeolithic tools, while Cueva del Bolomor can
918 be characterized as a short-term camp with more generalized hunting and stable expeditive Middle
919 Palaeolithic industry. Despite these differences both sites provide evidence for a change in lithic
920 assemblages occurring at the end of MIS 6/ beginning of MIS 5: the disappearance of handaxes and
921 generalization of Levallois flakes in Lazaret, and the intensification and standardization of flint flakes
922 in Bolomor.

a mis en forme : Espace Avant : 12 pt

923 ~~Changes in land use and mobility pattern have been evidenced in north-central Iberia, and can~~
924 ~~be viewed as adaptations to the severe climatic conditions of MIS 6: increasing mobility, more short-~~
925 ~~term occupations and reliance on more local resources for subsistence strategies (Diez Martín, 2010;~~
926 ~~Diez Martín et al., 2008; Rios Garaizar, 2016; Sánchez Yustos, 2009). According to this view, the~~
927 ~~emergence of the "classical Neanderthal" world in Europe after the MIS 6/5 transition corresponds to~~
928 ~~the initialization of dynamics of repeated population contraction and expansion in response to the~~
929 ~~Upper Pleistocene instability (Sánchez Yustos, 2009).~~

930 ~~Indeed, the~~The fast climate dynamics during Termination II as evidenced in the ODP 976
931 paleoenvironmental record could have represented a critical period for human population. At the end
932 of MIS 6, more sites have been identified in the Iberian Peninsula than Southern France, showing the
933 latter could have represented a climate refugium~~a~~ at the time of maximum glacial expansion, with
934 more intense human occupation regionally. Many of these late MIS 6 sites present a chronological
935 boundary at the top of the sequence compatible with the onset of Termination II around 136 ka BP,
936 and with Heinrich Stadial~~HS~~-11, within the dating uncertainty: Matalascañas, Tarrazona, Los Aljezares,
937 Bolomor Unit III, Almonda, Pegos do Tejo, Puente Pino, Arlanpe Unit SQ2, Lazaret Unit CII, Payre layer
938 D, Vauffrey unit IV, and Pech de l'Azé II layer 5-. The extreme character of this event in the South-
939 Western Mediterranean as expressed in the ODP 976 sequence could have put further environmental
940 pressure on hominin groups already diminished. A niche modelling approach based on 41 sites of
941 Western Eurasia since 145 ka BP has shown that the projected potential niche space ~~reconstructed~~
942 for Neanderthals at the end of MIS 6 (~145ka BP)- ~~was very reduced~~~~is very reduced~~, and concentrated
943 in Western Europe (Yaworsky et al., 2024). ~~This coincides with the end of pollen zone/phase 2 in the~~
944 ODP 976 record, the most cold and arid phase of the penultimate Glacial before HS11. Then, the

945 authors reconstruct a progressive expansion of Neanderthal potential niche space between 145 and
946 130 ka, compatible with the climatic warming and moistening during pollen zone/phase 3 in the ODP
947 976 record (Yaworsky et al., 2024). The temporal resolution of the model (1000 years) does not allow
948 to detect the impact of HS11 on the niche projection, and only a small slowdown and decline of the
949 projected niche is visible at ~130 ka BP, before the MIS 5e optimum (Yaworsky et al., 2024, Fig. 5). A
950 regional study focused on North-Western Spain ~~also~~ argued in favour of a demographic vacuum at the
951 end of MIS 6, compatible with HS11 and leading to a population reorganization implying ~~population~~
952 ~~retreat-contraction~~ or micro-extinction, before the generalization of Middle Palaeolithic industries ~~and~~
953 during MIS 5 (Sánchez-Yustos and Díez-Martín, 2015). According to the same authors, following this
954 crisis, Neanderthal population entered a “reorganisation phase” leading to demographical stability
955 (Peyrégne et al., 2019) and more technological standardization, visible in the explosion of the number
956 of sites in Europe in general, especially after the MIS 5e climatic optimum (Bringmans, 2007; Lewis et
957 al., 2011; Wenzel, 2007).- This statement is supported by niche modelling which shows a peak in
958 projected potential niche space of Neanderthal during MIS 5e (Yaworsky et al., 2024), and by recent
959 genetic data which provided evidence for at least two radiation events linked with the environmental
960 conditions of the last interglacial (Vernot et al., 2021), and Neanderthal population continuity since
961 ~120 ka BP (Peyrégne et al., 2019). Thus, HS11 did not lead to complete extinction of hominin groups
962 but might have induced deep demographical and technological reorganization, representing the first
963 and one of the most intense abrupt changes that Neanderthal population had to face in South-Western
964 Europe before the Last Glacial largest oscillations (HS4-4e). According to this view, the emergence of
965 the “classical Neanderthal” world in Europe after the MIS 6/5 transition corresponds to the
966 initialization of dynamics of repeated population contraction and expansion in response to the Upper
967 Pleistocene instability, especially during MIS 4-2 (Sánchez-Yustos, 2009). In that sense, the subdued
968 environmental instability during MIS 6 evidenced in the ODP site 976 record compared to the last
969 glacial period (Section 5.5 and Fig. 9) could also have implications for human populations, with less
970 fragmented (although harsh) habitats and more stable (although reduced) population during MIS 6.
971 This hypothesis remains however hard to test based on the very different nature and quality of
972 preservation of the archaeological record during MIS 6 compared to MIS 4-2 (e.g. Charton et al.,
973 2025),(Peyrégne et al., 2019)(Vernot et al., 2021)~~Thus, HS11 did not lead to complete extinction of~~
974 ~~hominin groups but might have induced deep demographical and technological reorganization,~~
975 ~~representing the first and one of the most intense abrupt changes that Neanderthal population had to~~
976 ~~face in South-Western Europe before the Last Glacial largest oscillations (HS4-6).~~

977

978 6. Conclusion

979 The ODP 976 record sheds light on the environmental and climate changes during MIS 6 in the
980 SW Mediterranean. The sequence is characterized by the high representation of *Cedrus* and Ericaceae
981 pollen, resulting from the combined influence of African and Atlantic input respectively. ODP 976
982 position, at the confluence of Mediterranean versus Atlantic, and Eurasian versus African climatic
983 areas, is ideal to decipher the processes behind orbital and sub-orbital climate dynamics during past
984 glaciations. Three main phases have been distinguished during MIS 6 with different trends in
985 vegetation and climate changes. Millennial-scale oscillations are recorded especially during the early
986 part of MIS 6 (~187-166 ka BP) through the rapid increases of temperate and Mediterranean pollen,
987 some of which are ~~consistent similar to with Antarctic and millennial-scale warming D-O-like~~ events
988 identified in the ice-core and marine temperature records, ~~and as well as~~ other palynological
989 sequences in the Mediterranean region. This Early MIS 6 phase is characterized by overall warmer and
990 wetter climate conditions, in agreement with other paleoclimate archives in the Mediterranean
991 showing enhanced moisture availability at the beginning of MIS 6. This phase of enhanced moisture
992 availability was likely connected with enhanced Asian and African monsoon activity and was probably
993 at the origin of the deposition of ~~the an~~ Organic Rich Layer 607 in the Alboran Sea and sapropel S6 in
994 the eastern Mediterranean. The second phase (165-144 ka BP) shows the establishment of full glacial
995 conditions in the Mediterranean, with the maximum spread of steppe and semi-desert vegetation
996 associated to cold and arid climate conditions and limited rapid oscillations. Finally, the final stages of
997 MIS 6 are marked by increased humidity and the development of Ericaceae, with moderate millennial-
998 scale oscillations seen in the vegetation record. Termination II is very particular in the ODP 976 record,
999 with the continuous increase of temperate and Mediterranean vegetation being contemporaneous to
1000 a major episode of steppe expansion and aridity increase identified as ~~Heinrich Stadial 11~~ HS11. This
1001 event shows a particular three phases or “~~double- ψ W~~” shape, in agreement with other records, and
1002 ~~probably~~ had a major impact on the SW Mediterranean ~~region~~ environments. A comparison with the
1003 changes occurring during the last glacial period (MIS ~~42-42~~) inferred from the same core highlighted
1004 the limited duration, frequency and intensity of MIS 6 millennial-scale climatic events compared to
1005 the last Glacial D-O cycles and Heinrich ~~Events-Stadials~~ (MIS ~~2-44-2~~). These results support a subdued
1006 impact of the millennial-scale climatic oscillations on the continental vegetation in the Mediterranean
1007 region during the Penultimate glaciation compared to the Last Glacial. The only exception is HS11,
1008 which stands out by its notable intensity and duration and is of particular interest to understand the
1009 mechanisms behind Termination II.

1010 Human populations continuously inhabited the SW Mediterranean territory during MIS 6.
1011 While few sites are available and robustly dated to MIS 6 in Italy, Southern France and the Iberian

1012 Peninsula appear to have been intensely populated, supporting their nature of Pleistocene Climate
1013 refugia. More ecological data from well-dated archaeological sites during MIS 6 would be needed to
1014 increase the quality of human-environmental dynamics comparison. However, the synthesis drawn in
1015 the present study highlights the extreme nature of events characterizing Termination II, and
1016 particularly HS11, which could have represented an important environmental crisis for human
1017 population at that time, catalysing the end of the Lower to Middle Palaeolithic Transition and the onset
1018 of the “classical” Neanderthal world through a drastic population ~~contraction~~bottleneck.

1019 7. Data availability

1020 Pollen counts and climate reconstruction results from ODP 976 will be soon submitted to PANGAEA
1021 data repository (<https://www.pangaea.de/>).

Code de champ modifié

1022 8. Supplements

1023

1024 The supplementary figures and tables related to this study can be downloaded at the following
1025 link:

1026 9. Author contribution

1027

1028 LC, NC, AB and VL designed the project. LC and NC carried out the palynological analyses. LC, OP
1029 and MR applied the four methods of pollen-based climate reconstruction to the ODP 976 record. LC
1030 and MHM led the archaeological synthesis. LC made the figures and wrote the text. All authors
1031 contributed to improve the manuscript by their expertise.

1032 10. Acknowledgments

1033

1034 We want to thank the three anonymous reviewers and the editor for their very helpful
1035 comments on this manuscript. We acknowledge the International Ocean Drilling Project and the
1036 MARUM Bremen Core Repository for making available the ODP 976 samples. The sample processing
1037 was funded by the CNRS and the MNHN. We thank the European Research Council (ERC) under the
1038 European Union’s HORIZON1.1 research program (LATEUROPE project, grant agreement ID
1039 101052653) for funding this publication. L. Charton doctoral contract was funded by the French
1040 Ministère de l’Enseignement Supérieur et de la Recherche at the doctoral school ED 227 of the
1041 Muséum National d’Histoire Naturelle, Paris. The international cotutorship with the University of
1042 Florence is supported by the Ecole Franco-Italienne Vinci grant (project C2-166). We thank Lionel
1043 Dubost for assistance in laboratory treatment of samples to HF. We are grateful to Francisco Sierra for

1044 sharing the isotopic data on AICC2012 timescale, to Jon Camuera for the pollen data from Padul and
1045 to Katherine Roucoux for the pollen data from Ioannina. This is an ISEM contribution.

1046

1047 11. References

1048

1049 de Abreu, L., Shackleton, N. J., Schönfeld, J., Hall, M., and Chapman, M.: Millennial-scale oceanic
1050 climate variability off the Western Iberian margin during the last two glacial periods, *Marine Geology*,
1051 196, 1–20, [https://doi.org/10.1016/S0025-3227\(03\)00046-X](https://doi.org/10.1016/S0025-3227(03)00046-X), 2003.

1052 Allen, J. R. M. and Huntley, B.: Last Interglacial palaeovegetation, palaeoenvironments and chronology:
1053 a new record from Lago Grande di Monticchio, southern Italy, *Quaternary Science Reviews*, 28, 1521–
1054 1538, <https://doi.org/10.1016/j.quascirev.2009.02.013>, 2009.

1055 Álvarez-Alonso, D.: First Neanderthal settlements in northern Iberia: The Acheulean and the
1056 emergence of Mousterian technology in the Cantabrian region, *Quaternary International*, 326–327,
1057 288–306, <https://doi.org/10.1016/j.quaint.2012.12.023>, 2014.

1058 Aranguren, B., Grimaldi, S., Benvenuti, M., Capalbo, C., Cavanna, F., Cavulli, F., Ciani, F., Comencini, G.,
1059 Giuliani, C., Grandinetti, G., Mariotti Lippi, M., Masini, F., Mazza, P. P. A., Pallecchi, P., Santaniello, F.,
1060 Savorelli, A., and Revedin, A.: Poggetti Vecchi (Tuscany, Italy): A late Middle Pleistocene case of
1061 human–elephant interaction, *Journal of Human Evolution*, 133, 32–60,
1062 <https://doi.org/10.1016/j.jhevol.2019.05.013>, 2019.

1063 Arsuaga, J. L., Fernández Peris, J., Gracia-Téllez, A., Quam, R., Carretero, J. M., Barciela González, V.,
1064 Blasco, R., Cuartero, F., and Sañudo, P.: Fossil human remains from Bolomor Cave (Valencia, Spain),
1065 *Journal of Human Evolution*, 62, 629–639, <https://doi.org/10.1016/j.jhevol.2012.02.002>, 2012.

1066 Auffret, G.-A., Pastouret, L., Chamley, H., and Lanoix, F.: Influence of the prevailing current regime on
1067 sedimentation in the Alboran Sea, *Deep Sea Research and Oceanographic Abstracts*, 21, 839–849,
1068 [https://doi.org/10.1016/0011-7471\(74\)90003-5](https://doi.org/10.1016/0011-7471(74)90003-5), 1974.

1069 Aureli, D. and Ronchitelli, A.: The Lower Tyrrhenian Versant: was it a techno-cultural area during the
1070 Middle Palaeolithic? Evolution of the lithic industries of the Riparo del Molare sequence in the frame
1071 of Neanderthal peopling dynamics in Italy, 59–94, 2018.

1072 Ayalon, A., Bar-Matthews, M., and Kaufman, A.: Climatic conditions during marine oxygen isotope
1073 stage 6 in the eastern Mediterranean region from the isotopic composition of speleothems of Soreq
1074 Cave, Israel, *Geology*, 30, [https://doi.org/10.1130/0091-7613\(2002\)030<0303:CCDMOI>2.0.CO;2](https://doi.org/10.1130/0091-7613(2002)030<0303:CCDMOI>2.0.CO;2),
1075 2002a.

1076 Ayalon, A., Bar-Matthews, M., and Kaufman, A.: Climatic conditions during marine oxygen isotope
1077 stage 6 in the eastern Mediterranean region from the isotopic composition of speleothems of Soreq
1078 Cave, Israel, *Geol*, 30, 303, [https://doi.org/10.1130/0091-7613\(2002\)030<0303:CCDMOI>2.0.CO;2](https://doi.org/10.1130/0091-7613(2002)030<0303:CCDMOI>2.0.CO;2),
1079 2002b.

1080 Baena, J., Moncel, M.-H., Cuartero, F., Chacón Navarro, M. G., and Rubio, D.: Late Middle Pleistocene
1081 genesis of Neanderthal technology in Western Europe: The case of Payre site (south-east France),
1082 *Quaternary International*, 436, 212–238, <https://doi.org/10.1016/j.quaint.2014.08.031>, 2017.

- 1083 Bailey, G., Carrión, J., Fa, D., Finlayson, C., Finlayson, G., and Vidal, J.: The coastal shelf of the
 1084 Mediterranean and beyond: Corridor and refugium for human populations in the Pleistocene
 1085 Introduction, *Quaternary Science Reviews*, 27, 2095–2099,
 1086 <https://doi.org/10.1016/j.quascirev.2008.08.005>, 2008.
- 1087 Bajo, P., Drysdale, R. N., Woodhead, J. D., Hellstrom, J. C., Hodell, D., Ferretti, P., Voelker, A. H. L.,
 1088 Zanchetta, G., Rodrigues, T., Wolff, E., Tyler, J., Frisia, S., Spötl, C., and Fallick, A. E.: Persistent influence
 1089 of obliquity on ice age terminations since the Middle Pleistocene transition, *Science*, 367, 1235–1239,
 1090 <https://doi.org/10.1126/science.aaw1114>, 2020.
- 1091 Barbante, C., Barnola, J.-M., Becagli, S., Beer, J., Bigler, M., Boutron, C., Blunier, T., Castellano, E.,
 1092 Cattani, O., Chappellaz, J., Dahl-Jensen, D., Debret, M., Delmonte, B., Dick, D., Falourd, S., Faria, S.,
 1093 Federer, U., Fischer, H., Freitag, J., Frenzel, A., Fritzsche, D., Fundel, F., Gabrielli, P., Gaspari, V.,
 1094 Gersonde, R., Graf, W., Grigoriev, D., Hamann, I., Hansson, M., Hoffmann, G., Hutterli, M. A.,
 1095 Huybrechts, P., Isaksson, E., Johnsen, S., Jouzel, J., Kaczmarska, M., Karlin, T., Kaufmann, P., Kipfstuhl,
 1096 S., Kohno, M., Lambert, F., Lambrecht, A., Lambrecht, A., Landais, A., Lawer, G., Leuenberger, M., Littot,
 1097 G., Loulergue, L., Lüthi, D., Maggi, V., Marino, F., Masson-Delmotte, V., Meyer, H., Miller, H., Mulvaney,
 1098 R., Narcisi, B., Oerlemans, J., Oerter, H., Parrenin, F., Petit, J.-R., Raisbeck, G., Raynaud, D.,
 1099 Röthlisberger, R., Ruth, U., Rybak, O., Severi, M., Schmitt, J., Schwander, J., Siegenthaler, U., Siggaard-
 1100 Andersen, M.-L., Spahni, R., Steffensen, J. P., Stenni, B., Stocker, T. F., Tison, J.-L., Traversi, R., Udisti,
 1101 R., Valero-Delgado, F., van den Broeke, M. R., van de Wal, R. S. W., Wagenbach, D., Wegner, A., Weiler,
 1102 K., Wilhelms, F., Winther, J.-G., Wolff, E., and EPICA Community Members: One-to-one coupling of
 1103 glacial climate variability in Greenland and Antarctica, *Nature*, 444, 195–198,
 1104 <https://doi.org/10.1038/nature05301>, 2006.
- 1105 Bard, E., Delaygue, G., Rostek, F., Antonioli, F., Silenzi, S., and Schrag, D. P.: Hydrological conditions
 1106 over the western Mediterranean basin during the deposition of the cold Sapropel 6 (ca. 175 kyr BP),
 1107 *Earth and Planetary Science Letters*, 202, 481–494, [https://doi.org/10.1016/S0012-821X\(02\)00788-4](https://doi.org/10.1016/S0012-821X(02)00788-4),
 1108 2002a.
- 1109 Bard, E., Antonioli, F., and Silenzi, S.: Sea-level during the penultimate interglacial period based on a
 1110 submerged stalagmite from Argentarola Cave (Italy), *Earth and Planetary Science Letters*, 196, 135–
 1111 146, [https://doi.org/10.1016/S0012-821X\(01\)00600-8](https://doi.org/10.1016/S0012-821X(01)00600-8), 2002b.
- 1112 Barker, S. and Knorr, G.: Millennial scale feedbacks determine the shape and rapidity of glacial
 1113 termination, *Nat Commun*, 12, 2273, <https://doi.org/10.1038/s41467-021-22388-6>, 2021.
- 1114 Barker, S., Knorr, G., Edwards, R. L., Parrenin, F., Putnam, A. E., Skinner, L. C., Wolff, E., and Ziegler, M.:
 1115 800,000 Years of Abrupt Climate Variability, *Science*, 334, 347–351,
 1116 <https://doi.org/10.1126/science.1203580>, 2011.
- 1117 Bayr, D., Plaza, M. P., Gilles, S., Kolek, F., Leier-Wirtz, V., Traidl-Hoffmann, C., and Damialis, A.: Pollen
 1118 long-distance transport associated with symptoms in pollen allergics on the German Alps: An old story
 1119 with a new ending?, *Sci Total Environ*, 881, 163310, <https://doi.org/10.1016/j.scitotenv.2023.163310>,
 1120 2023.
- 1121 Bazin, L., Landais, A., Lemieux-Dudon, B., Toyé Mahamadou Kele, H., Veres, D., Parrenin, F., Martinerie,
 1122 P., Ritz, C., Capron, E., Lipenkov, V., Loutre, M.-F., Raynaud, D., Vinther, B., Svensson, A., Rasmussen,
 1123 S. O., Severi, M., Blunier, T., Leuenberger, M., Fischer, H., Masson-Delmotte, V., Chappellaz, J., and
 1124 Wolff, E.: An optimized multi-proxy, multi-site Antarctic ice and gas orbital chronology (AICC2012):
 1125 120‐800 ka, *Climate of the Past*, 9, 1715–1731, <https://doi.org/10.5194/cp-9-1715-2013>, 2013.

- 1126 Benvenuti, M., Bahain, J.-J., Capalbo, C., Capretti, C., Ciani, F., D'Amico, C., Esu, D., Giachi, Gi., Giuliani,
 1127 C., Gliozzi, E., Lazzeri, S., Macchioni, N., Lippi, M. M., Masini, F., Mazza, P. P. A., Pallecchi, P., Revedin,
 1128 A., Savorelli, A., Spadi, M., Sozzi, L., Vietti, A., Voltaggio, M., and Aranguren, B.: Paleoenvironmental
 1129 context of the early Neanderthals of Poggetti Vecchi for the late middle Pleistocene of Central Italy,
 1130 *Quat. res.*, 88, 327–344, <https://doi.org/10.1017/qua.2017.51>, 2017.
- 1131 Bermúdez de Castro, J. M. and Martínón-Torres, M.: A new model for the evolution of the human
 1132 Pleistocene populations of Europe, *Quaternary International*, 295, 102–112,
 1133 <https://doi.org/10.1016/j.quaint.2012.02.036>, 2013.
- 1134 Bicho, N. and Carvalho, M.: Peninsular southern Europe refugia during the Middle Palaeolithic: an
 1135 introduction, *J Quaternary Science*, 37, 133–135, <https://doi.org/10.1002/jqs.3410>, 2022.
- 1136 Bisschop, K., Mortier, F., Etienne, R. S., and Bonte, D.: Transient local adaptation and source–sink
 1137 dynamics in experimental populations experiencing spatially heterogeneous environments,
 1138 *Proceedings of the Royal Society B: Biological Sciences*, 286, 20190738,
 1139 <https://doi.org/10.1098/rspb.2019.0738>, 2019.
- 1140 Blasco, R., Rosell, J., Fernández Peris, J., Arsuaga, J. L., Bermúdez de Castro, J. M., and Carbonell, E.:
 1141 Environmental availability, behavioural diversity and diet: a zooarchaeological approach from the
 1142 TD10-1 sublevel of Gran Dolina (Sierra de Atapuerca, Burgos, Spain) and Bolomor Cave (Valencia,
 1143 Spain), *Quaternary Science Reviews*, 70, 124–144, <https://doi.org/10.1016/j.quascirev.2013.03.008>,
 1144 2013.
- 1145 Bond, G., Heinrich, H., Broecker, W., Labeyrie, L., McManus, J., Andrews, J., Huon, S., Jantschik, R.,
 1146 Clasen, S., Simet, C., Tedesco, K., Klas, M., Bonani, G., and Ivy, S.: Evidence for massive discharges of
 1147 icebergs into the North Atlantic ocean during the last glacial period, *Nature*, 360, 245–249,
 1148 <https://doi.org/10.1038/360245a0>, 1992.
- 1149 Bond, G., Broecker, W., Johnsen, S., McManus, J., Labeyrie, L., Jouzel, J., and Bonani, G.: Correlations
 1150 between climate records from North Atlantic sediments and Greenland ice, *Nature*, 365, 143–147,
 1151 <https://doi.org/10.1038/365143a0>, 1993.
- 1152 Bond, G., Showers, W., Cheseby, M., Lotti, R., Almasi, P., Demenocal, P., Priore, P., Cullen, H., Hajdas,
 1153 I., and Bonani, G.: A pervasive millennial-scale cycle in the North Atlantic Holocene and glacial climates,
 1154 *sci*, 278, 1257, <https://doi.org/10.1126/science.278.5341.1257>, 1997.
- 1155 Bond, G. C., Showers, W., Elliot, M., Evans, M., Lotti, R., Hajdas, I., Bonani, G., and Johnson, S.: The
 1156 North Atlantic's 1-2 kyr climate rhythm: Relation to Heinrich events, Dansgaard/Oeschger cycles and
 1157 the Little Ice Age, *Washington DC American Geophysical Union Geophysical Monograph Series*, 112,
 1158 35–58, <https://doi.org/10.1029/GM112p0035>, 1999.
- 1159 Boswell, S. M., Toucanne, S., Pitel-Roudaut, M., Creyts, T. T., Eynaud, F., and Bayon, G.: Enhanced
 1160 surface melting of the Fennoscandian Ice Sheet during periods of North Atlantic cooling, *Geology*, 47,
 1161 664–668, <https://doi.org/10.1130/G46370.1>, 2019.
- 1162 Bout-Roumazeilles, V., Combourieu Nebout, N., Peyron, O., Cortijo, E., Landais, A., and Masson-
 1163 Delmotte, V.: Connection between South Mediterranean climate and North African atmospheric
 1164 circulation during the last 50,000yrBP North Atlantic cold events, *Quaternary Science Reviews*, 26,
 1165 3197–3215, <https://doi.org/10.1016/j.quascirev.2007.07.015>, 2007.

a mis en forme : Anglais (États-Unis)

- 1166 ter Braak, C. and Juggins, S.: Weighted Averaging Partial Least Squares Regression (WA-PLS): An
 1167 Improved Method for Reconstructing Environmental Variables from Species Assemblages,
 1168 *Hydrobiologia*, 269–270, 485–502, <https://doi.org/10.1007/BF00028046>, 1993.
- 1169 Bradtmöller, M., Pastoors, A., Weninger, B., and Weniger, G.-C.: The repeated replacement model –
 1170 Rapid climate change and population dynamics in Late Pleistocene Europe, *Quaternary International*,
 1171 247, 38–49, <https://doi.org/10.1016/j.quaint.2010.10.015>, 2012.
- 1172 Brauer, A., Allen, J. R. M., Mingram, J., Dulski, P., Wulf, S., and Huntley, B.: Evidence for last interglacial
 1173 chronology and environmental change from Southern Europe, *Proceedings of the National Academy*
 1174 *of Sciences*, 104, 450–455, <https://doi.org/10.1073/pnas.0603321104>, 2007.
- 1175 Bringmans, P.: First Evidence of Neanderthal Presence in Northwest Europe during the Late Saalian
 1176 “Zeifen Interstadial” (MIS 6.01) found at the VLL and VLB Sites at Veldwezelt-Hezerwater, Belgium,
 1177 *Journal of Archaeology of Northwest Europe*, 1, 2007.
- 1178 Broecker, W. S. and Henderson, G. M.: The sequence of events surrounding Termination II and their
 1179 implications for the cause of glacial-interglacial CO₂ changes, *Paleoceanography*, 13, 352–364, 1998.
- 1180 Burns, S. J., Welsh, L. K., Scroxton, N., Cheng, H., and Edwards, R. L.: Millennial and orbital scale
 1181 variability of the South American Monsoon during the penultimate glacial period, *Sci Rep*, 9, 1234,
 1182 <https://doi.org/10.1038/s41598-018-37854-3>, 2019.
- 1183 Buzi, C., Profico, A., Lorenzo, C., and Manzi, G.: The first preserved nasal cavity in the human fossil
 1184 record: The Neanderthal from Altamura, *Proceedings of the National Academy of Sciences*, 122,
 1185 e2426309122, <https://doi.org/10.1073/pnas.2426309122>, 2025.
- 1186 Cacho, I., Grimalt, J. O., Pelejero, C., Canals, M., Sierro, F. J., Flores, J. A., and Shackleton, N.: Dansgaard-
 1187 Oeschger and Heinrich event imprints in Alboran Sea paleotemperatures, *Paleoceanography*, 14, 698–
 1188 705, <https://doi.org/10.1029/1999PA900044>, 1999.
- 1189 Cacho, I., Shackleton, N., Elderfield, H., Sierro, F. J., and Grimalt, J. O.: Glacial rapid variability in deep-
 1190 water temperature and $\delta^{18}O$ from the Western Mediterranean Sea, *Quaternary Science Reviews*, 25,
 1191 3294–3311, <https://doi.org/10.1016/j.quascirev.2006.10.004>, 2006.
- 1192 Camuera, J., Jiménez-Moreno, G., Ramos-Román, M. J., García-Alix, A., Toney, J. L., Anderson, R. S.,
 1193 Jiménez-Espejo, F., Bright, J., Webster, C., Yanes, Y., and Carrión, J. S.: Vegetation and climate changes
 1194 during the last two glacial-interglacial cycles in the western Mediterranean: A new long pollen record
 1195 from Padul (southern Iberian Peninsula), *Quaternary Science Reviews*, 205, 86–105,
 1196 <https://doi.org/10.1016/j.quascirev.2018.12.013>, 2019.
- 1197 Camuera, J., Ramos-Román, M. J., Jiménez-Moreno, G., García-Alix, A., Ilvonen, L., Ruha, L., Gil-Romera,
 1198 G., González-Sampériz, P., and Seppä, H.: Past 200 kyr hydroclimate variability in the western
 1199 Mediterranean and its connection to the African Humid Periods, *Sci Rep*, 12, 9050,
 1200 <https://doi.org/10.1038/s41598-022-12047-1>, 2022.
- 1201 Caro Gómez, J. A., Díaz Del Olmo, F., Artigas, R. C., Recio Espejo, J. M., and Barrera, C. B.:
 1202 Geoarchaeological alluvial terrace system in Tarazona: Chronostratigraphical transition of Mode 2 to
 1203 Mode 3 during the middle-upper pleistocene in the Guadalquivir River valley (Seville, Spain),
 1204 *Quaternary International*, 243, 143–160, <https://doi.org/10.1016/j.quaint.2011.04.022>, 2011.

a mis en forme : Anglais (États-Unis)

- 1205 Chapman, M. R. and Shackleton, N. J.: Global ice-volume fluctuations, North Atlantic ice-rafting events,
1206 and deep-ocean circulation changes between 130 and 70 ka, *Geology*, 27, 795,
1207 [https://doi.org/10.1130/0091-7613\(1999\)027<0795:GIVFNA>2.3.CO;2](https://doi.org/10.1130/0091-7613(1999)027<0795:GIVFNA>2.3.CO;2), 1999.
- 1208 Chappellaz, J., Brook, E., Blunier, T., and Malaizé, B.: CH₄ and δ¹⁸O of O₂ records from Antarctic and
1209 Greenland ice: A clue for stratigraphic disturbance in the bottom part of the Greenland Ice Core Project
1210 and the Greenland Ice Sheet Project 2 ice cores, *J. Geophys. Res.*, 102, 26547–26557,
1211 <https://doi.org/10.1029/97JC00164>, 1997.
- 1212 Charton, L.: Vegetation and climate changes during the Middle to Upper Palaeolithic transition in the
1213 southwestern Mediterranean: What happened to the last Neanderthals during Heinrich stadial 4?,
1214 *Quaternary Science Reviews*, 2025.
- 1215 Charton, L., Combourieu-Nebout, N., Bertini, A., Lebreton, V., Peyron, O., Robles, M., Sassoone, D., and
1216 Moncel, M.-H.: Vegetation and climate changes during the Middle to Upper Palaeolithic transition in
1217 the southwestern Mediterranean: What happened to the last Neanderthals during Heinrich stadial 4?,
1218 2025.
- 1219 Cheddadi, R. and Rossignol-Strick, M.: Eastern Mediterranean Quaternary paleoclimates from pollen
1220 and isotope records of marine cores in the Nile Cone Area, *Paleoceanography*, 10, 291–300,
1221 <https://doi.org/10.1029/94PA02672>, 1995.
- 1222 Cheng, H., Edwards, R. L., Wang, Y., Kong, X., Ming, Y., Kelly, M. J., Wang, X., Gallup, C. D., and Liu, W.:
1223 A penultimate glacial monsoon record from Hulu Cave and two-phase glacial terminations, *Geology*,
1224 34, 217–220, <https://doi.org/10.1130/G22289.1>, 2006.
- 1225 Chevalier, M., Davis, B. A. S., Heiri, O., Seppä, H., Chase, B. M., Gajewski, K., Lacourse, T., Telford, R. J.,
1226 Finsinger, W., Guiot, J., Kühl, N., Maezumi, S. Y., Tipton, J. R., Carter, V. A., Brussel, T., Phelps, L. N.,
1227 Dawson, A., Zanon, M., Vallé, F., Nolan, C., Mauri, A., de Vernal, A., Izumi, K., Holmström, L., Marsicek,
1228 J., Goring, S., Sommer, P. S., Chaput, M., and Kupriyanov, D.: Pollen-based climate reconstruction
1229 techniques for late Quaternary studies, *Earth-Science Reviews*, 210,
1230 <https://doi.org/10.1016/j.earscirev.2020.103384>, 2020.
- 1231 Colleoni, F., Wekerle, C., Näslund, J.-O., Brandefelt, J., and Masina, S.: Constraint on the penultimate
1232 glacial maximum Northern Hemisphere ice topography (≈140 kyrs BP), *Quaternary Science Reviews*,
1233 137, 97–112, <https://doi.org/10.1016/j.quascirev.2016.01.024>, 2016.
- 1234 Combourieu-Nebout, N., Turon, J. L., Zahn, R., Capotondi, L., Londeix, L., and Pahnke, K.: Enhanced
1235 aridity and atmospheric high-pressure stability over the western Mediterranean during the North
1236 Atlantic cold events of the past 50 k.y., *Geol*, 30, 863, [https://doi.org/10.1130/0091-7613\(2002\)030<0863:EAAAHP>2.0.CO;2](https://doi.org/10.1130/0091-7613(2002)030<0863:EAAAHP>2.0.CO;2), 2002.
- 1238 Combourieu-Nebout, N., Peyron, O., Dormoy, I., Desprat, S., Célia, B., Kotthoff, U., and Marret, F.:
1239 Rapid climatic variability in the west Mediterranean during the last 25 000 years from high resolution
1240 pollen data, *Climate of the Past*, 5, <https://doi.org/10.5194/cpd-5-671-2009>, 2009.
- 1241 Cortina, A., Sierro, F. J., Flores, J. A., Martrat, B., and Grimalt, J. O.: The response of SST to insolation
1242 and ice sheet variability from MIS 3 to MIS 11 in the northwestern Mediterranean Sea (Gulf of Lions),
1243 *Geophysical Research Letters*, 42, 10,366-10,374, <https://doi.org/10.1002/2015GL065539>, 2015.
- 1244 Couture-Veschambre, C., López-Onaindia, D., Sala, N., Arlegi, M., Balzeau, A., Crevecoeur, I., Maureille,
1245 B., Tournepiche, J.-F., and Gómez-Olivencia, A.: Reassessment of the Neandertal fossil collection from

a mis en forme : Anglais (États-Unis)

- 1246 Abri Suard (La Chaise de Vouthon, Charente, France), *Bulletins et mémoires de la Société*
1247 *d'Anthropologie de Paris*. BMSAP, 33, <https://doi.org/10.4000/bmsap.6982>, 2021.
- 1248 Cueto, S., Preysler, J., Pérez-González, A., Torres, C., Pérez, I., and Miguel, J.: Acheulian flint quarries in
1249 the Madrid Tertiary basin, central Iberian Peninsula: First data obtained from geoarchaeological
1250 studies, *Quaternary International*, 411, <https://doi.org/10.1016/j.quaint.2016.01.041>, 2016.
- 1251 Cunha, P. P., Almeida, N. A. C., Aubry, T., Martins, A. A., Murray, A. S., Buylaert, J.-P., Sohbaty, R.,
1252 Raposo, L., and Rocha, L.: Records of human occupation from Pleistocene river terrace and aeolian
1253 sediments in the Arneiro depression (Lower Tejo River, central eastern Portugal), *Geomorphology*,
1254 165–166, 78–90, <https://doi.org/10.1016/j.geomorph.2012.02.017>, 2012.
- 1255 Cunha, P. P., Martins, A. A., Buylaert, J.-P., Murray, A. S., Raposo, L., Mozzi, P., and Stokes, M.: New
1256 data on the chronology of the Vale do Forno sedimentary sequence (Lower Tejo River terrace staircase)
1257 and its relevance as a fluvial archive of the Middle Pleistocene in western Iberia, *Quaternary Science*
1258 *Reviews*, 166, 204–226, <https://doi.org/10.1016/j.quascirev.2016.11.001>, 2017.
- 1259 Damialis, A., Kaimakamis, E., Konoglou, M., Akritidis, I., Traidl-Hoffmann, C., and Gioulekas, D.:
1260 Estimating the abundance of airborne pollen and fungal spores at variable elevations using an aircraft:
1261 how high can they fly?, *Sci Rep*, 7, 44535, <https://doi.org/10.1038/srep44535>, 2017.
- 1262 Dansgaard, W., Johnsen, S. J., Clausen, H. B., Dahl-Jensen, D., Gundestrup, N. S., Hammer, C. U.,
1263 Hvidberg, C. S., Steffensen, J. P., Sveinbjörnsdóttir, A. E., and Jouzel, J.: Evidence for general instability
1264 of past climate from a 250-kyr ice-core record, *Nature*, 364, 218–220, 1993.
- 1265 Davtian, N. and Bard, E.: A new view on abrupt climate changes and the bipolar seesaw based on
1266 paleotemperatures from Iberian Margin sediments, *Proceedings of the National Academy of Sciences*,
1267 120, e2209558120, <https://doi.org/10.1073/pnas.2209558120>, 2023.
- 1268 Dennell, R. W., Martínón-Torres, M., and Bermúdez de Castro, J. M.: Hominin variability, climatic
1269 instability and population demography in Middle Pleistocene Europe, *Quaternary Science Reviews*, 30,
1270 1511–1524, <https://doi.org/10.1016/j.quascirev.2009.11.027>, 2011.
- 1271 D'Errico, F. and Sánchez Goñi, M. F. S.: Neandertal extinction and the millennial scale climatic variability
1272 of OIS 3, *Quaternary Science Reviews*, 22, 769–788, [https://doi.org/10.1016/S0277-3791\(03\)00009-X](https://doi.org/10.1016/S0277-3791(03)00009-X),
1273 2003.
- 1274 Di Vincenzo, F. and Manzi, G.: *Homo heidelbergensis* as the Middle Pleistocene common ancestor of
1275 Denisovans, Neanderthals and modern humans, *Journal of Mediterranean Earth Sciences*, Vol. 15
1276 (2023): In progress, <https://doi.org/10.13133/2280-6148/18074>, 2023.
- 1277 Díez-Martín, F.: Evaluating the effect of plowing on the archaeological record: The early middle
1278 palaeolithic in the river Duero basin plateaus (north-central Spain), *Quaternary International*, 214, 30–
1279 43, <https://doi.org/10.1016/j.quaint.2009.10.024>, 2010.
- 1280 Díez-Martín, F., Sánchez-Yustos, P., Gómez-González, J. Á., and Gómez De La Rúa, D.: Earlier
1281 Palaeolithic Settlement Patterns: Landscape Archaeology on the River Duero Basin Plateaus (Castilla y
1282 León, Spain), *J World Prehist*, 21, 103–137, <https://doi.org/10.1007/s10963-008-9012-0>, 2008.
- 1283 D'Oliveira, L., Dugerdil, L., Ménot, G., Evin, A., Muller, S., Ansanay-Alex, S., Azuara, J., Bonnet, C.,
1284 Bremond, L., Shah, M., and Peyron, O.: Reconstructing 15 000 years of southern France temperatures
1285 from coupled pollen and molecular (branched glycerol dialkyl glycerol tetraether) markers (Canroute,
1286 Massif Central), *Climate of the Past*, 19, 2127–2156, <https://doi.org/10.5194/cp-19-2127-2023>, 2023.

- 1287 Drysdale, R. N., Zanchetta, G., Hellstrom, J. C., Fallick, A. E., and Zhao, J.: Stalagmite evidence for the
 1288 onset of the Last Interglacial in southern Europe at 129 ± 1 ka, *Geophysical Research Letters*, 32,
 1289 <https://doi.org/10.1029/2005GL024658>, 2005.
- 1290 Ehlers, J. and Gibbard, P. L.: The extent and chronology of Cenozoic Global Glaciation, *Quaternary*
 1291 *International*, 164–165, 6–20, <https://doi.org/10.1016/j.quaint.2006.10.008>, 2007a.
- 1292 Ehlers, J. and Gibbard, P. L.: The extent and chronology of Cenozoic Global Glaciation, *Quaternary*
 1293 *International*, 164–165, 6–20, <https://doi.org/10.1016/j.quaint.2006.10.008>, 2007b.
- 1294 Ehlers, J., Grube, A., Stephan, H.-J., and Wansa, S.: Pleistocene Glaciations of North Germany—New
 1295 Results, in: *Developments in Quaternary Sciences*, vol. 15, Elsevier, 149–162,
 1296 <https://doi.org/10.1016/B978-0-444-53447-7.00013-1>, 2011.
- 1297 Ehlers, J., Gibbard, P. L., and Hughes, P. D.: Chapter 4 - Quaternary Glaciations and Chronology, in: *Past*
 1298 *Glacial Environments* (Second Edition), edited by: Menzies, J. and van der Meer, J. J. M., Elsevier, 77–
 1299 101, <https://doi.org/10.1016/B978-0-08-100524-8.00003-8>, 2018.
- 1300 Emeis, K., Schulz, H., Struck, U., Rossignol-Strick, M., Erlenkeuser, H., Howell, M., Kroon, D.,
 1301 Mackensen, A., Ishizuka, S., Oba, T., Sakamoto, T., and Koizumi, I.: Eastern Mediterranean surface
 1302 water temperatures and $\delta^{18}O$ composition during deposition of sapropels in the late Quaternary,
 1303 *Paleoceanography*, 18, 1005, <https://doi.org/10.1029/2000PA000617>, 2003a.
- 1304 Emeis, K.-C., Schulz, H., Struck, U., Rossignol-Strick, M., Erlenkeuser, H., Howell, M. W., Kroon, D.,
 1305 Mackensen, A., Ishizuka, S., Oba, T., Sakamoto, T., and Koizumi, I.: Eastern Mediterranean surface
 1306 water temperatures and $\delta^{18}O$ composition during deposition of sapropels in the late Quaternary,
 1307 *Paleoceanography*, 18, <https://doi.org/10.1029/2000PA000617>, 2003b.
- 1308 Eynaud, F., Zaragosi, S., Scourse, J. D., Mojtahid, M., Bourillet, J. F., Hall, I. R., Penaud, A., Locascio, M.,
 1309 and Reijonen, A.: Deglacial laminated facies on the NW European continental margin: The
 1310 hydrographic significance of British-Irish Ice Sheet deglaciation and Fleuve Manche paleoriver
 1311 discharges, *Geochemistry, Geophysics, Geosystems*, 8, <https://doi.org/10.1029/2006GC001496>, 2007.
- 1312 Faegri, K. and Iversen, J.: *Textbook of Pollen Analysis*, 4th Edition., John Wiley and Sons, Chichester,
 1313 UK, 338 pp., 1964.
- 1314 Fernández Peris, J., Barciela, V., Blasco, R., Cuartero, F., and Sañudo, P.: El Paleolítico Medio en el
 1315 territorio valenciano y la variabilidad tecno-económica de la Cova del Bolomor, *Treballs d'Arqueologia*,
 1316 141–169, 2008.
- 1317 Fernández-Rodríguez, S., Skjøth, C. A., Tormo-Molina, R., Brandao, R., Caeiro, E., Silva-Palacios, I.,
 1318 Gonzalo-Garijo, A., and Smith, M.: Identification of potential sources of airborne *Olea* pollen in the
 1319 Southwest Iberian Peninsula, *Int J Biometeorol*, 58, 337–348, <https://doi.org/10.1007/s00484-012-0629-4>, 2014.
- 1321 Finlayson, C. and Carrión, J. S.: Rapid ecological turnover and its impact on Neanderthal and other
 1322 human populations, *Trends in Ecology & Evolution*, 22, 213–222,
 1323 <https://doi.org/10.1016/j.tree.2007.02.001>, 2007.
- 1324 Fletcher, W. J. and Sánchez Goñi, M. F.: Orbital- and sub-orbital-scale climate impacts on vegetation of
 1325 the western Mediterranean basin over the last 48,000 yr, *Quaternary Research*, 70, 451–464,
 1326 <https://doi.org/10.1016/j.yqres.2008.07.002>, 2008.

a mis en forme : Anglais (États-Unis)

a mis en forme : Espagnol (Espagne)

a mis en forme : Anglais (États-Unis)

- 1327 Fletcher, W. J., Sánchez Goñi, M. F., Allen, J. R. M., Cheddadi, R., Combourieu-Nebout, N., Huntley, B.,
1328 Lawson, I., Londeix, L., Magri, D., Margari, V., Müller, U. C., Naughton, F., Novenko, E., Roucoux, K., and
1329 Tzedakis, P. C.: Millennial-scale variability during the last glacial in vegetation records from Europe,
1330 *Quaternary Science Reviews*, 29, 2839–2864, <https://doi.org/10.1016/j.quascirev.2009.11.015>, 2010.
- 1331 Foerster, V., Asrat, A., Bronk Ramsey, C., Brown, E. T., Chapot, M. S., Deino, A., Duesing, W., Grove, M.,
1332 Hahn, A., Junginger, A., Kaboth-Bahr, S., Lane, C. S., Opitz, S., Noren, A., Roberts, H. M., Stockhecke,
1333 M., Tiedemann, R., Vidal, C. M., Vogelsang, R., Cohen, A. S., Lamb, H. F., Schaebitz, F., and Trauth, M.
1334 H.: Pleistocene climate variability in eastern Africa influenced hominin evolution, *Nat Geosci*, 15, 805–
1335 811, <https://doi.org/10.1038/s41561-022-01032-y>, 2022.
- 1336 Follieri, M., Magri, D., and Sadori, L.: A 250 000-years pollen record from Valle di Castiglione (Roma),
1337 *Pollen et Spores*, 30, 329–356, 1988.
- 1338 Fontana, F., Nenzioni, G., and Peretto, C.: The southern Po plain area (Italy) in the mid-late Pleistocene:
1339 Human occupation and technical behaviours, *Quaternary International*, 223, 465–471,
1340 <https://doi.org/10.1016/j.quaint.2010.02.013>, 2010.
- 1341 Gouzy, A., Malaizé, B., Pujol, C., and Charlier, K.: Climatic “pause” during Termination II identified in
1342 shallow and intermediate waters off the Iberian margin, *Quaternary Science Reviews*, 23, 1523–1528,
1343 <https://doi.org/10.1016/j.quascirev.2004.03.002>, 2004.
- 1344 von Grafenstein, R., Zahn, R., and Tiedemann, R.: Planktonic d18O records at Sites 976 and 977,
1345 Alboran Sea: stratigraphy, forcing, and paleoceanographic implications. In Curry, W.B., Shackleton,
1346 N.J., and Richter, C, *Proceedings Ocean Drilling Program Scientific Results*, 154, 299–318, 1999.
- 1347 Guiot, J.: Methodology of the last climatic cycle reconstruction in France from pollen data,
1348 *Palaeogeography, Palaeoclimatology, Palaeoecology*, 80, 49–69, [https://doi.org/10.1016/0031-](https://doi.org/10.1016/0031-0182(90)90033-4)
1349 [0182\(90\)90033-4](https://doi.org/10.1016/0031-0182(90)90033-4), 1990.
- 1350 Guiot, J., Pons, A., De Beaulieu, J. L., and Reille, M.: A 140,000-year continental climate reconstruction
1351 from two European pollen records, *Nature*, 338, 309–313, <https://doi.org/10.1038/338309a0>, 1989.
- 1352 Guiot, J., De Beaulieu, J. L., Cheddadi, R., David, F., Poncelet, P., and Reille, M.: The climate in Western
1353 Europe during the last Glacial/Interglacial cycle derived from pollen and insect remains,
1354 *Palaeogeography, Palaeoclimatology, Palaeoecology*, 103, 73–93, [https://doi.org/10.1016/0031-](https://doi.org/10.1016/0031-0182(93)90053-L)
1355 [0182\(93\)90053-L](https://doi.org/10.1016/0031-0182(93)90053-L), 1993.
- 1356 Heinrich, H.: Origin and Consequences of Cyclic Ice Rafting in the Northeast Atlantic Ocean During the
1357 Past 130,000 Years, *Quaternary Research*, 29, 142–152, [https://doi.org/10.1016/0033-](https://doi.org/10.1016/0033-5894(88)90057-9)
1358 [5894\(88\)90057-9](https://doi.org/10.1016/0033-5894(88)90057-9), 1988.
- 1359 Held, F., Cheng, H., Edwards, R. L., Tüysüz, O., Koç, K., and Fleitmann, D.: Dansgaard-Oeschger cycles
1360 of the penultimate and last glacial period recorded in stalagmites from Türkiye, *Nat Commun*, 15, 1183,
1361 <https://doi.org/10.1038/s41467-024-45507-5>, 2024.
- 1362 Hemming, S. R.: Heinrich events: Massive late Pleistocene detritus layers of the North Atlantic and
1363 their global climate imprint, *Reviews of Geophysics*, 42, <https://doi.org/10.1029/2003RG000128>,
1364 2004.
- 1365 Hérison, D., Brenet, M., Cliquet, D., Moncel, M.-H., Richter, J., Scott, B., Van Baelen, A., Di Modica, K.,
1366 Loecker, D., Ashton, N., Bourguignon, L., Delagnes, A., Faivre, J.-P., Folgado-Lopez, M., Loch, J.-L.,
1367 Pope, M., Raynal, J.-P., Roebroeks, W., Santagata, C., and Peer, P.: The emergence of the Middle

- 1368 Palaeolithic in north-western Europe and its southern fringes, *Quaternary International*, 411,
1369 <https://doi.org/10.1016/j.quaint.2016.02.049>, 2016.
- 1370 Hersbach, H., Bell, B., Berrisford, P., Hirahara, S., Horányi, A., Muñoz-Sabater, J., Nicolas, J., Peubey, C.,
1371 Radu, R., Schepers, D., Simmons, A., Soci, C., Abdalla, S., Abellan, X., Balsamo, G., Bechtold, P., Biavati,
1372 G., Bidlot, J., Bonavita, M., De Chiara, G., Dahlgren, P., Dee, D., Diamantakis, M., Dragani, R., Flemming,
1373 J., Forbes, R., Fuentes, M., Geer, A., Haimberger, L., Healy, S., Hogan, R. J., Hólm, E., Janisková, M.,
1374 Keeley, S., Laloyaux, P., Lopez, P., Lupu, C., Radnoti, G., de Rosnay, P., Rozum, I., Vamborg, F., Villaume,
1375 S., and Thépaut, J.-N.: The ERA5 global reanalysis, *Quarterly Journal of the Royal Meteorological
1376 Society*, 146, 1999–2049, <https://doi.org/10.1002/qj.3803>, 2020.
- 1377 Hodell, D. A., Channell, J. E. T., Curtis, J. H., Romero, O. E., and Röhl, U.: Onset of “Hudson Strait”
1378 Heinrich events in the eastern North Atlantic at the end of the middle Pleistocene transition (~640
1379 ka)?, *Paleoceanography*, 23, 2008PA001591, <https://doi.org/10.1029/2008PA001591>, 2008.
- 1380 Hodell, D. A., Crowhurst, S. J., Lourens, L., Margari, V., Nicolson, J., Rolfe, J. E., Skinner, L. C., Thomas,
1381 N. C., Tzedakis, P. C., Mlenek-Vautravets, M. J., and Wolff, E. W.: A 1.5-million-year record of orbital
1382 and millennial climate variability in the North Atlantic, *Clim. Past*, 19, 607–636,
1383 <https://doi.org/10.5194/cp-19-607-2023>, 2023.
- 1384 Hodge, E., Richards, D., Smart, P., Andreo, B., Hoffmann, D., Matthey, D., and González-Ramón, A.:
1385 Effective precipitation in southern Spain (~ 266 to 46 ka) based on a speleothem stable carbon isotope
1386 record, *Quaternary Research*, 69, 447–457, <https://doi.org/10.1016/j.yqres.2008.02.013>, 2008.
- 1387 Hublin, J. J.: The origin of Neandertals, *Proceedings of the National Academy of Sciences*, 106, 16022–
1388 16027, <https://doi.org/10.1073/pnas.0904119106>, 2009.
- 1389 Jiménez-Amat, P. and Zahn, R.: Offset timing of climate oscillations during the last two glacial-
1390 interglacial transitions connected with large-scale freshwater perturbation, *Paleoceanography*, 30,
1391 768–788, <https://doi.org/10.1002/2014PA002710>, 2015.
- 1392 Jiménez-Moreno, G., Anderson, R. S., Ramos-Román, M. J., Camuera, J., Mesa-Fernández, J. M., García-
1393 Alix, A., Jiménez-Espejo, F. J., Carrión, J. S., and López-Avilés, A.: The Holocene *Cedrus* pollen record
1394 from Sierra Nevada (S Spain), a proxy for climate change in N Africa, *Quaternary Science Reviews*, 242,
1395 106468, <https://doi.org/10.1016/j.quascirev.2020.106468>, 2020.
- 1396 Johnsen, S. J., Clausen, H. B., Dansgaard, W., Fuhrer, K., Gundestrup, N., Hammer, C. U., Iversen, P.,
1397 Jouzel, J., Stauffer, B., and Steffensen, J. P.: Irregular glacial interstadials recorded in a new Greenland
1398 record, *Nature*, 359, 311–313, 1992.
- 1399 Jouzel, J., Masson-Delmotte, V., Cattani, O., Dreyfus, G., Falourd, S., Hoffmann, G., Minster, B., Nouet,
1400 J., Barnola, J. M., Chappellaz, J., Fischer, H., Gallet, J. C., Johnsen, S., Leuenberger, M., Loulergue, L.,
1401 Luethi, D., Oerter, H., Parrenin, F., Raisbeck, G., Raynaud, D., Schilt, A., Schwander, J., Selmo, E.,
1402 Souchez, R., Spahni, R., Stauffer, B., Steffensen, J. P., Stenni, B., Stocker, T. F., Tison, J. L., Werner, M.,
1403 and Wolff, E. W.: Orbital and millennial Antarctic climate variability over the past 800,000 years,
1404 *Science*, 317, 793–796, <https://doi.org/10.1126/science.1141038>, 2007.
- 1405 Kallel, N., Duplessy, J.-C., Labeyrie, L., Fontugne, M., Paterne, M., and Montacer, M.: Mediterranean
1406 pluvial periods and sapropel formation over the last 200 000 years, *Palaeogeography,
1407 Palaeoclimatology, Palaeoecology*, 157, 45–58, [https://doi.org/10.1016/S0031-0182\(99\)00149-2](https://doi.org/10.1016/S0031-0182(99)00149-2),
1408 2000.

- 1409 Kelly, M., Edwards, R., Cheng, H., Yuan, D., Cai, Y., Zhang, M., Lin, Y., and An, Z.: High resolution
 1410 characterization of the Asian Monsoon between 146,000 and 99,000 years B.P. from Dongge Cave,
 1411 China and global correlation of events surrounding Termination II, *Palaeogeography,*
 1412 *Palaeoclimatology, Palaeoecology*, 236, 20–38, <https://doi.org/10.1016/j.palaeo.2005.11.042>, 2006.
- 1413 Key, A. J. M., Jarić, I., and Roberts, D. L.: Modelling the end of the Acheulean at global and continental
 1414 levels suggests widespread persistence into the Middle Palaeolithic, *Humanit Soc Sci Commun*, 8, 55,
 1415 <https://doi.org/10.1057/s41599-021-00735-8>, 2021.
- 1416 Koltai, G., Spötl, C., Shen, C.-C., Wu, C.-C., Rao, Z., Palcsu, L., Kele, S., Surányi, G., and Bárányi-Kevei, I.:
 1417 A penultimate glacial climate record from southern Hungary, *Journal of Quaternary Science*, 32, 946–
 1418 956, <https://doi.org/10.1002/jqs.2968>, 2017.
- 1419 Koutsodendris, A., Dakos, V., Fletcher, W. J., Knipping, M., Kotthoff, U., Milner, A. M., Müller, U. C.,
 1420 Kaboth-Bahr, S., Kern, O. A., Kolb, L., Vakhrameeva, P., Wulf, S., Christanis, K., Schmiedl, G., and Pross,
 1421 J.: Atmospheric CO₂ forcing on Mediterranean biomes during the past 500 kyrs, *Nat Commun*, 14,
 1422 1664, <https://doi.org/10.1038/s41467-023-37388-x>, 2023.
- 1423 Laskar, J., Robutel, P., Joutel, F., Gastineau, M., Correia, A. C. M., and Levrard, B.: A long-term numerical
 1424 solution for the insolation quantities of the Earth, *A&A*, 428, 261–285, <https://doi.org/10.1051/0004-6361:20041335>, 2004.
- 1426 Lewis, S., Ashton, N., and Jacobi, R.: 9 - Testing Human Presence During the Last Interglacial (MIS 5e):
 1427 A Review of the British Evidence, in: *Developments in Quaternary Sciences*, vol. 14, edited by: Ashton,
 1428 N., Lewis, S. G., and Stringer, C., Elsevier, 125–164, <https://doi.org/10.1016/B978-0-444-53597-9.00009-1>, 2011.
- 1430 Li, T.-Y., Shen, C.-C., Huang, L.-J., Jiang, X.-Y., Yang, X.-L., Mii, H.-S., Lee, S.-Y., and Lo, L.: Stalagmite-
 1431 inferred variability of the Asian summer monsoon during the penultimate glacial–interglacial period,
 1432 *Climate of the Past*, 10, 1211–1219, <https://doi.org/10.5194/cp-10-1211-2014>, 2014.
- 1433 Lionello, P., Malanotte-Rizzoli, P., Boscolo, R., Alpert, P., Artale, V., Li, L., Luterbacher, J., May, W., Trigo,
 1434 R., Tsimplis, M., Ulbrich, U., and Xoplaki, E.: The Mediterranean climate: An overview of the main
 1435 characteristics and issues, in: *Developments in Earth and Environmental Sciences*, vol. 4, edited by:
 1436 Lionello, P., Malanotte-Rizzoli, P., and Boscolo, R., Elsevier, 1–26, [https://doi.org/10.1016/S1571-9197\(06\)80003-0](https://doi.org/10.1016/S1571-9197(06)80003-0), 2006.
- 1438 Lisiecki, L. and Raymo, M.: Pliocene-Pleistocene stack of 57 globally distributed benthic $\delta^{18}O$ records.,
 1439 *Paleoceanography*, 20, <https://doi.org/10.1029/2004PA001071>, 2005.
- 1440 Lisiecki, L. E. and Stern, J. V.: Regional and global benthic $\delta^{18}O$ stacks for the last glacial cycle,
 1441 *Paleoceanography*, 31, 1368–1394, <https://doi.org/10.1002/2016PA003002>, 2016.
- 1442 Liu, J., Fang, N., Wang, F., Yang, F., and Ding, X.: Features of ice-rafted debris (IRD) at IODP site U1312
 1443 and their palaeoenvironmental implications during the last 2.6 Myr, *Palaeogeography,*
 1444 *Palaeoclimatology, Palaeoecology*, 511, 364–378, <https://doi.org/10.1016/j.palaeo.2018.09.002>,
 1445 2018.
- 1446 de Lumley, M. A.: Les restes humains fossiles de la grotte du Lazaret. Généralités, approche
 1447 démographique., in: *Les restes humains fossiles de la grotte du Lazaret, Nice, Alpes-Maritimes. Des*
 1448 *Homo erectus européens évolués en voie de néandertalisation*, CNRS Editions, 217–220, 2018.

a mis en forme : Anglais (États-Unis)

1449 Macklin, M. G., Fuller, I. C., Lewin, J., Maas, G. S., Passmore, D. G., Rose, J., Woodward, J. C., Black, S.,
1450 Hamlin, R. H. B., and Rowan, J. S.: Correlation of fluvial sequences in the Mediterranean basin over the
1451 last 200 ka and their relationship to climate change, *Quaternary Science Reviews*, 21, 1633–1641,
1452 [https://doi.org/10.1016/S0277-3791\(01\)00147-0](https://doi.org/10.1016/S0277-3791(01)00147-0), 2002.

1453 Magri, D. and Parra, I.: Late Quaternary western Mediterranean pollen records and African winds,
1454 *Earth and Planetary Science Letters*, 200, 401–408, [https://doi.org/10.1016/S0012-821X\(02\)00619-2](https://doi.org/10.1016/S0012-821X(02)00619-2),
1455 2002.

1456 Margari, V., Skinner, L. C., Tzedakis, P. C., Ganopolski, A., Vautravers, M., and Shackleton, N. J.: The
1457 nature of millennial-scale climate variability during the past two glacial periods, *Nature Geosci*, 3, 127–
1458 131, <https://doi.org/10.1038/ngeo740>, 2010.

1459 Margari, V., Skinner, L., Hodell, D., Martrat, B., Toucanne, S., Gibbard, P., Lunkka, J., and Tzedakis, C.:
1460 Land-ocean changes on orbital and millennial time scales and the penultimate glaciation, *Geology*,
1461 <https://doi.org/10.1130/G35070.1>, 2014.

1462 Martrat, B., Grimalt, J. O., Lopez-Martinez, C., Cacho, I., Sierro, F. J., Flores, J. A., Zahn, R., Canals, M.,
1463 Curtis, J. H., and Hodell, D. A.: Abrupt Temperature Changes in the Western Mediterranean over the
1464 Past 250,000 Years, *Science*, 306, 1762–1765, <https://doi.org/10.1126/science.1101706>, 2004.

1465 Martrat, B., Grimalt, J. O., Shackleton, N. J., de Abreu, L., Hutterli, M. A., and Stocker, T. F.: Four Climate
1466 Cycles of Recurring Deep and Surface Water Destabilizations on the Iberian Margin, *Science*, 317, 502–
1467 507, <https://doi.org/10.1126/science.1139994>, 2007.

1468 Martrat, B., Jimenez-Amat, P., Zahn, R., and Grimalt, J. O.: Similarities and dissimilarities between the
1469 last two deglaciations and interglaciations in the North Atlantic region, *Quaternary Science Reviews*,
1470 99, 122–134, <https://doi.org/10.1016/j.quascirev.2014.06.016>, 2014.

1471 Masson-Delmotte, V., Stenni, B., Pol, K., Braconnot, P., Cattani, O., Falourd, S., Kageyama, M., Jouzel,
1472 J., Landais, A., Minster, B., Barnola, J. M., Chappellaz, J., Krinner, G., Johnsen, S., Röthlisberger, R.,
1473 Hansen, J., Mikolajewicz, U., and Otto-Bliesner, B.: EPICA Dome C record of glacial and interglacial
1474 intensities, *Quaternary Science Reviews*, 29, 113–128,
1475 <https://doi.org/10.1016/j.quascirev.2009.09.030>, 2010.

1476 Mathias, C., Bourguignon, L., Brenet, M., Grégoire, S., and Moncel, M.-H.: Between new and inherited
1477 technical behaviours: a case study from the Early Middle Palaeolithic of Southern France, *Archaeol*
1478 *Anthropol Sci*, 12, 146, <https://doi.org/10.1007/s12520-020-01114-1>, 2020.

1479 Matthews, A., Affek, H. P., Ayalon, A., Vonhof, H. B., and Bar-Matthews, M.: Eastern Mediterranean
1480 climate change deduced from the Soreq Cave fluid inclusion stable isotopes and carbonate clumped
1481 isotopes record of the last 160 ka, *Quaternary Science Reviews*, 272, 107223,
1482 <https://doi.org/10.1016/j.quascirev.2021.107223>, 2021.

1483 McCarron, A. P., Bigg, G. R., Brooks, H., Leng, M. J., Marshall, J. D., Ponomareva, V., Portnyagin, M.,
1484 Reimer, P. J., and Rogerson, M.: Northwest Pacific ice-rafted debris at 38°N reveals episodic ice-sheet
1485 change in late Quaternary Northeast Siberia, *Earth and Planetary Science Letters*, 553, 116650,
1486 <https://doi.org/10.1016/j.epsl.2020.116650>, 2021.

1487 McManus, J. F., Oppo, D. W., and Cullen, J. L.: A 0.5-Million-Year Record of Millennial-Scale Climate
1488 Variability in the North Atlantic, *Science*, 283, 971–975,
1489 <https://doi.org/10.1126/science.283.5404.971>, 1999.

a mis en forme : Anglais (États-Unis)

- 1490 Melchionna, M., Di Febbraro, M., Carotenuto, F., Rook, L., Mondanaro, A., Castiglione, S., Serio, C.,
 1491 Vero, V. A., Tesone, G., Piccolo, M., Diniz-Filho, J. A. F., and Raia, P.: Fragmentation of Neanderthals'
 1492 pre-extinction distribution by climate change, *Palaeogeography, Palaeoclimatology, Palaeoecology*,
 1493 496, 146–154, <https://doi.org/10.1016/j.palaeo.2018.01.031>, 2018.
- 1494 Menviel, L., Capron, E., Govin, A., Dutton, A., Tarasov, L., Abe-Ouchi, A., Drysdale, R. N., Gibbard, P. L.,
 1495 Gregoire, L., He, F., Ivanovic, R. F., Kageyama, M., Kawamura, K., Landais, A., Otto-Bliesner, B. L., Oyabu,
 1496 I., Tzedakis, P. C., Wolff, E., and Zhang, X.: The penultimate deglaciation: protocol for Paleoclimate
 1497 Modelling Intercomparison Project (PMIP) phase 4 transient numerical simulations between 140 and
 1498 127 ka, version 1.0, *Geoscientific Model Development*, 12, 3649–3685,
 1499 <https://doi.org/10.5194/gmd-12-3649-2019>, 2019.
- 1500 Michel, V., Shen, G., Shen, C.-C., Duval, M., Woodhead, J., Chou, Y.-M., Hu, H.-M., Wu, C.-C., Kan, Y.-C.,
 1501 Yang, H., Yu, T.-L., Gallet, S., and Valensi, P.: Datations radioisotopiques (U-Th, U-Pb) et
 1502 paléodosimétriques (ESR) des plus anciens sites préhistoriques des Alpes-Maritimes: la grotte du
 1503 Vallonnet, le site de plein air de Terra Amata et la grotte du Lazaret, in: *Bulletin du Musée*
 1504 *d'Anthropologie préhistorique de Monaco*, vol. 61, 65–80, 2022.
- 1505 Moncel, M., Vaissié, E., Marin, J., Fernandes, P., Abrunhosa, A., Hardy, B., Richard, M., Torres, C., and
 1506 Baena, J.: Early Middle Palaeolithic Occupations Dated to MIS 7 at the Abri du Maras (Ardèche,
 1507 Southeast France), *Journal of Paleolithic Archaeology*, 2025.
- 1508 Moncel, M.-H., Ashton, N., Arzarello, M., Fontana, F., Lamotte, A., Scott, B., Muttillio, B., Berruti, G.,
 1509 Nenzioni, G., Tuffreau, A., and Peretto, C.: Early Levallois core technology between Marine Isotope
 1510 Stage 12 and 9 in Western Europe, *Journal of Human Evolution*, 139, 102735,
 1511 <https://doi.org/10.1016/j.jhevol.2019.102735>, 2020.
- 1512 Moseley, G. E., Spötl, C., Cheng, H., Boch, R., Min, A., and Edwards, R. L.: Termination-II
 1513 interstadial/stadial climate change recorded in two stalagmites from the north European Alps,
 1514 *Quaternary Science Reviews*, 127, 229–239, <https://doi.org/10.1016/j.quascirev.2015.07.012>, 2015.
- 1515 Mudie, P.: Pollen distribution in recent marine sediments, eastern Canada, *Canadian Journal of Earth*
 1516 *Sciences*, 19, 729–747, <https://doi.org/10.1139/e82-062>, 2011.
- 1517 Murat, A. (Ed.): Chapitre 41: Pliocene–pleistocene occurrence of sapropels in the western
 1518 mediterranean sea and their relation to eastern mediterranean sapropels, in: *Proceedings of the*
 1519 *Ocean Drilling Program*, 161 Scientific Results, vol. 161, *Ocean Drilling Program*,
 1520 <https://doi.org/10.2973/odp.proc.sr.161.1999>, 1999.
- 1521 Nehme, C., Verheyden, S., Breitenbach, S. F. M., Gillikin, D. P., Verheyden, A., Cheng, H., Edwards, R.
 1522 L., Hellstrom, J., Noble, S. R., Farrant, A. R., Sahy, D., Goovaerts, T., Salem, G., and Claeys, P.: Climate
 1523 dynamics during the penultimate glacial period recorded in a speleothem from Kanaan Cave, Lebanon
 1524 (central Levant), *Quaternary Research*, 90, 10–25, <https://doi.org/10.1017/qua.2018.18>, 2018.
- 1525 Nehme, C., Kluge, T., Verheyden, S., Nader, F., Charalambidou, I., Weissbach, T., Gucel, S., Cheng, H.,
 1526 Edwards, R. L., Satterfield, L., Eiche, E., and Claeys, P.: Speleothem record from Pentadactylos cave
 1527 (Cyprus): new insights into climatic variations during MIS 6 and MIS 5 in the Eastern Mediterranean,
 1528 *Quaternary Science Reviews*, 250, 106663, <https://doi.org/10.1016/j.quascirev.2020.106663>, 2020.
- 1529 Obrochta, S. P., Crowley, T. J., Channell, J. E. T., Hodell, D. A., Baker, P. A., Seki, A., and Yokoyama, Y.:
 1530 Climate variability and ice-sheet dynamics during the last three glaciations, *Earth and Planetary Science*
 1531 *Letters*, 406, 198–212, <https://doi.org/10.1016/j.epsl.2014.09.004>, 2014.

a mis en forme : Anglais (États-Unis)

- 1532 Ochando, J., Carrión, J. S., Blasco, R., Fernández, S., Amorós, G., Munuera, M., Sañudo, P., and
 1533 Fernández Peris, J.: Silvicolous Neanderthals in the far West: the mid-Pleistocene palaeoecological
 1534 sequence of Bolomor Cave (Valencia, Spain), *Quaternary Science Reviews*, 217, 247–267,
 1535 <https://doi.org/10.1016/j.quascirev.2019.03.015>, 2019.
- 1536 Okuda, M., Yasuda, Y., and Setoguchi, T.: Middle to Late Pleistocene vegetation history and climatic
 1537 changes at Lake Kopais, Southeast Greece, *Boreas*, 30, 73–82, <https://doi.org/10.1111/j.1502-3885.2001.tb00990.x>, 2001.
- 1539 Oppo, D. W., Keigwin, L. D., McManus, J. F., and Cullen, J. L.: Persistent suborbital climate variability in
 1540 marine isotope stage 5 and termination II, *Paleoceanography*, 16, 280–292,
 1541 <https://doi.org/10.1029/2000PA000527>, 2001.
- 1542 Oppo, D. W., McManus, J. F., and Cullen, J. L.: Evolution and demise of the Last Interglacial warmth in
 1543 the subpolar North Atlantic, *Quaternary Science Reviews*, 25, 3268–3277,
 1544 <https://doi.org/10.1016/j.quascirev.2006.07.006>, 2006.
- 1545 Ovsepyan, E. A. and Murdmaa, I. O.: Response of the bering sea to Heinrich Event 11, *Lithol Miner
 1546 Resour*, 52, 442–446, <https://doi.org/10.1134/S0024490217060062>, 2017.
- 1547 Panera, J., Torres, T., Pérez-González, A., Ortiz, J. E., Rubio-Jara, S., and Val, D. U. del: Geocronología
 1548 de la Terraza Compleja de Arganda en el valle del río Jarama (Madrid, España), *Estudios Geológicos*,
 1549 67, 495–504, <https://doi.org/10.3989/egeol.40550.204>, 2011.
- 1550 Panera, J., Rubio-Jara, S., Yravedra, J., Blain, H.-A., Sesé, C., and Pérez-González, A.: Manzanares Valley
 1551 (Madrid, Spain): A good country for Proboscideans and Neanderthals, *Quaternary International*, 326–
 1552 327, 329–343, <https://doi.org/10.1016/j.quaint.2013.09.009>, 2014.
- 1553 Penaud, A., Eynaud, F., Turon, J. L., Zaragosi, S., Malaizé, B., Toucanne, S., and Bourillet, J. F.: What
 1554 forced the collapse of European ice sheets during the last two glacial periods (150 ka B.P. and 18 ka
 1555 cal B.P.)? Palynological evidence, *Palaeogeography, Palaeoclimatology, Palaeoecology*, 281, 66–78,
 1556 <https://doi.org/10.1016/j.palaeo.2009.07.012>, 2009.
- 1557 Penaud, A., Eynaud, F., Voelker, A. H. L., and Turon, J.-L.: Palaeohydrological changes over the last 50
 1558 ky in the central Gulf of Cadiz: complex forcing mechanisms mixing multi-scale processes,
 1559 *Biogeosciences*, 13, 5357–5377, <https://doi.org/10.5194/bg-13-5357-2016>, 2016.
- 1560 Pereira, T., Cunha, P. P., Martins, A. A., Nora, D., Paixão, E., Figueiredo, O., Raposo, L., Henriques, F.,
 1561 Caninas, J., Moura, D., and Bridgland, D. R.: Geoarchaeology of the Cobrinhos site (Vila Velha de Ródão,
 1562 Portugal) - a record of the earliest Mousterian in western Iberia, *Journal of Archaeological Science:
 1563 Reports*, 24, 640–654, <https://doi.org/10.1016/j.jasrep.2018.11.026>, 2019.
- 1564 Pérez-Asensio, J. N., Frigola, J., Pena, L. D., Sierro, F. J., Reguera, M. I., Rodríguez-Tovar, F. J., Dorador,
 1565 J., Asioli, A., Kuhlmann, J., Huhn, K., and Cacho, I.: Changes in western Mediterranean thermohaline
 1566 circulation in association with a deglacial Organic Rich Layer formation in the Alboran Sea, *Quaternary
 1567 Science Reviews*, 228, 106075, <https://doi.org/10.1016/j.quascirev.2019.106075>, 2020.
- 1568 Peyrégne, S., Slon, V., Mafessoni, F., de Filippo, C., Hajdinjak, M., Nagel, S., Nickel, B., Essel, E., Le Cabec,
 1569 A., Wehrberger, K., Conard, N. J., Kind, C. J., Posth, C., Krause, J., Abrams, G., Bonjean, D., Di Modica,
 1570 K., Toussaint, M., Kelso, J., Meyer, M., Pääbo, S., and Prüfer, K.: Nuclear DNA from two early
 1571 Neandertals reveals 80,000 years of genetic continuity in Europe, *Science Advances*, 5, eaaw5873,
 1572 <https://doi.org/10.1126/sciadv.aaw5873>, 2019.

a mis en forme : Espagnol (Espagne)

a mis en forme : Anglais (États-Unis)

- 1573 Pini, R., Ravazzi, C., and Donegana, M.: Pollen stratigraphy, vegetation and climate history of the last
 1574 215 ka in the Azzano Decimo core (plain of Friuli, north-eastern Italy), *Quaternary Science Reviews*,
 1575 28, 1268–1290, <https://doi.org/10.1016/j.quascirev.2008.12.017>, 2009.
- 1576 Prasad, A. M., Iverson, L. R., and Liaw, A.: Newer Classification and Regression Tree Techniques:
 1577 Bagging and Random Forests for Ecological Prediction, *Ecosystems*, 9, 181–199,
 1578 <https://doi.org/10.1007/s10021-005-0054-1>, 2006.
- 1579 Quézel, P.: *Réflexions sur l'évolution de la flore et de la végétation au Maghreb Méditerranéen*, Ibis
 1580 Press., Paris, 117 pp., 2000.
- 1581 Raia, P., Mondanaro, A., Melchionna, M., Di Febraro, M., Diniz-Filho, J. A., Rangel, T., Holden, P.,
 1582 Carotenuto, F., Edwards, N., Lima-Ribeiro, M., Profico, A., Maiorano, L., Castiglione, S., Serio, C., and
 1583 Rook, L.: Past Extinctions of Homo Species Coincided with Increased Vulnerability to Climatic Change,
 1584 *One Earth*, 3, 480–490, <https://doi.org/10.1016/j.oneear.2020.09.007>, 2020.
- 1585 Railsback, L. B., Gibbard, P. L., Head, M. J., Voarintsoa, N. R. G., and Toucanne, S.: An optimized scheme
 1586 of lettered marine isotope substages for the last 1.0 million years, and the climatostratigraphic nature
 1587 of isotope stages and substages, *Quaternary Science Reviews*, 111, 94–106,
 1588 <https://doi.org/10.1016/j.quascirev.2015.01.012>, 2015.
- 1589 Rasmussen, S. O., Bigler, M., Blockley, S. P., Blunier, T., Buchardt, S. L., Clausen, H. B., Cvijanovic, I.,
 1590 Dahl-Jensen, D., Johnsen, S. J., Fischer, H., Gkinis, V., Guillevic, M., Hoek, W. Z., Lowe, J. J., Pedro, J. B.,
 1591 Popp, T., Seierstad, I. K., Steffensen, J. P., Svensson, A. M., Vallelonga, P., Vinther, B. M., Walker, M. J.
 1592 C., Wheatley, J. J., and Winstrup, M.: A stratigraphic framework for abrupt climatic changes during the
 1593 Last Glacial period based on three synchronized Greenland ice-core records: refining and extending
 1594 the INTIMATE event stratigraphy, *Quaternary Science Reviews*, 106, 14–28,
 1595 <https://doi.org/10.1016/j.quascirev.2014.09.007>, 2014.
- 1596 Rasmussen, T. L., Oppo, D. W., Thomsen, E., and Lehman, S. J.: Deep sea records from the southeast
 1597 Labrador Sea: Ocean circulation changes and ice-rafting events during the last 160,000 years,
 1598 *Paleoceanography*, 18, <https://doi.org/10.1029/2001PA000736>, 2003.
- 1599 Regattieri, E., Zanchetta, G., Drysdale, R. N., Isola, I., Hellstrom, J. C., and Roncioni, A.: A continuous
 1600 stable isotope record from the penultimate glacial maximum to the Last Interglacial (159–121 ka) from
 1601 Tana Che Urla Cave (Apuan Alps, central Italy), *Quaternary Research*, 82, 450, 2014.
- 1602 Renault, L., Oguz, T., Pascual, A., Vizoso, G., and Tintore, J.: Surface circulation in the Alborán Sea
 1603 (western Mediterranean) inferred from remotely sensed data, *J. Geophys. Res.*, 117, 2011JC007659,
 1604 <https://doi.org/10.1029/2011JC007659>, 2012.
- 1605 Rios-Garaizar, J.: Early Middle Palaeolithic occupations at Ventalaperra cave (Cantabrian Region,
 1606 Northern Iberian Peninsula), *Journal of Lithic Studies*, 3, <https://doi.org/10.2218/jls.v3i1.1287>, 2016.
- 1607 Robles, M., Peyron, O., Ménot, G., Brugiapaglia, E., Wulf, S., Appelt, O., Blache, M., Vannière, B.,
 1608 Dugerdil, L., Paura, B., Ansanay-Alex, S., Cromartie, A., Charlet, L., Guédron, S., De Beaulieu, J.-L., and
 1609 Joannin, S.: Climate changes during the Lateglacial in South Europe: new insights based on pollen and
 1610 brGDGTs of Lake Matese in Italy, <https://doi.org/10.5194/cp-2022-54>, 2022.
- 1611 Robles, M., Peyron, O., Ménot, G., Elisabetta, B., Wulf, S., Appelt, O., Blache, M., Vannière, B., Dugerdil,
 1612 L., Paura, B., Ansanay-Alex, S., Cromartie, A., Charlet, L., Guedron, S., de Beaulieu, Jacques-L., and
 1613 Joannin, S.: Climate changes during the Late Glacial in southern Europe: new insights based on pollen
 1614 and brGDGTs of Lake Matese in Italy, 19, 493–515, <https://doi.org/10.5194/cp-19-493-2023>, 2023.

a mis en forme : Anglais (États-Unis)

- 1615 Rogerson, M., Cacho, I., Jimenez-Espejo, F., Reguera, M. I., Sierro, F. J., Martinez-Ruiz, F., Frigola, J.,
1616 and Canals, M.: A dynamic explanation for the origin of the western Mediterranean organic-rich layers,
1617 *Geochemistry, Geophysics, Geosystems*, 9, <https://doi.org/10.1029/2007GC001936>, 2008.
- 1618 Rohling, E. J., Marino, G., and Grant, K. M.: Mediterranean climate and oceanography, and the periodic
1619 development of anoxic events (sapropels), *Earth-Science Reviews*, 143, 62–97,
1620 <https://doi.org/10.1016/j.earscirev.2015.01.008>, 2015.
- 1621 Rohling, E. J., Hibbert, F. D., Williams, F. H., Grant, K. M., Marino, G., Foster, G. L., Hennekam, R., de
1622 Lange, G. J., Roberts, A. P., Yu, J., Webster, J. M., and Yokoyama, Y.: Differences between the last two
1623 glacial maxima and implications for ice-sheet, $\delta^{18}O$, and sea-level reconstructions, *Quaternary Science
1624 Reviews*, 176, 1–28, <https://doi.org/10.1016/j.quascirev.2017.09.009>, 2017.
- 1625 Rojo, J., Orlandi, F., Pérez-Badia, R., Aguilera, F., Ben Dhiab, A., Bouziane, H., Díaz de la Guardia, C.,
1626 Galán, C., Gutiérrez-Bustillo, A. M., Moreno-Grau, S., Msallem, M., Trigo, M. M., and Fornaciari, M.:
1627 Modeling olive pollen intensity in the Mediterranean region through analysis of emission sources,
1628 *Science of The Total Environment*, 551–552, 73–82, <https://doi.org/10.1016/j.scitotenv.2016.01.193>,
1629 2016.
- 1630 Roucoux, K. H., de Abreu, L., Shackleton, N. J., and Tzedakis, P. C.: The response of NW Iberian
1631 vegetation to North Atlantic climate oscillations during the last 65kyr, *Quaternary Science Reviews*, 24,
1632 1637–1653, <https://doi.org/10.1016/j.quascirev.2004.08.022>, 2005.
- 1633 Roucoux, K. H., Tzedakis, P. C., Lawson, I. T., and Margari, V.: Vegetation history of the penultimate
1634 glacial period (Marine isotope stage 6) at Ioannina, north-west Greece, *Journal of Quaternary Science*,
1635 26, 616–626, <https://doi.org/10.1002/jqs.1483>, 2011.
- 1636 Rousseau, D.-D., Antoine, P., Boers, N., Lacroix, F., Ghil, M., Lomax, J., Fuchs, M., Debret, M., Christine,
1637 H., Moine, O., Gauthier, C., Jordanova, D., and Jordanova, N.: Dansgaard-Oeschger-like events of the
1638 penultimate climate cycle: the loess point of view, *Climate of the Past*, 16, 713–727,
1639 <https://doi.org/10.5194/cp-16-713-2020>, 2020.
- 1640 Rubio-Jara, S. and Panera, J.: Unravelling an essential archive for the European Pleistocene. The human
1641 occupation in the Manzanares valley (Madrid, Spain) throughout nearly 800,000 years, *Quaternary
1642 International*, 520, 5–22, <https://doi.org/10.1016/j.quaint.2018.08.007>, 2019.
- 1643 Rubio-Jara, S., Panera, J., Rodríguez-de-Tembleque, J., Santonja, M., and Pérez-González, A.: Large
1644 flake Acheulean in the middle of Tagus basin (Spain): Middle stretch of the river Tagus valley and lower
1645 stretches of the rivers Jarama and Manzanares valleys, *Quaternary International*, 411, 349–366,
1646 <https://doi.org/10.1016/j.quaint.2015.12.023>, 2016.
- 1647 Ruddiman, W. F.: Late Quaternary deposition of ice-rafted sand in the subpolar North Atlantic (lat 40°
1648 to 65°N), *Geol Soc America Bull*, 88, 1813, [https://doi.org/10.1130/0016-7606\(1977\)88<1813:LQDOIS>2.0.CO;2](https://doi.org/10.1130/0016-7606(1977)88<1813:LQDOIS>2.0.CO;2), 1977.
- 1650 Sadori, L., Koutsodendris, A., Panagiotopoulos, K., Masi, A., Bertini, A., Combourieu-Nebout, N.,
1651 Francke, A., Kouli, K., Joannin, S., Mercuri, A. M., Peyron, O., Torri, P., Wagner, B., Zanchetta, G.,
1652 Sinopoli, G., and Donders, T. H.: Pollen-based paleoenvironmental and paleoclimatic change at Lake
1653 Ohrid (south-eastern Europe) during the past 500 ka, *Biogeosciences*, 13, 1423–1437,
1654 <https://doi.org/10.5194/bg-13-1423-2016>, 2016.

a mis en forme : Anglais (États-Unis)

- 1655 Salonen, J. S., Korpela, M., Williams, J. W., and Luoto, M.: Machine-learning based reconstructions of
 1656 primary and secondary climate variables from North American and European fossil pollen data, *Sci*
 1657 *Rep*, 9, 15805, <https://doi.org/10.1038/s41598-019-52293-4>, 2019.
- 1658 Sánchez Goñi, M.: The climatic and environmental context of the Late Pleistocene, in: *Updating*
 1659 *Neanderthals. Understanding Behavioural Complexity in the Late Middle Palaeolithic.*,
 1660 Elsevier/Academic Press, London, 165–169, <https://doi.org/10.1016/B978-0-12-823498-3.00012-1>,
 1661 2022.
- 1662 Sánchez Goñi, M. F.: Millennial-scale variability during the last glacial in vegetation records from
 1663 Europe, *Quaternary Science Reviews*, 2010.
- 1664 Sánchez Goñi, M. S., I, C., J, T., J, G., F, S., J, P., J, G., and N, S.: Synchronicity between marine and
 1665 terrestrial responses to millennial scale climatic variability during the last glacial period in the
 1666 Mediterranean region, *Climate Dynamics*, 19, 95, 2002.
- 1667 Sánchez-Laulhé, J. M., Jansa, A., and Jiménez, C.: Alboran Sea Area Climate and Weather, in: *Alboran*
 1668 *Sea - Ecosystems and Marine Resources*, edited by: Báez, J. C., Vázquez, J.-T., Camiñas, J. A., and
 1669 Malouli Idrissi, M., Springer International Publishing, Cham, 31–83, [https://doi.org/10.1007/978-3-](https://doi.org/10.1007/978-3-030-65516-7_3)
 1670 [030-65516-7_3](https://doi.org/10.1007/978-3-030-65516-7_3), 2021.
- 1671 Sánchez-Yustos, P.: El paleolítico antiguo en la cuenca del Duero. Instrumentos teóricos para la
 1672 construcción de un modelo interpretativo de arqueología económica, 2009.
- 1673 Sánchez-Yustos, P. and Díez-Martín, F.: Dancing to the rhythms of the Pleistocene? Early Middle
 1674 Paleolithic population dynamics in NW Iberia (Duero Basin and Cantabrian Region), *Quaternary Science*
 1675 *Reviews*, 121, <https://doi.org/10.1016/j.quascirev.2015.05.005>, 2015.
- 1676 Santonja, M., Pérez-González, A., Panera, J., Rubio-Jara, S., and Méndez-Quintas, E.: The coexistence
 1677 of Acheulean and Ancient Middle Palaeolithic techno-complexes in the Middle Pleistocene of the
 1678 Iberian Peninsula, *Quaternary International*, 411, 367–377,
 1679 <https://doi.org/10.1016/j.quaint.2015.04.056>, 2016.
- 1680 Santonja, M., Pérez-González, A., Baena, J., Panera, J., Méndez-Quintas, E., Uribebarrea, D., Demuro,
 1681 M., Arnold, L., Abrunhosa, A., and Rubio-Jara, S.: The Acheulean of the Upper Guadiana River Basin
 1682 (Central Spain). Morphostratigraphic Context and Chronology, *Front. Earth Sci.*, 10,
 1683 <https://doi.org/10.3389/feart.2022.912007>, 2022.
- 1684 Sasso, D., Lebreton, V., Comboureu-Nebout, N., Peyron, O., and Moncel, M.-H.:
 1685 Palaeoenvironmental changes in the southwestern Mediterranean (ODP site 976, Alboran sea) during
 1686 the MIS 12/11 transition and the MIS 11 interglacial and implications for hominin populations,
 1687 *Quaternary Science Reviews*, 304, 108010, <https://doi.org/10.1016/j.quascirev.2023.108010>, 2023.
- 1688 Sasso, D., Comboureu-Nebout, N., Peyron, O., Bertini, A., Toti, F., Lebreton, V., and Moncel, M.-H.:
 1689 Pollen-based climatic reconstructions for the interglacial analogues of MIS 1 (MIS 19, 11, and 5) in the
 1690 southwestern Mediterranean: insights from ODP Site 976, *Clim. Past*, 21, 489–515,
 1691 <https://doi.org/10.5194/cp-21-489-2025>, 2025.
- 1692 Savannah, M., Eelco, R., Timme, D., Katharine, G., Jörg, K., Gianluca, M., Francesca, S., Francesca, C.,
 1693 Caterina, M., Anna, S., and Alessandra, N.: The “glacial” sapropel S6 (172 ka; MIS 6): A multiproxy
 1694 approach to solve a Mediterranean “cold case,” *Palaeogeography, Palaeoclimatology, Palaeoecology*,
 1695 650, 112384, <https://doi.org/10.1016/j.palaeo.2024.112384>, 2024.

a mis en forme : Espagnol (Espagne)

a mis en forme : Anglais (États-Unis)

- 1696 Scott, B.: *Becoming Neanderthals: the earlier British middle palaeolithic*, Oxbow books, Oxford, 2011.
- 1697 Shackleton, N. J.: Oxygen isotopes, ice volume and sea level, *Quaternary Science Reviews*, 6, 183–190,
1698 [https://doi.org/10.1016/0277-3791\(87\)90003-5](https://doi.org/10.1016/0277-3791(87)90003-5), 1987.
- 1699 Shackleton, N. J., Hall, M. A., and Vincent, E.: Phase relationships between millennial-scale events
1700 64,000–24,000 years ago, *Paleoceanography*, 15, 565–569, <https://doi.org/10.1029/2000PA000513>,
1701 2000.
- 1702 Shackleton, N. J., Sánchez-Goñi, M. F., Pailler, D., and Lancelot, Y.: Marine Isotope Substage 5e and the
1703 Eemian Interglacial, *Global and Planetary Change*, 36, 151–155, <https://doi.org/10.1016/S0921->
1704 8181(02)00181-9, 2003.
- 1705 Shackleton, N. J., Fairbanks, R. G., Chiu, T., and Parrenin, F.: Absolute calibration of the Greenland time
1706 scale: implications for Antarctic time scales and for $\Delta^{14}C$, *Quaternary Science Reviews*, 23, 1513–1522,
1707 <https://doi.org/10.1016/j.quascirev.2004.03.006>, 2004.
- 1708 Shaw, A., Bates, M., Conneller, C., Gamble, C., Julien, M.-A., McNabb, J., Pope, M., and Scott, B.: The
1709 archaeology of persistent places: the Palaeolithic case of La Cotte de St Brelade, Jersey, *Antiquity*, 90,
1710 1437–1453, <https://doi.org/10.15184/aqy.2016.212>, 2016.
- 1711 Shin, J., Nehrbass-Ahles, C., Grilli, R., Chowdhry Beeman, J., Parrenin, F., Teste, G., Landais, A.,
1712 Schmidely, L., Silva, L., Schmitt, J., Bereiter, B., Stocker, T. F., Fischer, H., and Chappellaz, J.: Millennial-
1713 scale atmospheric CO₂ variations during the Marine Isotope Stage 6 period (190–135 ka),
1714 *Climate of the Past*, 16, 2203–2219, <https://doi.org/10.5194/cp-16-2203-2020>, 2020.
- 1715 Sierro, F. J. and Andersen, N.: An exceptional record of millennial-scale climate variability in the
1716 southern Iberian Margin during MIS 6: Impact on the formation of sapropel S6, *Quaternary Science*
1717 *Reviews*, 286, 107527, <https://doi.org/10.1016/j.quascirev.2022.107527>, 2022.
- 1718 Sierro, F. J., Hodell, D. A., Andersen, N., Azibeiro, L. A., Jimenez-Espejo, F. J., Bahr, A., Flores, J. A., Ausin,
1719 B., Rogerson, M., Lozano-Luz, R., Lebreiro, S. M., and Hernandez-Molina, F. J.: Mediterranean Overflow
1720 Over the Last 250 kyr: Freshwater Forcing From the Tropics to the Ice Sheets, *Paleoceanography and*
1721 *Paleoclimatology*, 35, e2020PA003931, <https://doi.org/10.1029/2020PA003931>, 2020.
- 1722 Silva, P. G., López-Recio, M., Tapias, F., Roquero, E., Morín, J., Rus, I., Carrasco-García, P., Giner-Robles,
1723 J. L., Rodríguez-Pascua, M. A., and Pérez-López, R.: Stratigraphy of the Arriaga Palaeolithic sites.
1724 Implications for the geomorphological evolution recorded by thickened fluvial sequences within the
1725 Manzanares River valley (Madrid Neogene Basin, Central Spain), *Geomorphology*, 196, 138–161,
1726 <https://doi.org/10.1016/j.geomorph.2012.10.019>, 2013.
- 1727 Sinopoli, G., Peyron, O., Masi, A., Holtvoeth, J., Francke, A., Wagner, B., and Sadori, L.: Pollen-based
1728 temperature and precipitation changes in the Ohrid Basin (western Balkans) between 160 and 70 ka,
1729 *Climate of the Past*, 15, 53–71, <https://doi.org/10.5194/cp-15-53-2019>, 2019.
- 1730 Skinner, L. C. and Shackleton, N. J.: Deconstructing Terminations I and II: revisiting the glacioeustatic
1731 paradigm based on deep-water temperature estimates, *Quaternary Science Reviews*, 25, 3312–3321,
1732 <https://doi.org/10.1016/j.quascirev.2006.07.005>, 2006a.
- 1733 Skinner, L. C. and Shackleton, N. J.: Deconstructing Terminations I and II: revisiting the glacioeustatic
1734 paradigm based on deep-water temperature estimates, *Quaternary Science Reviews*, 25, 3312–3321,
1735 <https://doi.org/10.1016/j.quascirev.2006.07.005>, 2006b.

a mis en forme : Anglais (États-Unis)

- 1736 Stocker, T. F.: The Seesaw Effect, *Science*, 282, 61–62, <https://doi.org/10.1126/science.282.5386.61>,
1737 1998.
- 1738 Sumner, G., Homar, V., and Ramis, C.: Precipitation seasonality in eastern and southern coastal Spain,
1739 *Intl Journal of Climatology*, 21, 219–247, <https://doi.org/10.1002/joc.600>, 2001.
- 1740 Svendsen, J. I., Alexanderson, H., Astakhov, V. I., Demidov, I., Dowdeswell, J. A., Funder, S., Gataullin,
1741 V., Henriksen, M., Hjort, C., Houmark-Nielsen, M., Hubberten, H. W., Ingólfsson, Ó., Jakobsson, M.,
1742 Kjær, K. H., Larsen, E., Lokrantz, H., Lunkka, J. P., Lyså, A., Mangerud, J., Matiouchkov, A., Murray, A.,
1743 Möller, P., Niessen, F., Nikolskaya, O., Polyak, L., Saarnisto, M., Siegert, C., Siegert, M. J., Spielhagen, R.
1744 F., and Stein, R.: Late Quaternary ice sheet history of northern Eurasia, *Quaternary Science Reviews*,
1745 23, 1229–1271, <https://doi.org/10.1016/j.quascirev.2003.12.008>, 2004.
- 1746 Terradillos-Bernal, M., Demuro, M., Arnold, L. J., Jordá-Pardo, J. F., Clemente-Conte, I., Benito-Calvo,
1747 A., and Díez Fernández-Lomana, J. C.: San Quirce (Palencia, Spain): new chronologies for the Lower to
1748 Middle Palaeolithic transition of south-west Europe, *Journal of Quaternary Science*, 38, 21–37,
1749 <https://doi.org/10.1002/jqs.3460>, 2023.
- 1750 Thabet, A. A., Maas, A. E., Lawson, G. L., and Tarrant, A. M.: Life cycle and early development of the
1751 thecosomatous pteropod *Limacina retroversa* in the Gulf of Maine, including the effect of elevated
1752 CO₂ levels, *Mar Biol*, 162, 2235–2249, <https://doi.org/10.1007/s00227-015-2754-1>, 2015.
- 1753 Torres, C., Tapias, F., Demuro, M., Arnold, L., Arriolabengoa, M., Pérez, S., and Preysler, J.: The
1754 Acheulian site of Cantera Vieja (Madrid, Spain) and the Lower to Middle Palaeolithic transition in
1755 central Spain, <https://doi.org/10.21203/rs.3.rs-4195503/v1>, 2024.
- 1756 Toucanne, S., Zaragosi, S., Bourillet, J. F., Cremer, M., Eynaud, F., Van Vliet-Lanoë, B., Penaud, A.,
1757 Fontanier, C., Turon, J. L., Cortijo, E., and Gibbard, P. L.: Timing of massive ‘Fleuve Manche’ discharges
1758 over the last 350 kyr: insights into the European ice-sheet oscillations and the European drainage
1759 network from MIS 10 to 2, *Quaternary Science Reviews*, 28, 1238–1256,
1760 <https://doi.org/10.1016/j.quascirev.2009.01.006>, 2009.
- 1761 Tzedakis, P. C.: Long-term tree populations in northwest Greece through multiple Quaternary climatic
1762 cycles, *Nature*, 364, 437–440, <https://doi.org/10.1038/364437a0>, 1993.
- 1763 Tzedakis, P. C.: Towards an understanding of the response of southern European vegetation to orbital
1764 and suborbital climate variability, *Quaternary Science Reviews*, 24, 1585–1599,
1765 <https://doi.org/10.1016/j.quascirev.2004.11.012>, 2005.
- 1766 Tzedakis, P. C., Frogley, M. R., Lawson, I. T., Preece, R. C., Cacho, I., and de Abreu, L.: Ecological
1767 thresholds and patterns of millennial-scale climate variability: The response of vegetation in Greece
1768 during the last glacial period, *Geology*, 32, 109, <https://doi.org/10.1130/G20118.1>, 2004.
- 1769 Tzedakis, P. C., Hooghiemstra, H., and Pälike, H.: The last 1.35 million years at Tenaghi Philippon:
1770 revised chronostratigraphy and long-term vegetation trends, *Quaternary Science Reviews*, 25, 3416–
1771 3430, <https://doi.org/10.1016/j.quascirev.2006.09.002>, 2006.
- 1772 Tzedakis, P. C., Drysdale, R. N., Margari, V., Skinner, L. C., Menviel, L., Rhodes, R. H., Taschetto, A. S.,
1773 Hodell, D. A., Crowhurst, S. J., Hellstrom, J. C., Fallick, A. E., Grimalt, J. O., McManus, J. F., Martrat, B.,
1774 Mokeddem, Z., Parrenin, F., Regattieri, E., Roe, K., and Zanchetta, G.: Enhanced climate instability in
1775 the North Atlantic and southern Europe during the Last Interglacial, *Nat Commun*, 9, 4235,
1776 <https://doi.org/10.1038/s41467-018-06683-3>, 2018.

1777 Valensi, P., Aouraghe, H., Bailon, S., Cauche, D., Combiér, J., Desclaux, E., Gagnepain, J., Gaillard, C.,
1778 Khatib, S., Lumley, H., Moigne, A.-M., Moncel, M.-H., and Notter, O.: Les peuplements préhistoriques
1779 dans le sud-est de la France à la fin du Pléistocène moyen : 400 - 120 000 ans. Terra Amata, Orgnac 3,
1780 Baume Bonne, Lazaret. Cadre géochronologique et biostratigraphique, paléoenvironnements et
1781 évolution culturelle des derniers anténéandertaliens., 2005.

1782 Valensi, P., Michel, V., El Guennouni, K., and Liouville, M.: New data on human behavior from a 160,000
1783 year old Acheulean occupation level at Lazaret cave, south-east France: An archaeozoological
1784 approach, *Quaternary International*, 316, <https://doi.org/10.1016/j.quaint.2013.10.034>, 2013.

a mis en forme : Anglais (États-Unis)

1785 Vernot, B., Zavala, E., Gómez-Olivencia, A., Jacobs, Z., Slon, V., Mafessoni, F., Romagné, F., Pearson, A.,
1786 Petr, M., Sala, N., Pablos, A., Aranburu, A., Bermúdez de Castro, J.-M., Carbonell, E., Li, B., Krajcarz, M.,
1787 Krivoschapkin, A., Kolobova, K., Kozlikin, M., and Meyer, M.: Unearthing Neanderthal population history
1788 using nuclear and mitochondrial DNA from cave sediments, *Science*, 372, eabf1667,
1789 <https://doi.org/10.1126/science.abf1667>, 2021.

1790 Vidal-Matutano, P., Blasco, R., Sañudo, P., and Fernández Peris, J.: The Anthropogenic Use of Firewood
1791 During the European Middle Pleistocene: Charcoal Evidence from Levels XIII and XI of Bolomor Cave,
1792 Eastern Iberia (230–160 ka), *Environmental Archaeology*, 24, 269–284,
1793 <https://doi.org/10.1080/14614103.2017.1406026>, 2019.

1794 Voelker, A. H. L. and de Abreu, L.: A Review of Abrupt Climate Change Events in the Northeastern
1795 Atlantic Ocean (Iberian Margin): Latitudinal, Longitudinal, and Vertical Gradients, in: Abrupt Climate
1796 Change: Mechanisms, Patterns, and Impacts, American Geophysical Union (AGU), 15–37,
1797 <https://doi.org/10.1029/2010GM001021>, 2011.

1798 Wagner, B., Vogel, H., Francke, A., Friedrich, T., Donders, T., Lacey, J. H., Leng, M. J., Regattieri, E.,
1799 Sadori, L., Wilke, T., Zanchetta, G., Albrecht, C., Bertini, A., Combourieu-Nebout, N., Cvetkoska, A.,
1800 Giaccio, B., Grazhdani, A., Hauffe, T., Holtvoeth, J., Joannin, S., Jovanovska, E., Just, J., Kouli, K., Kousis,
1801 I., Koutsodendris, A., Krastel, S., Lagos, M., Leicher, N., Levkov, Z., Lindhorst, K., Masi, A., Melles, M.,
1802 Mercuri, A. M., Nomade, S., Nowaczyk, N., Panagiotopoulos, K., Peyron, O., Reed, J. M., Sagnotti, L.,
1803 Sinopoli, G., Stelbrink, B., Sulpizio, R., Timmermann, A., Tofilovska, S., Torri, P., Wagner-Cremer, F.,
1804 Wonik, T., and Zhang, X.: Mediterranean winter rainfall in phase with African monsoons during the
1805 past 1.36 million years, *Nature*, 573, 256–260, <https://doi.org/10.1038/s41586-019-1529-0>, 2019.

1806 Wainer, K., Genty, D., Blamart, D., Daëron, M., Bar-Matthews, M., Vonhof, H., Dublyansky, Y., Pons-
1807 Branchu, E., Thomas, L., Calsteren, P., Quinif, Y., and Caillon, N.: Speleothem record of the last 180 ka
1808 in Villars cave (SW France): Investigation of a large δ 18O shift between MIS6 and MIS5, *Quaternary*
1809 *Science Reviews - QUATERNARY SCI REV*, 30, 130–146,
1810 <https://doi.org/10.1016/j.quascirev.2010.07.004>, 2011.

a mis en forme : Anglais (États-Unis)

1811 Wainer, K., Genty, D., Blamart, D., Bar-Matthews, M., Quinif, Y., and Plagnes, V.: Millennial climatic
1812 instability during penultimate glacial period recorded in a south-western France speleothem,
1813 *Palaeogeography, Palaeoclimatology, Palaeoecology*, 376, 122–131,
1814 <https://doi.org/10.1016/j.palaeo.2013.02.026>, 2013.

1815 Wang, Q., Wang, Y., Shao, Q., Liang, Y., Zhang, Z., and Kong, X.: Millennial-scale Asian monsoon
1816 variability during the late Marine Isotope Stage 6 from Hulu Cave, China, *Quat. res.*, 90, 394–405,
1817 <https://doi.org/10.1017/qua.2018.75>, 2018.

1818 Wang, Y. J., Cheng, H., Edwards, R. L., An, Z. S., Wu, J. Y., Shen, C. C., and Dorale, J. A.: A high-resolution
1819 absolute-dated late Pleistocene Monsoon record from Hulu Cave, China, *Science*, 294, 2345–2348,
1820 <https://doi.org/10.1126/science.1064618>, 2001.

1821 Wenzel, S.: Neanderthal presence and behaviour in central and Northwestern Europe during MIS 5e,
1822 in: *Developments in Quaternary Sciences*, 173–193, <https://doi.org/10.13140/2.1.2747.7442>, 2007.

1823 White, M. J. and Pettitt, P. B.: The British Late Middle Palaeolithic: An Interpretative Synthesis of
1824 Neanderthal Occupation at the Northwestern Edge of the Pleistocene World, *Journal of World*
1825 *Prehistory*, 24, <https://doi.org/10.1007/s10963-011-9043-9>, 2011.

1826 Willis, K. J., Bennett, K. D., Walker, D., Gamble, C., Davies, W., Pettitt, P., and Richards, M.: Climate
1827 change and evolving human diversity in Europe during the last glacial, *Philosophical Transactions of*
1828 *the Royal Society of London. Series B: Biological Sciences*, 359, 243–254,
1829 <https://doi.org/10.1098/rstb.2003.1396>, 2004.

1830 Wilson, G. P., Frogley, M. R., Hughes, P. D., Roucoux, K. H., Margari, V., Jones, T. D., Leng, M. J., and
1831 Tzedakis, P. C.: Persistent millennial-scale climate variability in Southern Europe during Marine Isotope
1832 Stage 6, *Quaternary Science Advances*, 3, 100016, <https://doi.org/10.1016/j.qsa.2020.100016>, 2021.

1833 Xue, G., Cai, Y., Ma, L., Cheng, X., Cheng, H., Edwards, R. L., Li, D., and Tan, L.: A new speleothem record
1834 of the penultimate deglacial: Insights into spatial variability and centennial-scale instabilities of East
1835 Asian monsoon, *Quaternary Science Reviews*, 210, 113–124,
1836 <https://doi.org/10.1016/j.quascirev.2019.02.023>, 2019.

1837 Yaworsky, P. M., Nielsen, E. S., and Nielsen, T. K.: The Neanderthal niche space of Western Eurasia 145
1838 ka to 30 ka ago, *Sci Rep*, 14, 7788, <https://doi.org/10.1038/s41598-024-57490-4>, 2024.

1839 Yravedra, J., Rubio-Jara, S., Panera, J., Made, J. van der, and Pérez-González, A.: Neanderthal diet in
1840 fluvial environments at the end of the Middle Pleistocene/early Late Pleistocene of PRERESA site in the
1841 Manzanares Valley (Madrid, Spain), *Quaternary International*, 520, 72–83,
1842 <https://doi.org/10.1016/j.quaint.2018.01.030>, 2019.

1843 Zahn, R., Comas, M. C., and Klaus, A. (Eds.): *Proceedings of the Ocean Drilling Program*, 161 Scientific
1844 Results, Ocean Drilling Program, <https://doi.org/10.2973/odp.proc.sr.161.1999>, 1999.

1845 Zhang, J., Zolitschka, B., Hogrefe, I., Tsukamoto, S., Binot, F., and Frechen, M.: High-resolution
1846 luminescence-dated sediment record for the last two glacial-interglacial cycles from Rodderberg,
1847 Germany, *Quaternary Geochronology*, 82, 101535, <https://doi.org/10.1016/j.quageo.2024.101535>,
1848 2024.

1849 Ziegler, M., Tuenter, E., and Lourens, L.: The precession phase of the boreal summer monsoon as
1850 viewed from the eastern Mediterranean (ODP Site 968), *Quaternary Science Reviews*, 29,
1851 <https://doi.org/10.1016/j.quascirev.2010.03.011>, 2010.

1852